Modulation of pollen tube growth by ethylene signaling

Rasha Althiab Almasaud

THÈSE

En vue de l'obtention du

DOCTORAT DE L'UNIVERSITÉ DE TOULOUSE

Délivré par :

Institut National Polytechnique de Toulouse (Toulouse INP)

Discipline ou spécialité :

Développement des Plantes

Présentée et soutenue par :

Mme RASHA ALTHIAB ALMASAUD

le vendredi 8 octobre 2021

Titre :

Modulation of pollen tube growth by ethylene signaling

Ecole doctorale :

Sciences Ecologiques, Vétérinaires, Agronomiques et Bioingénieries (SEVAB)

Unité de recherche :

Laboratoire de Génomique et Biotechnologie des Fruits (GBF)

Directeurs de Thèse :

M. CHRISTIAN CHERVIN

MME HUGUETTE SALLANON

Rapporteurs :

MME CATHERINE RAYON, UNIVERSITE AMIENS

Membres du jury :

MME FRANÇOISE CORBINEAU, UNIVERSITE SORBONNE, Présidente

M. CHRISTIAN CHERVIN, TOULOUSE INP, Membre

MME HUGUETTE SALLANON, UNIVERSITE D'AVIGNON, Membre

M. MONDHER BOUZAYEN, TOULOUSE INP, Invité

M. PHILIPPE GALLUSCI, UNIVERSITE BORDEAUX 1, Membre

Acknowledgements

I thank all the people who contributed in some way to the work described in this thesis. First, I would like to thank Dr Mondher Bouzayen for accepting me in his group and giving me helpful suggestions during my thesis.

I deeply thank my supervisor, Dr Christian Chervin. During my thesis, he contributed to a rewarding graduate school experience by giving me intellectual freedom in my work, supporting my attendance at various conferences, engaging me in new ideas. Additionally, I thank my other supervisor, Dr Huguette Sallanon for her interest and support in my work.

Specials thanks to Drs Jean-Claude Mollet, Elisabeth Jamet and Christian Mazars for their participation to the second chapter. Special thanks to Dr Caren Chang for her participation to the third chapter.

I am grateful to Drs Françoise Corbineau, Catherine Rayon and Philippe Gallusci for their participation to my PhD jury.

I am grateful to scientists of my PhD committee: Drs Caren Chang, Jean-Claude Mollet, and Nicolas Frei-dit-Frey. I greatly benefited from their keen scientific insight, their knack for solving seemingly intractable practical difficulties, and their ability to put complex ideas into simple terms.

I would like to thank all members of the GBF team. They provided a friendly and cooperative atmosphere at work and also useful feedback and insightful comments on my work.

I would thank my family for supporting me during my thesis's years. Thank to my husband and love of my life, Mohamed, for keeping things going and for always showing how proud he is of me. Thank to my daughters Yara and Alma who have been the light of my life and who have

given me the extra strength and motivation to get things done. The last word goes for my mother for always believing in me and encouraging me to follow my dreams.

Publications

Related to my PhD work

Althiab-Almasaud, R., Chen, Y., Maza, E., Djari, A., Frasse, P., Mollet, J.C. et al. (2021) Ethylene signaling modulates tomato pollen tube growth, through modifications of cell wall remodeling and calcium gradient. **Plant Journal**, 107, 893–908. https://doi.org/10.1111/tpj.15353

An J.*, **Althiab Almasaud R**.*, Bouzayen M., Zouine M. Chervin C. (2019). Auxin and Ethylene Regulation of Fruit Set. **Plant Science**, 292: 110381. https://doi.org/10.1016/j.plantsci.2019.110381

Althiab-Almasaud, R., Sallanon, H., Chang, C. and Chervin, C**.** (2021) 1-aminocyclopropane-1-carboxylic acid (ACC) stimulates tomato pollen tube growth independently of ethylene receptors . *Physiol. Plant.*, 1–7**.** https://doi.org/10.1111/ppl.13579

Teyssier E. *, **Althiab-Almasaud R**. *, Chervin C., Mollet J.C. (2021). Pollen viability and longevity in angiosperms: biotechnological, physiological and environmental issues. Submitted to **Annals of Botany**

Althiab-Almasaud R., Alkassem M., Bouzayen M., Chervin C. (2021). Fruit set stages identification using Deep Learning. in preparation

Side project

Chen Y., **Althiab Almasaud R**., Carrie E., Desbrosses G., Binder B., Chervin C. (2020). Ethanol, at physiological concentrations, affects ethylene sensing in tomato germinating seeds and seedlings. **Plant Science**, 291:110368. https://doi.org/10.1016/j.plantsci.2019.110368

* premiers auteurs joints

Abstract

Ethylene is a phytohormone controlling many processes of plant development. The importance of this hormone in fruit set regulation has been reported, but there are still gaps in our knowledge.

The first chapter is dedicated to a review of the role of ethylene in the different stages of fruit set, as well as the role of auxin. Briefly, ethylene is involved in the pollen germination in the stigma, the pollen tube growth through the transmission tissues in the style and finally the fertilization of the ovule.

The second chapter is centered on pollen tube (PT) elongation. Two opposite lines of Ethylene Receptors (ETRs) mutants were used: *etr3-ko*, a loss-of-function (LOF) mutant; and *NR* (*Never Ripe*), a gain of function (GOF) mutant. We showed that PT of etr*3-ko* grew faster than WT (Wild Type). On the contrary, *NR* PT elongation was slower than WT. Moreover, we confirmed that PT growth is enhanced by exogenous ethylene and inhibited by an ethylene perception inhibitor, 1-methylcyclopropene (1-MCP). The transcriptome profiling of PTs in *etr3-ko* and *NR* mutants, revealed that ethylene perception has major impacts on cell wall- and calcium signaling-related genes.

The third chapter is focused on the role of 1-aminocyclopropane-1-carboxylic acid (ACC), a precursor of ethylene, as a signal by itself, independent of ethylene perception, on PT growth. We discovered that exogenous ACC stimulated PT growth even when ethylene perception was inhibited by 1-MCP treatment or the *NR* mutation. Furthermore, in *EBS:GUS* transgenic pollen, GUS activity was stimulated by ACC in the presence of 1-MCP. These data suggest that ACC signaling can bypass the ethylene receptor step to stimulate PT growth.

Résumé

L'éthylène est une phytohormone contrôlant de nombreux processus de développement des plantes. L'importance de cette hormone dans la régulation de la mise à fruit a été décrite, mais il y a encore des points non éclaircis.

Le premier chapitre constitue une synthèse sur le rôle de l'éthylène dans les différentes étapes de la mise à fruit, ainsi que le rôle de l'auxine. En bref, l'éthylène est impliqué dans la germination du pollen dans le stigmate, la croissance du tube pollinique à travers les tissus du style et enfin la fécondation de l'ovule.

Le deuxième chapitre porte sur l'allongement du tube pollinique (TP). Nous avons utilisé deux lignées opposées de mutants des récepteurs de l'éthylène (ETR): *etr3-ko*, un mutant perte de fonction (LOF); et *NR* (Never Ripe), un mutant gain de fonction (GOF). Nous avons montré que les TPs de *etr3-ko* se développaient plus rapidement que ceux du WT (Wild Type). Au contraire, l'allongement des TPs de *NR* était plus lent que ceux du WT. De plus, nous avons confirmé que la croissance du TP est stimulée par l'éthylène exogène et inhibée par un inhibiteur de la perception de l'éthylène, le 1-méthylcyclopropène (1-MCP). L'analyse transcriptomique des TPs de mutants *etr3-ko* et *NR*, a révélé que la perception de l'éthylène a des impacts majeurs sur les gènes liés à la modification de la paroi cellulaire et de la signalisation calcique.

Le troisième chapitre est axé sur le rôle de l'acide 1-aminocyclopropane-1-carboxylique (ACC), un précurseur de l'éthylène, en tant que signal en soi (indépendant de la perception de l'éthylène) sur la croissance du TP. Nous avons découvert que l'ACC exogène stimulait la croissance des TPs même lorsque la perception de l'éthylène était inhibée par le traitement au 1-MCP ou la mutation *NR*. De plus, dans le pollen transgénique *EBS:GUS*, l'activité GUS a été stimulée par ACC en présence de 1-MCP. Ces données suggèrent que la signalisation ACC peut contourner l'étape du récepteur de l'éthylène pour stimuler la croissance de TPs.

Abbreviations

1-MCP: 1-MethylCycloPropene:

A. thaliana: Arabidopsis thaliana

ACC: 1-AminoCyclopropane-1-Carboxylic acid

ACO: 1-AminoCyclopropane-1-Carboxylic acid Oxydase

ACS: 1-AminoCyclopropane-1-Carboxylic acid Synthase

AVG: AminoethoxyVinylGlycine

cDNA: complementary DeoxyriboNucleic Acid

CDS: Coding sequence

CTR1: CONSTITUTIVE TRIPLE RESPONSE 1

DPA: Days Post Anthesis

EDTA: EthyleneDiamine Tetraacetic Acid

EIN2: ETHYLENE INSENSITIVE 2

ER: Endoplasmic Reticulum

ERS: Ethylene Response Sensor

ETR: EThylene Receptor

GOF: Gain-Of-Function

GUS: β-Glucuronidase

KO: Knock-Out

LOF: Loss-Of-Function

MS: Murashige and Skoog

NR: Never Ripe

PCR: Polymerase Chain Reaction

qPCR: quantitative PCR

WT: Wild Type

WTB: Wild Type Brazil

Content

General Introduction

My doctorate work covers ethylene roles in tomato fruit set. My main topic was the studyof the effects of ethylene signaling on tomato pollen tube elongation by using transcriptome profiling, and also by looking at the potential role of the ethylene precursor, 1-aminocyclopropane carboxylic acid, which has recently been identified a potential signal by itself.

In recent years, the research in plant reproduction has gained interest as it is a key element to control plant yield and food production to match the growth of world population (Pereira and Coimbra, 2019). The transition from flower to young fruit, namely fruit set, is an initial step of fruit development to ensure successful sexual plant reproduction, and fruit set efficiency which is important features to determine the production and yield of various crops (An *et al.*, 2020). Fruit set starts by the landing of pollen grains on stigma and the pollen grain germination, then the pollen tube grows through the style towards the ovule where the fertilization occurs (An *et al.*, 2020).

This latter review article, the first chapter of my PhD work, covers the roles of ethylene and auxin in fruit set, as I co-authored it with a companion PhD student, Jing An, working on the auxin roles. Many reports pointed the role of ethylene in fruit set including pollen germination, pollen tube elongation and fertilization (Holden *et al.*, 2003; Jia *et al.*, 2018; Zhang *et al.*, 2018). In mature pollen grain the content of the ethylene precursor, 1- aminocyclopropane carboxylic acid (ACC), start to increase, one day before anthesis, which may induce pollen germinationethylene. Also, ethylene led to transmission tissues degradationin the style, which facilitates pollen tube growth. After pollination, the ethylene initiates egg cell differentiation in ovules. Finally, ethylene promotes programmed cell death of synergid cells, which prevent other pollen tube attraction.

In chapter two, I describe our studies about the role of ethylene perception in pollen tube elongation by using two ETR3 mutants with opposite effects, a loss-of-function (LOF) mutation, the *etr3-ko* mutant, and a gain-of-function (GOF) mutant, called *NR* for Never Ripe. We discovered that ethylene receptors block PT growth, in absence of ethylene. The

transcriptome profiling analyses for *etr3-ko* and *NR* mutants showed that cell wall-related genes and calcium signaling-related genes were mostly affected. Moreover, the distribution of the methylesterified homogalacturonan pectic motifs in the pollen tubes were modified in *NR*. Additionally, the calcium gradient was differently altered in *etr3-ko* and *NR* mutants. All these results reveal that the ethylene signal is able to remodel cell wall structureand calcium gradient in the pollen tubes.

Finally, my third chapter focuses on ACC, a biosynthetic precursor of ethylene, which was often used as a tool to identify the genetic and molecular mechanisms regulating the ethylene response. Recently, some studies showed that ACC can act as a signal by itself, independent of ethylene signaling or bypassing ethylene perception. Here, we provide additional evidence for the role of ACC in the regulation of pollen tube growth, independently of ethylene perception. ACC treatment stimulated PT growth despite ethylene perception was blocked either chemically by treating with 1-methylcyclopropene (1-MCP) or genetically by using the ethylene-insensitive *NR* mutant. Reducing endogenous ACC levels by aminoethoxyvinylglycine (AVG) treatment led to a reduction of PT growth. Moreover, GUS activity driven by an EIN3 Binding Site promoter *(EBS:GUS* transgene) was triggered by ACC in the presence of 1-MCP. Taken together these results suggest that ACC signaling can bypass the ethylene receptor to induce PT growth.

Finally, I was also involved in the development of methods to detect the different stages of tomato fruit set by using deep learning. This work will provide a new method to help the researchers detect the different flower stages by image analyses, which could replace the visual method. This work is in progress and has been added in Annex.

Chapter I: Review: Auxin and Ethylene Regulation of Fruit Set

(Published in Plant Science by An et al., 2020)

Review: Auxin and Ethylene Regulation of Fruit Set

Abstract

With the forecasted fast increase in world population and global climate change, it becomes a major challenge for human society to provide sufficient amounts of quality food. Seed and fruit crop yield is determined by developmental processes including flower initiation, pollen fertility and fruit set. Fruit set is defined as the transition from flower to young fruit, a key step in the development of sexually reproducing higher plants. Plant hormones have important roles during flower pollination and fertilization, leading to fruit set. Moreover, it is well established that fruit set can be triggered by phytohormones like auxin and gibberellins (GAs), in the absence of fertilization, both hormones being commonly used to produce parthenocarpic fruits and to increase fruit yield. Additionally, a number of studies highlighted the role of ethylene in plant reproductive organ development. The present review integrates current knowledge on the roles of auxin and ethylene in different steps of the fruit set process with a specific emphasis on the interactions between the two hormones. A deeper understanding of the interplay between auxin and ethylene may provide new leads towards designing strategies for a better control of fruit initiation and ultimately yield.

1. Introduction

Fruit set is known as the initial step of fruit development in sexual reproduction of flowering plants, a process by which the flower turns into a fruit. The transition from flower to fruit corresponds to a developmental shift that is naturally triggered upon flower fertilization and leading to the activation of a high number of metabolic pathways and anatomical transformations that result in the change in organ identity. Fruit set relies on successful pollination of the stigma, followed by pollen germination and subsequent growth of the pollen tube towards the ovule (Vriezen *et al.*, 2008). Then, the fertilization of the ovule triggers the division and expansion of the cells surrounding the embryo (Vriezen *et al.*, 2008), and it is

widely accepted that the whole process is regulated by plant growth substances, such as phytohormones, with auxin playing a pivotal role in the regulation of this developmental shift (Wang *et al.*, 2005; Pandolfini, 2009).

Notably, the role of auxins in the development of fruit from unfertilized ovules, a process called parthenocarpy, has been largely documented, and it was proposed that auxin can serve as alternative signal replacing pollination and fertilization to initiate the fruit growth program. It was also shown that auxins interact with the GAs, and that both hormones stimulate cell division and expansion during the fruit set. In particular, auxin was reported to increase GA content, by upregulating GA biosynthesis genes (Serrani *et al.*, 2008). Further insights into the molecular mechanisms involving the two hormones in the regulation of fruit initiation were provided by the discovery of SlARF7, an auxin response factor, which mediates a crosstalk between auxin and GA signaling (Jong *et al.*, 2011). Recent studies showed that abscisic acid also plays an important role in regulating tomato fruit set, further adding to the complexity of the network that regulates this process (Serrani *et al.*, 2008; Jong *et al.*, 2011; Vriezen *et al.*, 2008).

Ethylene has been recognized as an important hormone in several plant development processes and ethylene production increases in the flowers of many plant species after pollination (Holden *et al.*, 2003), although it was also reported that ethylene biosynthesis starts to decrease once fruit set is completed (Pandolfini, 2009). However, our understanding of the function of ethylene during carpel development and fruit set in tomato is mostly limited to transcriptome profiling of tomato ovaries which revealed alterations in a high number of ethylene related genes involved in the flower-to-fruit transition (Pascual *et al.*, 2009; Vriezen *et al.*, 2008). The role of ethylene in pollination-independent fruit set has also been suggested based on treatments with the ethylene perception inhibitors, silver thiosulphate and 1-methylcyclopropene (1-MCP) or with the ethylene biosynthesis inhibitor, 2-aminoethoxyvinyl glycine, that leads to parthenocarpic fruit formation (Carbonell-Bejerano *et al.*, 2011). Taken together, these findings support the idea that ethylene plays an active role in the regulation of fruit set, although its precise contribution to this process and its mode of action remain to be further clarified.

The present review addresses various aspects of the regulation of the fruit set by ethylene and auxin, and provides new leads towards unravelling the mechanisms underlying this hormonal crosstalk. For a better clarity, the roles of ethylene and auxin are considered at different stages of fruit set, including sexual organ formation, pollination, fertilization, and in parthenocarpic fruit formation.

1.1. Auxin biosynthesis, transport and signaling pathway.

In higher plants, there are two major routes for indole acetic acid (IAA) biosynthesis: the tryptophan (Trp)-dependent and the Trp-independent pathways (Normanly *et al.*, 1993; Zhao, 2014; Wang *et al.*, 2015). In the Trp-dependent pathways, IAA is biosynthesized from L-Trp by a two-step process: the first step corresponds to the transformation of Trp to indole-3-pyruvic acid (IPA) catalyzed by TRYPTOPHAN AMINOTRANSFERASE OF ARABIDOPSIS (TAA/TAR) family, then IPA is decarboxylated by YUCCA flavin monooxygenase enzymes to form IAA (Zhao, 2014). The Trp-independent pathway was discovered two decades ago. It assumes that IAA can be produced *de novo* without Trp (Normanly *et al.*, 1993). In this pathway, the indole-3-glycerol phosphate (IGP) is converted to indole by indole synthase, which initiates IAA synthesis without Trp (Wang *et al.*, 2015).

Auxin transport can be operated either by diffusion (passive movement) or by specific transporters (active movement) (Zazímalová *et al.*, 2010). IAA is protonated in the apoplasmic compartment, crossing the plasma membrane to diffuse into the cell. Once in the cytosol, IAA is mainly deprotonated due to the higher pH, and the resulting charged molecule (IAA-) is membrane impermeable. Then transporters are required to help auxins to to cross the plasma membranes. Several auxin carrier families have been identified, such as AUXIN-RESISTANT 1/LIKE AUX1 (AUX1/LAX) influx carriers, PIN-FORMED (PIN) and ATP-BINDING CASSETTE (ABCB) auxin efflux carriers which mediate auxin distribution in and between cells (Zazímalová *et al.*, 2010).

Auxin is perceived by the cytoplasmic F-box-domain-containing proteins named TRANSPORT INHIBITOR RESPONSE1/AUXIN SIGNALING F-BOX (TIR1/AFB) (Dharmasiri *et al.*, 2005). The pathway linking auxin perception to gene expression involves the ubiquitination of AUXIN RESISTANT/INDOLE-3-ACETIC ACID INDUCIBLE

(Aux/IAA) proteins by the TIR1/AFB subunit of the SCFTIR1/AFB ubiquitin ligase and their degradation by the 26S proteasome. Then the Aux/IAA-mediated inhibition of AUXIN RESPONSE FACTORs (ARFs) is released, which allows ARFs to modulate the expression of their downstream target genes, known as auxin-responsive genes (Chapman and Estelle, 2009).

1.2. Ethylene biosynthesis and signaling pathways.

The biosynthesis of ethylene includes three steps, the first leading from methionine to S-Adenosyl-Methionine (SAM) catalyzed by the S-adenosyl-methionine synthetase (SAM synthetase), the second transforming SAM into 1-aminocyclopropane-1-carboxylic acid (ACC) by ACC synthase (ACS) and finally the production of ethylene from ACC by ACC oxidase (ACO). The pool of ACC is also regulated by conjugation via ACC acyl-transferases leading to the formation of ACC derivatives like malonyl-ACC, glutamyl-ACC, and jasmonyl-ACC, which affects the pools of free ACC and hence ethylene biosynthesis (Van de Poel *et al.*, 2015).

Ethylene is perceived by different ethylene receptor proteins (ETRs), located in the endoplasmic reticulum membrane. The number of ETRs varies among species with five receptors reported in Arabidopsis, ETR1, ETR2, EIN4, ERS1, and ERS2 (Binder *et al.*, 2007) and seven ethylene receptors in the tomato, ETR1, ETR2, ETR3, ETR4, ETR5, ETR6, and ETR7, each having a distinct pattern of expression throughout development and in response to external stimuli (Liu *et al.*, 2015). The ETRs are negative regulators of ethylene responses and interact with other protein partners like CONSTITUTIVE TRIPLE RESPONSE (CTRs) protein kinases which are also negative regulators of the downstream signal. In the absence of ethylene, the ETR-CTR complex maintains the ETHYLENE INSENSITIVE2 protein (EIN2) in a phosphorylated state at its C-terminus domain which prevents its cleavage (Stepanova and Alonso, 2009). In the presence of ethylene, the protein complex (ETR-CTRs) is dephosphorylated and inactivated, thus causing the cleavage of the EIN2 C-terminus domain by proteases, and this C-terminus domain moves into the nucleus, promoting the accumulation of EIN3/EILs by preventing its degradation via EBF1 and EBF2 (Binder *et al.*, 2007). The EIN3/EIL3 proteins activate the transcription of ethylene response factors (ERFs), which in

turn lead to expression of hundreds of ethylene responsive genes, through binding to GCC-boxes and other cis-acting elements (Liu *et al.*, 2015; Stepanova and Alonso, 2009).

Ethylene and auxin can interact synergistically or antagonistically to control a variety of plant development processes, such as fruit development, fruit ripening, root formation and hypocotyl elongation (Shin *et al.*, 2019; Růzicka *et al.*, 2007).

2. Ethylene and auxin regulate the formation of plant male and female organs.

2.1 Male reproductive organs

In flowering plants, the stamen male reproductive organ is made of the filament and the anther where pollen is produced (Figure 1A). The formation and development of normal stamens are essential for male fertility, and therefore for successful fruit set. A number of studies highlighted the expression dynamics of genes encoding various components of ethylenesignaling and responses in male reproductive organs suggesting an active role for ethylene in pollen development (Hua *et al.*, 1998; Yau, 2004). For instance, in Arabidopsis, *AtEIN4* and *AtERS2* exhibit high expression at the transcript level in stamen, including pollen and tapetumcells. These latter form a specialized cell layer feeding the developing pollen grains. High expression of ethylene receptors in these tissues suggests that ethylene is important in these processes (Hua *et al.*, 1998). *AtERS2* gene shows a similar expression pattern to the ethylene receptor gene *Os-ERS1* in rice that is up-regulated during early pollen development, corresponding to meiotic and microspore stages (Yau, 2004). In tomato, the ethylene productioncapacity of pollen grains is consistent with the expression of ethylene biosynthesis and signaling genes in these tissues (Jegadeesan *et al.*, 2018a). Moreover, the application of high concentration of exogenous ethylene on male gametophyte induces the degradation of the generative cell at meiosis stage resulting in male sterility (Kovaleva *et al.*, 2011). Regarding auxins, many studies showed that they are involved in pollen development. For example, IAA accumulates in anthers prior to pollination, specifically in pollen grains, tapetum, endotheciumand epidermis cells of anther (Feng *et al.*, 2006). Moreover, the repression of the *iaaL* gene

encoding indoleacetic acid–lysine synthetase, which converts free IAA to its inactive form IAA-lysine, results in low free IAA content in anther and reduced pollen viability due to defective mitosis (Feng *et al.*, 2006). In tomato, the down-regulation of *SlPIN8*, a gene encodingan auxin-transporter specifically expressed in tomato pollen, resulted in up to 80% abnormal pollen grains with extremely poor viability (Gan *et al.*, 2019). Altogether, these data suggestthat ethylene and auxin play important roles in pollen development, and that high amount of ethylene may have detrimental effect on the process.

Additionally, several studies showed that ethylene has critical roles in pollen release. The process of anther dehiscence involves two main steps sequentially consisting of (i) degeneration of the middle layer and tapetum; (ii) breakage of the anther wall at the region of stomium between the two locules of each anther (Goldberg *et al.*, 1993). It has been reported, using transgenetic tabacco plants, that the mutant melon ethylene receptor gene *Cm-ERS1/H70A* exhibits delay in tapetum programmed cell death, resulting in the production of abnormal pollen (Takada *et al.*, 2006). In the Arabidopsis ethylene insensitive mutant *etr1-1*, the (i) stomium cells showed delayed degeneration and then (ii) anther dehiscence is delayed (Rieu *et al.*, 2003). These two events have been related to ethylene production peaks in petunia (Kovaleva *et al.*, 2011). Moreover, application of ethylene-perception inhibitors 2,5-norbornadiene and 1-MCP impaired anther dehiscence in petunia and tobacco, respectively, whereas ethylene treatment accelerated this process (Rieu *et al.*, 2003). Similarly, in Petunia, the down-regulation lines of ethylene receptor gene *PhETR2* hastened stomium degeneration and anther dehiscence, making these process happened before anthesis, which is earlier than in wild type, indicating that PhETR2 regulates the timing of anther dehiscence (Wang and Kumar, 2007). This seems to indicate that through promoting anther dehiscence, ethylene promotes pollen release. It was shown that auxin also involves in anther dehiscence process, the quadruple mutant *tir1/ afb1/ afb2/ afb3* displaying auxin perception defects shows early anther dehiscence due to premature lignification of endothecium cell walls and precocious breakage of the stomium (Cecchetti *et al.*, 2008).

Regarding male sterility, ethylene and auxin also appear to be involved in the arrest of stamen development (Rieu et al., 2003; Okada., 1991). In Arabidopsis, it shows the stamen

development arrest in *CsACO2* overexpressed lines, suggesting that the increase in ethylene production inhibits stamen development (Duan *et al.*, 2008). Also, down regulation of cucumber *ETR1* ethylene receptor gene induced abnormal stamen development leading to female flower only (Wang *et al.*, 2010). Moreover, it was shown in tobacco that ethylene perception is critical for filament elongation (Takada *et al.*, 2005). However, it was shown that auxin positively regulates stamen development, including filament elongation and pollen maturation (Takada *et al.*, 2005; Okada et al., 1991). Indeed, in the Arabidopsis *yuc2-yuc6* double mutant, the down regulation of auxin biosynthesis caused the failure of filament elongation and pollen maturation (Cheng *et al.*, 2006), similar observations were performed when auxin perception were altered (Cecchetti *et al.*, 2008). When auxin transport is affected, in Arabidopsis *pin1-1* and *pin1-2* mutants, no stamen developed (C).

Finally, cross-talks between auxin and ethylene, have been observed in *Gaillardia grandiflora* at the stamen level, as auxin promotes pollen tube elongation and ethylene production at the same stage. This auxin-induced ethylene has an important role in the later stigma opening stage (Koning, 1983). Taken together, these findings support the idea that ethylene and auxin play important roles in male reproductive organs of higher plants.

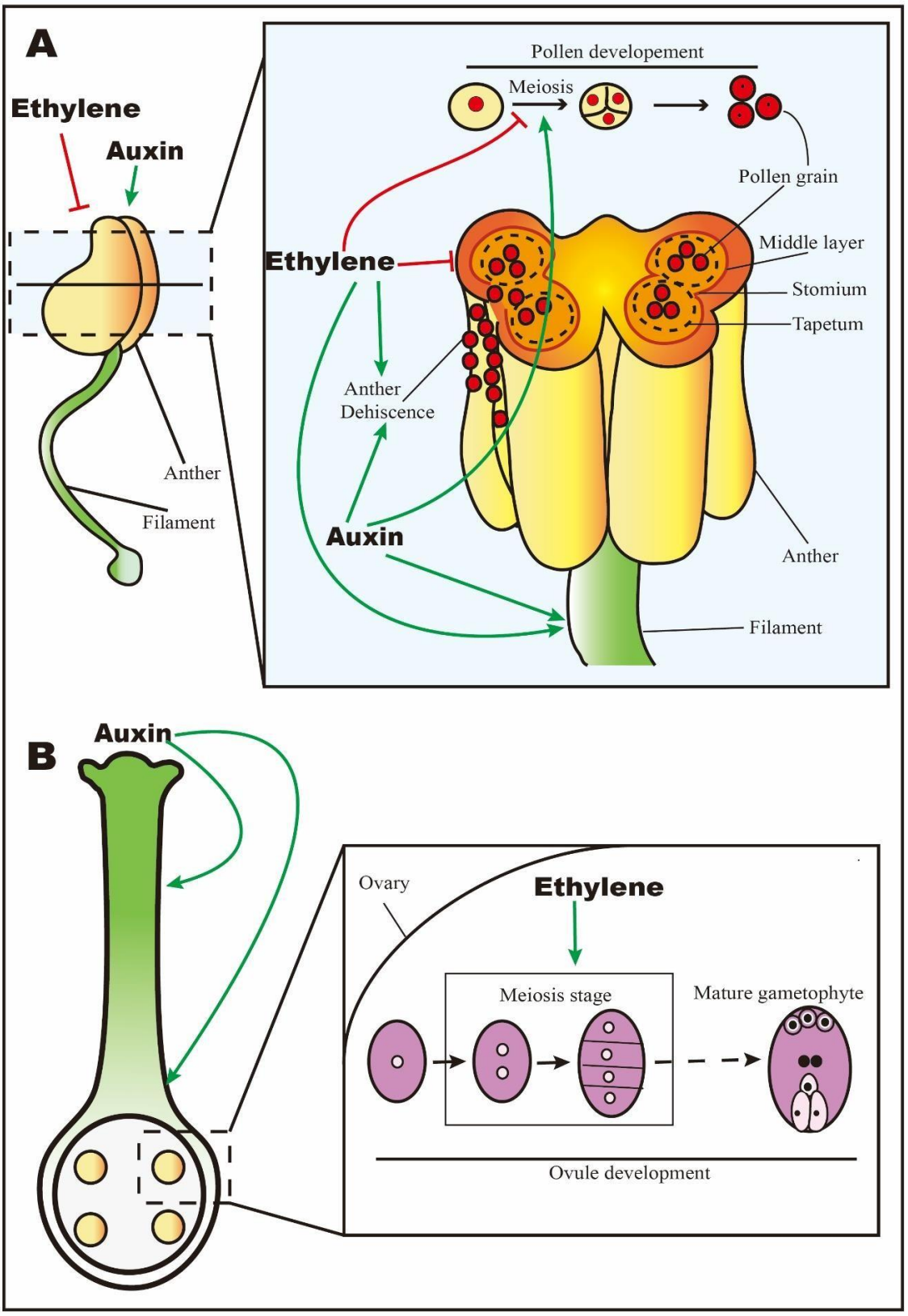
A
Ethylene
Auxin
Anther
Filament
Pollen developement
Meiosis
Pollen grain
Middle layer
Stomium
Tapetum
Ethylene
Anther
Dehiscence
Auxin
Anther
Filament
B
Auxin
Ovary
Ethylene
Meiosis stage
Mature gametophyte
Ovule development

Figure. 1. **Ethylene and auxin regulate the development of plant male and female organs**. Green lines stand for positive regulations. Red lines stand for negative regulations. **(A) Ethylene and auxin regulate stamen formation and development.** This panel illustrates ethylene and auxin roles detailed in the 2.1 paragraph. Briefly, ethylene and auxin participate in pollen formation and development, and play important roles at the meiosis stage; ethylene induces the programmed cell death (PCD) of the tapetum and middle layer, which leads to anther dehiscence and pollen release; auxin may induce anther dehiscence; ethylene and auxin may promote filament elongation. **(B) Ethylene and auxin regulates pistil formation and development.** This panel illustrates ethylene and auxin roles detailed in the 2.2 paragraph. Briefly, ethylene induces the early stage of ovule development; auxin synthesis in apical domain of gynoecium plays an important role in style and ovary formation.

2.2. Female reproductive organs

In female reproductive organ, the pistil (Figure 1B) provides protection for the ovules, enables pollen capture and pollen tube guidance, and supports self- and inter-specific incompatibility. Following fertilization of the ovules, in true fruit, such as grape and tomato, the gynoecium develops into a fruit, which protects the developing seeds and ultimately facilitates mature seed dispersal; in false fruit, such as apple and pears, the fruit derives from other flower parts, after fertilization (Ferrándiz *et al.*, 2010). Gynoecium development involves the differentiation of specialized functional modules, including the stigma which forms at the apex of pistil, and will capture and stimulate the pollen grain germination (Martínez-Fernández *et al.*, 2014). The style or pistil is located immediately below the stigma and contains transmitting tissues that conduct pollen tubes to the ovary, the basal structure containing the ovules (Martínez-Fernández *et al.*, 2014). The formation of normal and functional gynoecium is essential for female fertility, and hence for successful fruit set. The role of ethylene in female gametophyte development, and ultimately in promoting ovule fertilization, has been addressed in several studies (Martínez-Fernández *et al.*, 2014; Martinis and Mariani, 1999). Intobacco, the ethylene biosynthesis gene, *ACO*, is expressed during early stages of ovule development (meiosis stage), and its silencing results in the arrest of ovule development and failure to reach the maturity stage. Similar effect was obtained by the application of the ethylene

biosynthesis inhibitor, silver thiosulfate (Martinis and Mariani, 1999). Notably, upon exogenous ethylene treatment, the ovules recover their functionality and restore the guidance of pollen tubes to the ovule micropyle (Martinis and Mariani, 1999).

The role of auxin in female reproductive organ was revealed through the characterization of the *AGAMOUS*-clade of MADS-box genes showing that members of MADS-box B3 domain transcription factors *NGATHA* (*NGA1* to *NGA4*) play an essential role in style development; the loss-of-function of these four *NGA* genes results in complete loss of style and stigma development, and this phenotype is due to the failure of activating *YUCCA*-mediated auxin synthesis in apical domain of gynoecium (Trigueros *et al.*, 2009). These studies emphasize the role of auxin in apical-basal gynoecium pattern.

3. Ethylene and auxin regulate pollination-dependent fruit set

3.1. Pollen germination and tube growth

In plants, pollination refers to the release of the pollen from the anther and its deposition at the surface of the stigma (Figure 2A). When the pollen grain rehydrates and germinates on the stigma, the pollen tube starts to grow inside the style. The pollen grain contains a nucleus and a generative cell, which divides into two sperm cells (Edlund *et al.*, 2004). The pollen tube grows navigating through transmitting tissue in the style towards the ovule where it releases the sperm cells for double fertilization (Palanivelu *et al.*, 2003). The reality and the nature of the pollination signal remains a matter of debate, even though auxin, or ACC, have been proposed as the acting molecular signals (Whitehead *et al.*, 1983; Zhang & O'Neill, 1993). In petunia, the level of ACC increases 100 fold in mature pollen grain and in anthers one day before anthesis (Lindstrom *et al.*, 1999). In tomato, it was shown that pollen grain has the capacity to produce and sense ethylene before germination, as suggested by the expression of several ethylene biosynthesis and signaling genes including *SlACS3*, *SlACS11*, *SlETR3* and *SlCTR2* (Jegadeesan *et al.*, 2018a). Nevertheless, exogenous application of ACC in flowers cannot induce the post-pollination development (O'Neill *et al.*, 1993). When applying the synthetic auxin, NAA, to the stigma of orchids, the ethylene production was stimulated in flowers (Zhang & O'Neill, 1993). Although these findings support the idea that auxin and ethylene are

important for pollination initiation, other factors might also contribute to the regulation of this process.

It was suggested that auxins regulate pollen germination (Wu *et al.*, 2008a; Aloni *et al.*, 2006). In support to this hypothesis, IAA accumulates at high levels in the stigma when most pollen grains germinate (Chen and Zhao, 2008) and, free IAA is high in the growing tip of the pollen tube where it was suggested to promote rapid pollen tube growth (Aloni *et al.*, 2006). It has also been reported that IAA treatment results in straighter and more slender pollen tube growth which facilitates its elongation (Wang *et al.*, 1996; Wu *et al.*, 2008b). Notably, plasma membrane H^+ ATPase has been shown to interact with 14-3-3 proteins, an interaction that is important for pollen germination (Pertl *et al.*, 2001). However, when the pollen tube enters the style, the amount of auxin decreases in the style tissues (Chen and Zhao, 2008).

The growth and elongation of the pollen tube is essential for successful fertilization and subsequent fruit set since it carries two male gametes to the ovary and ovule over a long distance in the pistil (Figure 2B). The transmission tissues in the style play an important role in providing nutrition and mechanical support for pollen tube growth and, after pollination, transmission tissues begin to be malformed and deteriorate, which could provide nutrition to surrounding tissues (Wang *et al.*, 1996). In addition, the cellular degeneration of transmission tissues in the style provides more space, allowing the penetration of the pollen tube in the stigma. This degeneration facilitates the passage of pollen tube in the style to reach the ovary, and these events are considered as a programmed cell death process (Wang *et al.*, 1996). Several studies have shown the important role of ethylene in pollen tube growth (Kovaleva and Zakharova, 2003; Holden *et al.*, 2003). Both ACC and ethylene have a role in the degeneration of transmitting tissues, by promoting the shortening of the polyA tail of some RNAs specific to these transmitting tissues (Wang *et al.*, 1996). On one hand, the treatment with 1-MCP reduces pollen tube growth in petunia (Holden *et al.*, 2003). On the other hand, it was shown that ethylene promotes pollen tube growth by increasing the relative amount of F-actin, which is important for the polarized growth of this tube (Jia *et al.*, 2018). Upon pollination, the increase

in ethylene production reaches a maximum in the stigma and is associated with enhanced expression of *ACS* and *ACO* genes in the ovary. By contrast, control emasculated flowers did not exhibit such a change in ethylene production (Llop-Tous *et al.*, 2000). In orchid gynoecium, *ACS* and *ACO* genes reach an expression peak 24 to 48 hours after pollination, and then decline (O'Neill *et al.*, 1993), and similar expression patterns for *ACS* or *ACO* were observed in petunia and carnation (Tang and Woodson, 1996).

3.2. Changes to ovary development

The presence of auxin and ethylene is required to initiate changes in ovary development and to induce ovule differentiation (Figure 2C). It has been found that following pollination with fresh pollen, enhanced ethylene synthesis and auxin transport are necessary to initiate the egg cell differentiation in maize ovules (Mól *et al.*, 2004). Before fertilization, auxin production is suppressed by FIS-PRC2 in the central cell, and this suppression is released upon fertilization. In *fis* mutants impaired in the FIS-PRC2 block system, auxin biosynthesis is induced before fertilization and initiates autonomous endosperm formation (Figueiredo *et al.*, 2015).

In flowering plants, when the pollen tube reaches the ovule, two male sperm cells are released to fuse with two female gametes, the egg cell and the central cell (Figure 2D). The fused egg cell will develop into an embryo, and the fused central cell will give the endosperm, which provides nutrition and support to embryo (Berger *et al.*, 2008). The two synergids are responsible for pollen tube attraction, but only one pollen tube will fertilize the ovule (Maruyama *et al.*, 2015). Recent studies demonstrate that ethylene signal is critical to prevent the attraction of a second pollen tube and it was shown that egg cell fertilization induces the activation of EIN3- and EIN2-dependent ethylene response pathway necessary for the programmed cell death of the synergid cell (Völz *et al.*, 2013). In addition, the over-accumulation of EIN3 in synergid cells leads to the block of pollen tube attraction (Zhang *et al.*, 2018). Auxin has been suggested to regulate maize endosperm proliferation. A study in the maize mutant *defective endosperm18 (de18)* showed that IAA biosynthesis is impaired and the total cell number is lower in the endosperm, and the level of endoreduplication of the endosperm is reduced (Bernardi *et al.*, 2012).

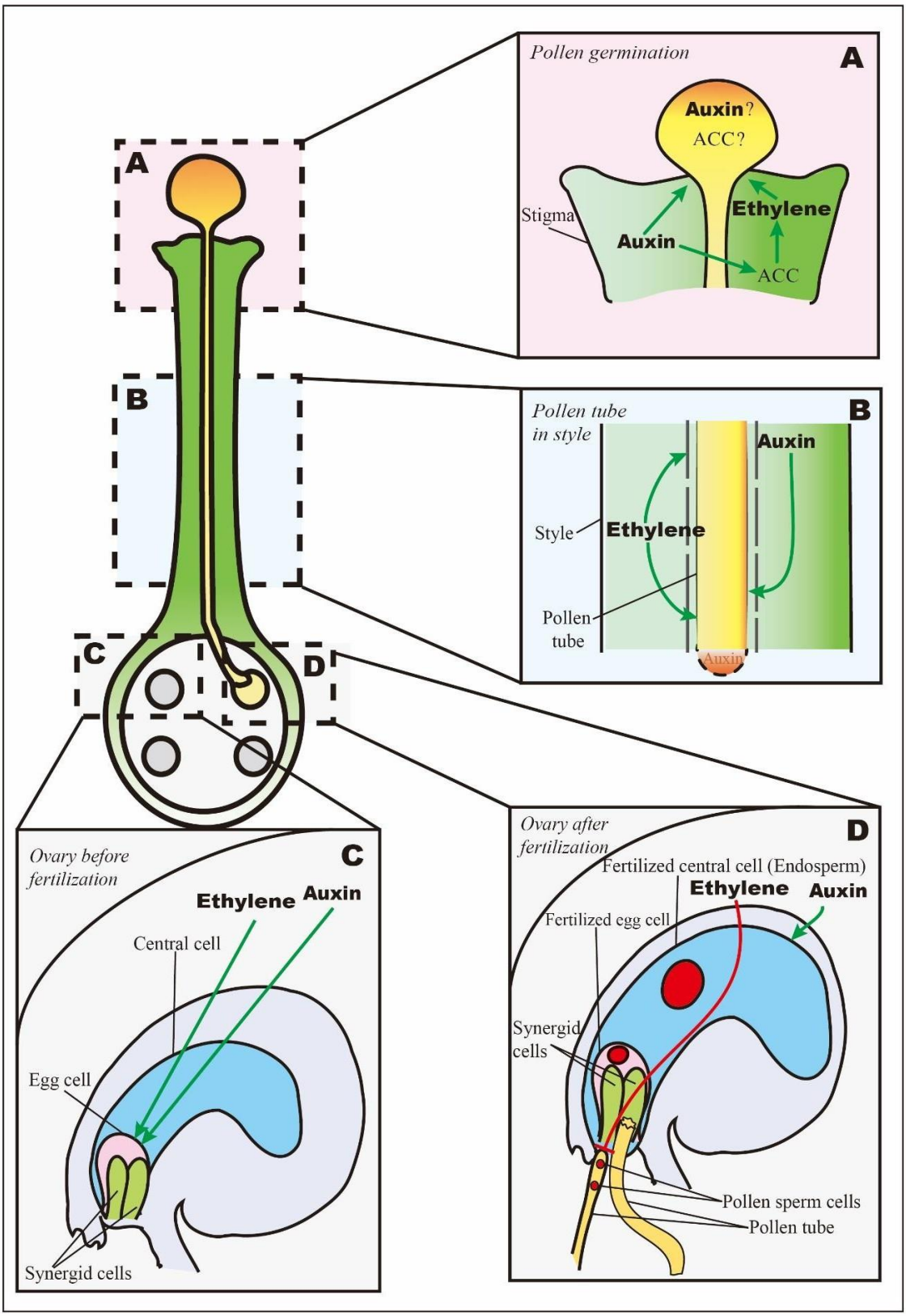
A
B
C
D
Pollen germination
A
Auxin?
ACC?
Stigma
Auxin
Ethylene
ACC
Pollen tube
in style
B
Auxin
Style
Ethylene
Pollen
tube
Auxin
Ovary before
fertilization
C
Ethylene
Auxin
Central cell
Egg cell
Synergid cells
Ovary after
fertilization
D
Fertilized central cell (Endosperm)
Ethylene
Auxin
Fertilized egg cell
Synergid
cells
Pollen sperm cells
Pollen tube

Figure 2. Ethylene and auxin regulate plant pollination and fertilization process. Green lines stand for positive regulations. Red lines stand for negative regulations. ***(A) Pollen germination.*** This panel illustrates ethylene and auxin roles detailed in the 3.1 paragraph. Briefly, mature pollen grain contains ACC and auxin, which may induce pollen germination; ethylene and auxin both induce pollen germination in stigma, and auxin stimulates ACC synthesis. ***(B) Pollen tube growth in style***. This panel illustrates ethylene and auxin roles detailed in the 3.2 paragraph. Briefly, ethylene helps degradation of transmission tissues in the style, which facilitates pollen tube growth. Auxin accumulates in the tip of pollen tube, and this facilitates pollen tube growth. ***(C) Ovary before fertilization.*** This panel illustrates ethylene and auxin roles detailed in the 3.2 paragraph. Briefly, the increase of ethylene and auxin concentrations are necessary to initiate egg cells differentiation in ovules after pollination.
(D) Ovary after fertilization. This panel illustrates ethylene and auxin roles detailed in the 3.2 paragraph. Briefly, ethylene promotes programmed cell death of synergid cell, which prevents second pollen tube attraction; auxin is important for endosperm development, especially in endoreduplication.

4. Ethylene and auxin roles in parthenocarpy

Parthenocarpy corresponds to the ovary development in the absence of pollination and fertilization (Varoquaux *et al.*, 2000). In this regard, it is considered as a desirable agronomic trait to improve fruit set in adverse climate conditions. In addition, the seedless fruits due to parthenocarpic development are preferred by consumers (Varoquaux *et al.*, 2000). It has long been known that applying synthetic phytohormones like auxin and gibberellic acid (GA) to unpollinated flower buds induces parthenocarpic fruit set (Sjut and Bangerth, 1982). However, exogenous application of plant hormones to get seedless fruits is costly, thus genetic engineering strategies are promoted, aiming at altering hormone biosynthesis or signaling in order to obtain parthenocarpic fruits. Pioneering work, in this domain, targeted the up-regulation of the *iaaM* gene to promote the synthesis of indolacetamide, which can be converted to IAA (Rotino *et al.*, 1997). The expression of this auxin biosynthesis gene, driven by the

promoter of *DefH9*, a MADS-box gene expressed specifically in ovules, resulted in parthenocarpic fruit development in both tobacco and eggplant (Rotino *et al.*, 1997). Thereafter, the same gene was used to obtain parthenocarpic fruit in several horticultural crops, like tomato and cucumber (Plcader *et al.*, 2006). Another successful approach to produce parthenocarpic fruit dealt with the down-regulation of *SlIAA9,* encoding a negative regulator of auxin-dependent gene transcription (Wang *et al.*, 2005). Subsequently, the parthenocarpic trait was also achieved through up or down-regulation of members of auxin response factors in different species (Goetz *et al.*, 2006). In Arabidopsis, the loss of function mutation of *AtARF8* produced dehiscent and parthenocarpic siliques (Goetz *et al.*, 2006). In tomato, the down-regulation of *SlARF8* and *SlARF7* formed parthenocarpic fruit, and the over-expression of *SmARF8* in eggplant produced the same seedless trait (Du *et al.*, 2016; Goetz *et al.*, 2007; Jong *et al.*, 2011). Overall, auxin biosynthesis and signaling genes provide efficient targets to engineer parthenocarpic plants in a variety of species.

Most studies showed that ethylene acts as a negative regulator of parthenocarpy in plants (Carbonell-Bejerano *et al.*, 2011). For example, in Arabidopsis, ethylene is responsible for ovule senescence by preventing GA perception; hence, ethylene indirectly leads to the degradation of ovule tissues, thus reducing parthenocarpic fruit set (Carbonell-Bejerano *et al.*, 2011). On the other hand, preventing ethylene perception in emasculated flowers of tomato, either by using 1–MCP, or by using ethylene insensitive mutants (*etr1-1*), led to more parthenocarpic fruits (Shinozaki *et al.*, 2015). Similarly, blocking ethylene synthesis, by using 2-aminoethoxyvinyl glycine, or blocking ethylene perception, by using silver thiosulphate, induced parthenocarpy in zucchini squash (Martínez *et al.*, 2013).

To date, there is no study focusing on the crosstalk of auxin and ethylene during parthenocarpic fruit set.

5. Conclusions and perspectives

A large set of data supports the notion that both ethylene and auxin play active roles in controlling the fruit set process, at different steps of the flower-to-fruit transition. But there is a

need for research to detail the potential crosstalk between auxin and ethylene signals in the control of this transition. The two hormones impact all stages of stamen development, including elongation of stamen filament bringing anthers close to stigma, pollen maturation, and anther dehiscence to release pollen on stigma. Proper completion of these events is critical to the formation and development of reproductive sexual organs and then to successful initiation of the fruit set process (Kumar *et al.*, 2013). Ethylene and auxin are also involved in most events associated with the germination of pollen in the stigma, the growth of pollen tube through the transmission tissues in the style and finally the fertilization of the ovule. The use of mutant lines impaired in both auxin and ethylene responses will allow to better decipher the roles of auxin and ethylene in initiating and controlling the flower-to-fruit transition. By building on studies about crosstalk in other developmental processes, like root formation and hypocotyl elongation (Růzicka *et al.*, 2007), future research will allow to further detail the dialogue engaged between the two hormones in the different phases of the fruit set. For example, it was shown that mutants altered in AUX1 and EIR1/AGR/PIN2 with impaired auxin transport, and those affected in TIR1 auxin receptor, exhibit ethylene insensitive root growth, which supports the idea of interdependence of both hormones (Luschnig *et al.*, 1998; Muday *et al.*, 2012). More recently, it was reported that ERF109 binds directly to the promoters of *ASA1* and *YUC2* auxin biosynthesis genes, and ERF1 could bind with the promoter of *ASA1*, leading to auxin increase and ethylene-induced root growth inhibition (Cai *et al.*, 2014; Mao *et al.*, 2016). Similarly, the expression of *Sl-IAA27* is regulated by direct binding of ERF.B3 to its promoter (Liu *et al.*, 2018). The regulation of *ACS* expression by ARFs, and of *TAA1* by EIN3 have been documented (Robles *et al*., 2013) . Finally, the impaired expression on *SlSAUR69* in the tomato results in altered auxin distribution and change in ethylene sensitivity (Shin *et al.*, 2019). All these examples should lead to new studies about potential ethylene and auxin crosstalks in fruit set. These studies should cover the parthenocarpic fruit formation, which is becoming an important trait, offering a mean to ensure yield stability in unfavorable environmental conditions, these latter reducing pollen viability and depressing flower fertilization. Additionally, the epigenetic control is an emerging theme in developmental biology and its contribution to the fruit set process needs to be unveiled. It is therefore important to investigate

how epigenetic components impact the transcriptomic reprogramming underlying different steps of fruit set. Finally, while the present review emphasizes the role of ethylene and auxin in fruit set, input from gibberellins is also critical to control this process (Serrani *et al.*, 2008; Jong *et al.*, 2011). Thus, it will be interesting to expand the crosstalk studies to such hormones.

Chapter II: Ethylene signaling modulates tomato pollen tube growth, through modifications of cell wall remodeling and calcium gradient

(Published in Plant Journal by Althiab-Almasaud et al., 2021)

The supplementary data of this chapter have been placed in Annex I

Ethylene signaling modulates tomato pollen tube growth, through modifications of cell wall remodeling and calcium gradient

Abstract

Ethylene modulates plant developmental processes including flower development. Previous studies have suggested ethylene participation in pollen tube (PT) elongation, and both ethylene production and perception seem critical at fertilization time. The full gene set regulated by ethylene during PT growth is unknown. To study this, we used various EThylene Receptors (ETRs) tomato mutants: *etr3-ko*, a loss-of-function (LOF) mutant; and *NR* (*Never Ripe*), a gain of function (GOF) mutant. The *etr3-ko* PTs grew faster than its wild type, WT. Oppositely, *NR* PT elongation was slower than its wild type, and PTs displayed larger diameters. *ETR* mutations created feedbacks on ethylene production. Furthermore, the ethylene treatment of germinating pollen grains increased PT length in *etr-ko* mutants and WT, but not in *NR*. Treatments with the ethylene perception inhibitor, 1-MCP, decreased PT length in *etr-ko* mutants and wild types,but had no effect on *NR*. This confirmed that ethylene regulates PT growth. The comparison ofPT transcriptomes in LOF and GOF mutants, *etr3-ko* and *NR*, both mutated on the *ETR3* gene, revealed that ethylene perception has major impacts on cell wall- and calcium-related genes as confirmed by microscopic observations showing a modified distribution of the methylesterified homogalacturonan pectic motif and of calcium load. Our results establish links between PT growth, ethylene, calcium and cell wall metabolisms, and also constitute a transcriptomic resource.

1. Introduction

The human population growth and increasing food demand make food security a priority for the future (Gustavsson et al., 2011). Therefore, research on plant reproduction is critical for increasing crop productivity and fruit/seed yields. Sexual plant reproduction starts with pollen grain landing onto the stigma where it hydrates and starts to germinate; then, the pollen tube

(PT), carrying the two sperm cells, grows rapidly through the style and the ovary (Figure S1), to reach the ovule where the fertilization takes place (An et al., 2020). PT elongation is essential for fertilization (Michard., *et al.*, 2017). Many studies suggested that ethylene participates in this process (An et al., 2020). For example, a few hours after the penetration of PTs in the tomato stigma, a burst of ethylene was detected in the pistil (Llop-Tous *et al.*, 2000). Ethylene signaling starts with the binding of ethylene to specific receptors (Chang, 2016, Binder, 2020). In tomato, there are seven EThylene Receptors (ETRs), *Sl*ETR1-7, which are located in the endoplasmic reticulum, and their amount varies over plant development (Chen *et al.*, 2020a). ETRs are negative regulators of ethylene responses. In absence of ethylene, they maintain the downstream signaling partners in a "OFF" status, but in presence of ethylene their phosphorylation level changes and this turn "ON" the signaling partners (Bisson and Groth, 2015; Chang, 2016; Binder, 2020).

Some studies have highlighted the critical role of ethylene perception in PT elongation. For example, in *Petunia inflata*, ethylene perception was shown to be correlated with PT elongation (Holden et al., 2003). Indeed, the treatment with 1-MethylCycloPropene (1-MCP), an ethylene perception inhibitor, led to a strong inhibition of PT growth during the first six hours after pollination. Besides, Jia et al. (2018) have observed that ethylene promotes PT growth by interacting with cyclic Guanosine MonoPhosphate (cGMP) in *Arabidopsis thaliana*, thus leading to an increased number of actin filaments in PTs, which are important for their polarized growth. Moreover, in an ethylene-insensitive mutant (*etr1-1*), PT growth was reduced (Jia et al., 2018).

During PT growth, a number of cell wall components like pectins, cellulose, hemicelluloses and callose are required to build up the cell wall architecture (Mollet *et al.*, 2013). Pectins constitute a major component of the PT apical region, and the pectin methylesterase (PME) activity is critical for PT growth (Bosch, 2005). During fruit ripening, ethylene was shown to

modulate the expression of genes encoding cell-wall modifying enzymes such as *PMEs* and polygalacturonases *(PGs)* (Brummell, 2006). PGs are also known to be critical for PT growth (Dearnaley and Daggard, 2001). But a clear link between ethylene and cell wall remodelling during PT growth is yet to be demonstrated.

PT elongation, morphology, and orientation have been shown to be highly dependent on ions choreography. Namely, the combination of potassium, chloride, calcium and proton gradients play crucial roles in the development of pollen grains (Michard et al., 2017). Tip-focused Ca^{2+} gradients generated by the interplay of Ca^{2+} pumps and channels are observed during PT elongation and are correlated with pulses in growth rate (Zheng *et al.*, 2019). The link between Ca^{2+} and ethylene has been reported, in other organs than flowers. It was found that Ca^{2+} is required for ethylene biosynthesis (Jung *et al.*, 2000; Petruzzelli *et al.*, 2003; Li *et al.*, 2018). Moreover, it was shown that ethylene could enhance the endogenous Ca^{2+} concentration in tobacco cell suspension cultures by activating a plasma membrane Ca^{2+}-permeable channel (Zhao *et al.*, 2007). A recent study has shown that exogenous application of Ca^{2+} to root tissues was able to down-regulate the expression of *ETR* genes, and up-regulate gene expression of downstream elements of the ethylene signaling pathway (Yu *et al.*, 2019).

In the present study, we aimed at investigating the role of ETRs during PT growth in tomato. After identifying the main *ETRs* expressed during PT growth, we studied the effects of mutations affecting *ETRs* with opposite effects, a loss-of-function (LOF) mutation in the *etr3* mutant, and a gain-of-function (GOF) mutant carrying a constitutive functional ETR (*NR*, for *NEVER RIPE*). A RNA-seq comparative study between *etr3-ko*, *NR* and their respective wild-types, led us to focus on Ca^{2+} signaling- and cell wall-related genes, and on pectin remodeling to understand the observed phenotypes. In this study, we show links between metabolisms related to ethylene, calcium and cell wall during PT growth.

2. Material and methods

2.1 Plant material and growth conditions

Tomato lines (*Solanum lycopersicum* cv MicroTom): the *etr3-ko* and *etr4-ko* mutant lines were generated in our laboratory using the CRISPR-Cas9 technology, as described (Chen et al., 2020a), these *ko* lines are Loss-Of-Function (LOF). Briefly the sgRNAs "GAATCCTGTGATTGCATTGAGG" and "GCGATGTAACTGTGATGATGAGG" were designed to knock out *ETR3* and *ETR4*, respectively. The *etr3-ko* used in this study has an adenine missing at the 4th position before the PAM (protospacer adjacent motif) resulting in a frameshift mutation. For *etr4-ko*, a guanine was deleted at the 4th position before the PAM. The comparisons of the amino acid sequences of the mutated ETR proteins in *etr3-ko* and *etr4-ko* to their wild types are shown in Figure S8. Unfortunately, we did not succeed in the mutagenesis of *ETR5*. WTB and *NR* mutant lines were obtained from the L.E. Pereira Peres laboratory (Carvalho *et al.*, 2011), the *NR* line is a Gain-Of-Function line (GOF), due to a point-mutation in *ETR3*. All lines are MicroTom cultivar, but WTB and *NR* might have evolved slightly differently over the last 20 years since they were distributed by the Avi Levy's laboratory (Weizmann Institute, Israel). Thus, we used two wild-type lines, WT and WTB. WT is the wild type we used in the laboratory over the last 20 years, with which we performed the CRISPR-Cas9 constructs for *etr-ko*. In WTB, the "B" stands for Brazil. Plant sowing and growing conditions are detailed in Chen et al. (2020a).

2.2 In vitro pollen grain germination assay

For germination assays, pollen was sampled from flowers at one and two days post-anthesis (DPA) (Figure S9), at second and third positions of flower clusters. Pollen grains from 10 anthers were collected in 1.5 mL centrifuge tubes using an electric toothbrush body (Oral-B, France). The germination medium (GM) as in Firon *et al.*, (2012), containing 0.5 % (w/v) agarose or not. Pollen grains were spread over solid GM or suspended in 0.5 mL of liquid GM, and incubated at 25°C for various times in the dark. Images were acquired with an inverted microscope (Leitz DMIRB, Leica Microsystems, Germany) equipped with a 10M pixel CMOS camera (MC 190HD, Leica), with a 10x/0.22NA NPLAN objective (Leica). PT length and

diameter were measured with ImageJ (Abràmoff *et al.*, 2004). The lanthanum was applied at 50 µM $LaCl_3$ in liquid GM as described in Qu *et al.*, (2016).

2.3 Ethylene and 1-MCP

Pollen grains were spread on solid GM as described above, the Petri dishes were sealed with an electric tape, and ethylene or 1-MCP were injected in the headspace at the desired concentration, and incubated for 4 h before germination or PT length measurements. Preliminary experiments were performed to validate optimal concentrations, as in (Figure S7). Endogenous ethylene measurements by PTs were performed by sampling the headspace in a 2 mL brown glass vials containing around 10 mg of pollen grains in 0.5 mL of liquid GM, 4 h after imbibition, and analysing the headspace gas sample as previously detailed (Chen., *et al.*, 2020b). A vial with GM only was used as control. Numbers of pollen grains per µL were assessed by microscopy.

2.4 RNA extraction and RT-qPCR

Pollen grains (20 mg) were suspended 0.5 mL of liquid GM. After 4 h of germination at 25°C in the dark, PTs were centrifuged at 16,000 *g* for 5 min. The supernatant was removed and the pellet was frozen into liquid nitrogen and stored at -80°C. Samples were ground with a ball grinder using Tissue Lyser II (Qiagen, France) for 1 min. The pollen powder (20 mg) was used to extract total RNA using the ReliaPrep™ RNA Tissue Miniprep System kit (Promega, France) and treated with DNase I (Invitrogen, France). RT-qPCR analyses were performed as described (Chen et al., 2020a). Primers are listed in Table S1. *ETR6* transcripts were always below detection threshold. Thus, *ETR6* was not used in correlation analysis between RNA-seqreads and RT-qPCR results.

2.5 RNA-seq analyses

For each line (WT, WTB, *etr3-ko* and *NR),* four biological replicates were prepared, and RNA quality was checked on Agilent 2100 Bioanalyzer System, using the RNA 6000 Nano kit protocol (Agilent Technologies, Germany). RNA samples with RNA Integrity Number (RIN)

values greater than 7.5 were sent to the GENEWIZ company (Germany) for sequencing (standard service, 2x150bp, HiSeq Illumina Platform). Raw sequenced reads were treated using the pipeline described in Figure S10, implemented inside a data-driven computational pipeline called NextFlow (Tommaso *et al.*, 2017): raw sequenced reads in Fastq format were cleaned after quality check using fastQC version 0.11.05 (Andrews, 2010). To use only high-quality sequences, reads were cleaned by removing all left sequencing adaptors and by trimming low quality bases. This step was made using Trim Galore 0.6 (http://www.bioinformatics.babraham.ac.uk/projects/trim_galore/), a wrapping tool based on Cutadapt (Martin, 2011). Cleaned sequences were mapped to a new and improved reference tomato genome produced and assembled by the GBF lab with the annotation Slmic1.1 (http://tomatogenome.gbfwebtools.fr/) using STAR 2.5.1b, a spliced-aware mapper (Dobin *et al.*, 2013). The mapping parameters took into account each library size when paired-end sequencing was performed. Finally, featureCounts 1.6.0 (Liao *et al.*, 2014) was used to calculate read counts for each gene from the mapping file. The homologies between Slmic 1.1 (Sly nomenclature) and ITAG 2.4 (Solyc) annotation (https://solgenomics.net/organism/Solanum_lycopersicum/) is available at http://tomatogenome.gbfwebtools.fr/correspondence, and in Table S3A. The homologies between Slmic 1.1 and ITAG 4.1 are available in Table S3B, and all RNA sequences are available from the European Nucleotide Archive, accession number E-MTAB-9660.

2.6 Differential expression and downstream analyses

Without *a priori* knowledge of gene expression variances, we optimized our experimental design with four biological replicates for each condition of interest (Lamarre *et al.*, 2018). Differential expression (DE) analysis was performed with R software using DESeq2 package with default Relative Log Expression (RLE) normalization method, encompassing biases caused by library size and relative size of transcriptomes (Love *et al.*, 2014; Maza *et al.*, 2013; Maza, 2016). False discovery rate was limited by using a threshold for adjusted p-values equal to 0.05 (Benjamini and Hochberg, 1995). To visualize distances between samples, a PCA of

normalized expressions was performed with plotPCA function (DESeq2 package), to check the homogeneity of the biological replicates and relative distances between conditions. The RLE normalization method used in DESeq2 for the DE analysis, considering that transcripts have the same length in all conditions, do not normalize counts by transcript length. Thus, normalized counts generated by DESeq2 need to be normalized by transcript length to allow comparison between transcript levels within a condition. Then, DESeq2 normalized samples were multiplied by 100 (rough magnitude of read lengths, in bp) and divided by the transcript length(in bp). Finally, the mean of the biological replicates for a given condition was calculated. Thismean relates to the number of transcripts produced in this condition (Zouine *et al.*, 2017). Venn diagrams were generated with JVENN software (http://jvenn.toulouse.inra.fr/app/example.html). The RNA-seq results are available in Table S3.

The MAPMAN annotation (https://mapman.gabipd.org/mapman) and the *ProtAnnDB* (http://www.polebio.lrsv.ups-tlse.fr/ProtAnnDB/) tools were used to identify functional categories of genes and to determine genes that could be related to calcium signaling and cell wall modification. TAIR 11 annotation was selected to search for homologous genes in *Arabidopsis* by using BLAST+ tool, version 2.9.0. The calcium signaling-related genes are listed in Table S5. The proteins predicted to be secreted and having no more than one transmembrane domain and no intracellular retention signal have been selected as cell-wall related proteins (Table S4). They have been named following the nomenclature of *WallProtDB*, a database dedicated to cell wall proteins identified in cell wall proteomes (San Clemente and Jamet, 2015) and the CAZy database (http://www.cazy.org/).

2.7 Pectin immunolabeling and PME activity measurement

The immunolabeling was performed as described (Hocq *et al.*, 2020). Briefly, after 4 h of growth in liquid GM, PTs were treated with a fixation medium: 100 mM PIPES, 4 mM $MgSO_4$, 7 H_2O, 4 mM EGTA, 10% (w/v) sucrose, and 5% of paraformaldehyde pH 7.5 and stored at 4°C until use. The fixed PTs were centrifuged at 4,000 *g* for 7 min and washed 3 times with

250 µL PBS, pH 7.4, incubated in a blocking solution (PBS containing 3% fat-free milk) for 30 min at room temperature. After three washes, PTs were incubated overnight with the primary antibody, LM19 or LM20, for weakly or highly methylesterified HGs, respectively (PlantProbes, http://www.plantprobes.net/) (Verhertbruggen *et al.*, 2009) at 1:5 dilution in PBS at 4°C in the dark. After washing the pellet 3 times, it was incubated for 3 h at 30°C in the dark with the secondary Alexa488 anti-rat antibody at 1:50 dilution in PBS, followed by 3 washes with PBS. Controls were incubated with the secondary antibody only. Images were acquired with a Leica DMI6000 B inverted microscope equipped with DFC 450C camera and LAS V3.8 software. Alexa488 was detected with a filter cube L5, λ excitation at 460-500 nm and λ emission at 510–540 nm. All the samples were observed at the same exposure time.

For PME assays, the protein extraction from PT was carried out with 2M NaCl buffer according to Baldwin et al. (2014). After desalting, protein concentration was measured with the Bradford assay (Bio-Rad, France). The total PME activity was assayed according to Baldwin et al. (2014) by quantifying the amount of methanol released from citrus pectin with a degree of methylesterification > 85% (Sigma-Aldrich, France). The mean ± SD of PME activity is from 3 biological replicates.

2.8 Intracellular calcium detection and imaging

Intracellular Ca^{2+} was detected using Fluo-4 AcetoxyMethyl ester (Fluo-4/AM, Invitrogen, USA) as described (Qu *et al.*, 2016) with the following adjustments. Stock aliquots of fluo-4/AM were made of 50 µg fluo-4/AM dissolved in 91.2 µL anhydrous dimethyl sulfoxide solution, stored at -20°C. PTs were imbibed for 1 h in liquid GM at a concentration of 8×10^5 cells·mL^{-1}, treated with a final concentration of 1 µM fluo-4/AM, and incubated for 30 min at 22° C in the dark. Images were acquired with CLSM confocal microscope Leica SP8, driven by LAS X software, with water immersion objective 25x/0.95. Fluo-4/AM was excited at 488 nm and fluorescence was collected on photomultiplier between 500 and 690 nm. Images were acquired on one plan, every 2 s for a 30 min total duration. The maximum fluorescence intensity

observed over the time course, for one PT apex, was selected for quantification with ImageJ (Abràmoff et al., 2004), using the mean grey value, over a constant area, shown in figures with a yellow dashed line. The mean of maximum fluorescence of 10 individual PTs for each genotype was measured.

2.9 ACCESSION NUMBERS

All RNA-seq data were deposited in the European Nucleotide Archive under the accession number E-MTAB-9660.

3. Results

3.1 Expression of ETRs in germinating pollen grains

In WT PTs, we observed that *ETR3, ETR4*, and *ETR5* were the *ETR* genes with the highest expression levels 4 h after pollen imbibition, without significant differences between them (Figure 1A). *ETR1*, *2* and *7* were expressed at significantly lower levels, and *ETR6* transcripts were below the detection threshold. A preliminary experiment showed that 4 h after imbibition was the optimum time at which we were able to collect a sufficient amount of raw material and extract total RNA of good quality, with PTs being still in a linear phase of growth (Figure S2). In the following parts, we will focus on *etr3,* since we have LOF and GOF mutants for this gene, in the search for changes in gene expression between the two mutant types, to reveal the metabolisms driving PT growth under ETR control. Moreover, ETR3 has been shown to be involved in PT growth (Jegadeesan *et al.*, 2018a).

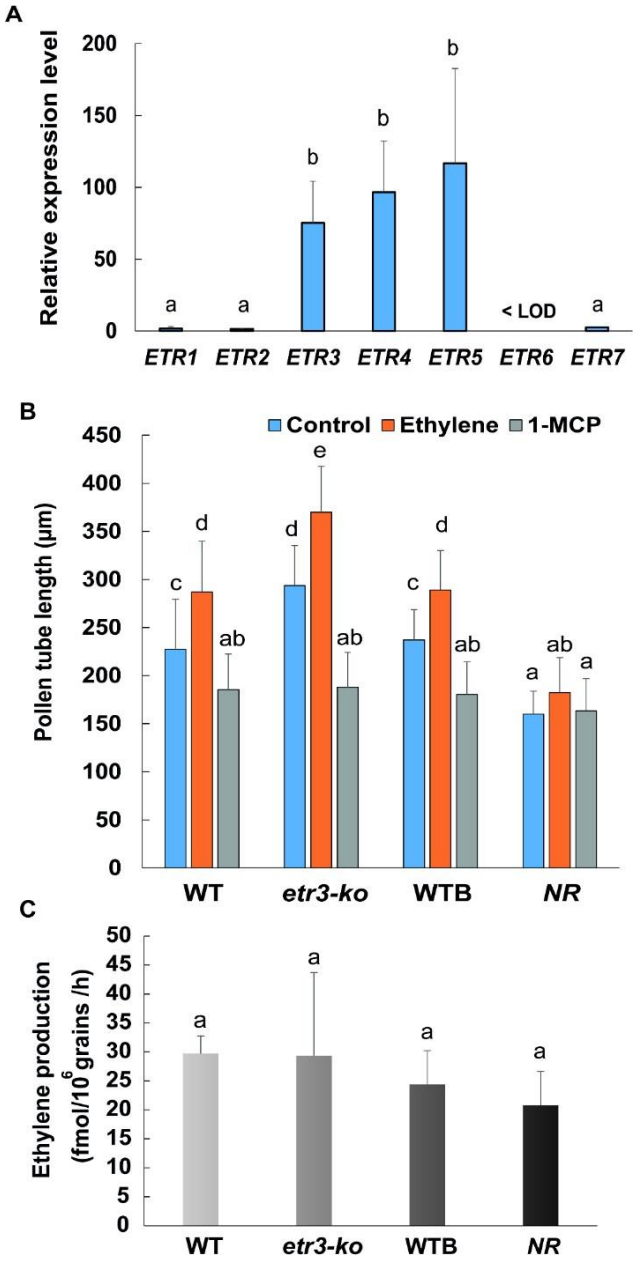

Figure 1. Regulation of germinating pollen grains by ethylene. (A) Expression levels of *ETR* genes in germinating tomato pollen grains. Total RNA was extracted from WT PTs 4 h after pollen harvest and imbibition, n = 4 biological replicates, LOD stands for lower limit of detection, Relative expression was calculated with regard to *ETR1*. The sequences of the gene-specific primers used for PCR are listed in Table S1. **(B)** PT length in WT, WTB, *NR* and *etr3-ko*, 4 h after pollen grain imbibition; and effects of 100 ppm ethylene and 2 ppm 1-MCP treatments on PT length. n = 90 PTs. **(C)** Ethylene production

by germinating pollen grains, 4 h after pollen grain imbibition, n = 6 biological replicates. For all panels, error bars show SE, different small letters indicate a significant difference between means at $P = 0.05$ (Tukey's HSD for panels A and B, Dunn's test for panel C).

3.2 ETRs modulate pollen tube growth, but not ethylene production by pollen tubes

To test whether ETRs modulate PT growth, we used two *ETR3* mutants: the *etr3-ko* line, a LOF mutant, and the *NR* line, a GOF mutant of *etr3*, and their corresponding wild types, *i.e.* WT and WTB, respectively (see Experimental Procedures for details). After 4 h of imbibition, PT growth was increased in *etr3-ko,* whereas PT growth was reduced in *NR* (Figure 1B). We observed a weak ethylene production by PTs, but without any significant difference between the tomato lines (Figure 1C). A similar stimulation of PT growth was also observed in another LOF affecting *ETR4*, *etr4-ko* (Figure S2A detailing growth kinetics), and in addition, we observed that the PTs of the *etr3-ko/etr4-ko* double mutant were growing faster than those of WT, but not significantly faster than those of *etr3-ko* or *etr4-ko* single mutants (Figure S2B).

3.3 Ethylene stimulates pollen tube growth, whereas 1-MCP inhibits it

We decided to check the impact of adding an ETR effector, the ethylene itself, or adding an ETR inhibitor, 1-methylcyclopropene (1-MCP) in the headspace above germinating pollen grains. In *etr3-ko*, and in both WT lines, the ethylene treatment stimulates PT elongation (Figure 1B). This was not the case in *NR*, which is ethylene-insensitive. On the contrary, the addition of 1-MCP limited PT growth in *etr3-ko* (Figure 1B), but no significant change was observed in both WT and *NR* lines. After showing that functional ETRs limit PT growth, an effect reversed by adding ethylene, we performed an RNA-seq experiment to look at changes in gene expression possibly driven by ETR signaling and impacting PT growth.

3.4 Transcriptome profiling of etr3-ko and NR pollen tubes

We compared the PT mRNAs of two *etr3* mutant lines, *etr3-ko* (*ETR3* LOF) and *NR* (*ETR3* GOF), and their respective WTs. Total RNA was extracted from PTs collected 4 h after pollen

grain imbibition. The overall quality of sequencing data was very good with a mean read quality of 35 (Illumina 1.9 encoding) (Figure S3A). A cleaning step was performed as 40.8% of the reads still had sequencing adaptors. After this step, more than 94% of the reads were mapped without ambiguity and less than 4 % were mapped at more than one location (Figure S3B). This showed a very good specificity of sequences confirmed by RNA-seq quantification. As shown in Figure S3C, more than 90% of sequenced reads were assigned to genes after the mapping process, making the analysis even more robust.

A principal component analysis (PCA), carried out on normalized RNA-seq counts, showed that the four biological replicates were well-clustered in the four conditions WT, WTB, *etr3-ko*, and *NR* (Figure 2A). This showed that all samples were of good quality, and that the biological variability was smaller than differences between the four conditions of interest. Moreover, the PCA revealed that the horizontal axis (first axis of the PCA), carrying 42% of the variability, discriminated the *NR* mutant from the three other conditions, which meant that *NR* was the condition creating the biggest differences. On the second axis carrying 26% of the variability, this PCA also underlined that both WT lines were close to each other. It could also be seen that *etr3-ko* was closer to WTs than *NR*.

There were 2452 Differentially Expressed Genes (DEGs) in *NR vs* WTB and 551 DEGs in *etr3-ko vs* WT (Figure 2B): 1131 were up-regulated genes in *NR vs* WTB, and 253 in *etr3-ko vs* WT, whereas the numbers of down-regulated genes were 1321 and 298, respectively. To validate the quality of the RNA-seq data by RT-qPCR analyses, we chose 15 genes, encoding proteins possibly impacting PT growth, and ranging from low to high expression levels in the RNA-seq experiment (Table S2). The chosen genes were associated to functions about ethylene perception or synthesis, or related to cell wall metabolism or calcium signaling. The data were generated with the same RNA samples as for the RNA-seq analysis. The values obtained from the four biological replicates were averaged, thus the correlation calculation between RNA-seq and RT-qPCR values was performed over 60 data points. The results showed a Pearson correlation coefficient of 0.864, a *P* value of $6.7\ 10^{-19}$ and a power of 1 (Table S2). These were good indicators of transcriptomic data quality. Because previous studies showed that tomato *ETRs* expression is altered in *ETR* mutants (Tieman et al., 2000, Chen et al., 2019), we checked if this was the case for the seven *ETRs* in PTs. The expression level of three *ETRs* was altered in the mutants: *ETR4* and *ETR5* were up-regulated in *NR*, whereas *ETR3* was down-regulated in *etr3-ko* (Figure 2C). These results were confirmed by RT-qPCR (Table S2). The expression of the other genes, tested in the qPCR check, did not reveal any trend or will be described below.

The full list of DEGs, genes with a $P < 0.05$, is available in Table S3. In the following part of the study, we focused on cell wall modification and calcium signaling based on the observation of DEG families (Figure 2D). This revealed that cell wall-related genes were up-regulated in *etr3-ko vs* WT and down-regulated in *NR vs* WTB, whereas calcium signaling-related genes were strongly down-regulated in *NR vs* WTB. The key genes attracting our attention, with opposite differences between GOF and LOF mutants were: pectin methylesterases (PMEs) involved in cell wall remodeling, and calcium-dependent protein kinases (CPKs), calcium-pumps (ACAs), and calcium channels (CNGCs) for calcium signaling. They will be detailed below.

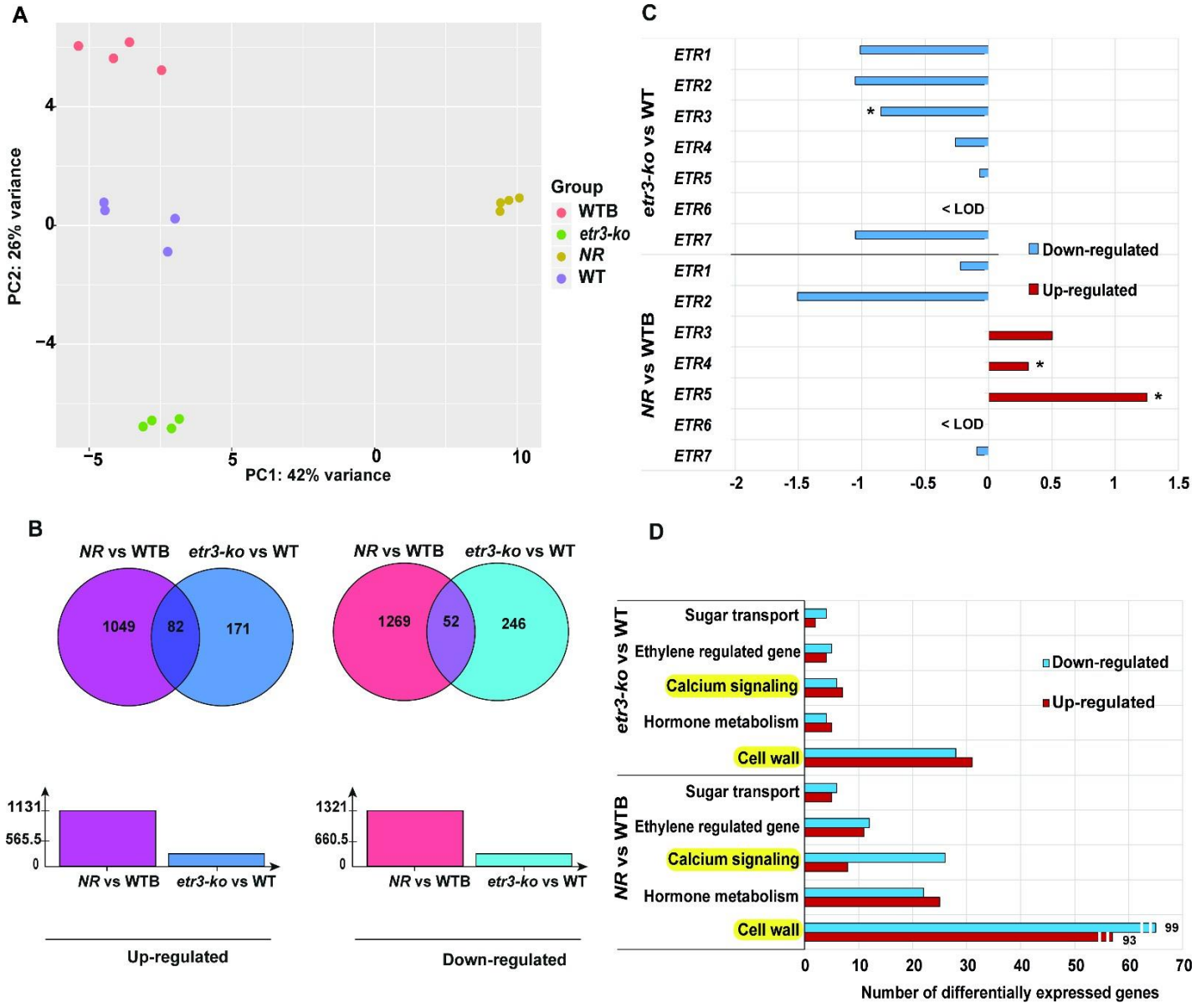

Figure 2. Transcriptome profiling of *etr3-ko* and *NR* PTs. (A) PCA of normalized samples. Axes 1 and 2 represent 68% of data information. Colored dots underline the four conditions of interest and the four biological replicates analysed by RNAseq. See Figure S3 for additional RNAseq quality indicators. (B) Venn diagrams showing the numbers of differentially expressed genes (DEGs) in *NR vs* WTB and *etr3-ko vs* WT, up-regulated DEGs, and down-regulated DEGs, base means of normalized counts > 5, and adjusted *P*-value <0.05. (C) *ETRs* are differentially expressed in *etr3-ko* and *NR*. Bar plot representing log2(fold change) shows differences in expression level between (i) *NR* vs WTB, and (ii) *etr3-ko vs* WT, * shows significant changes at $P < 0.05$ using Tukey HSD. (D) Functional classification of DEGs. The down-regulated genes are in blue (log2 fold change < 0, $P < 0.05$), and the up-regulated genes in red (log2 fold change > 0, $P < 0.05$). Four biological replicates were analyzed.

3.5 Transcriptomic analysis of the cell wall-related genes in etr3-ko and NR pollen tubes

In both comparisons (*NR vs* WTB and *etr3-ko vs* WT), around 10% of genes showing modified transcript levels encode proteins involved in cell wall protein or polysaccharide biosynthesis, in signaling at the plasma membrane interface or in cell wall metabolism, *e.g.* cell wall polysaccharides modifications (Table S4). Among these genes, there were 192 DEGs in *NR vs* WTB, and 59 in *etr3-ko vs* WT. The encoded cell wall-related proteins belong to five main functional classes: proteins acting on cell wall polysaccharides (29% in *NR* and in *etr3-ko*), proteases (11 *vs* 16%), proteins possibly related to lipid metabolism (9 *vs* 11%), proteins with interaction domains with cell wall polysaccharides or proteins (5 *vs* 10%) and proteins of yet unknown function (33% *vs* 20%). Only a few genes encoding oxido-reductases, mostly multicopper oxidases showed modified transcripts levels (Sedbrook et al., 2002). Among the proteins of yet unknown function, six DEGs in *NR* encoded proteins with six conserved cysteines exhibiting the same spacing as thionins (Silverstein et al., 2007).

A main feature regarding the cell wall-related genes was that 17% and 28% of them encoded proteins possibly involved in the pectin metabolism in *NR vs* WTB and in *etr3-ko* vs WT, respectively (Figure 3 and Table S4). These proteins belong to several families: polygalacturonases (PGs), of the glycosyl hydrolase family 28 (GH28), pectin methylesterases (PMEs), of the carbohydrate esterase family 8 (CE8), pectate lyases (PLs) of the PL1 family, PME inhibitors (PMEIs), trichome birefringence-like (TBLs) protein family and Pro-rich, Arabinogalactan conserved Cysteines (PAC) proteins (Hocq *et al.*, 2017; Stranne *et al.*, 2018). The number of DEGs encoding PGs and PMEs was higher in *NR vs* WTB than in *etr3-ko vs* WT. In *NR*, four *PG* genes had increased transcript levels, whereas four had decreased levels. Regarding the *PME* genes, three genes among the most highly expressed had slightly increased transcript levels, whereas seven *PME* genes were down-regulated (Table S4). In *etr3-ko*, four *PME* genes had higher transcript levels than in WT, among which two of the most highly expressed (Table S4). The *PL* genes showed the same kind of regulation in *NR* and *etr3*, with decreased transcript levels for four genes in *NR* and two in *etr3-ko*, and increased transcript

levels for one gene in each case. In *etr3-ko*, two of the most highly expressed genes, *Solyc01g068120* and *Solyc06g084620*, encode PMEs and showed increased transcript levels compared to WT. The transcript level of two *PMEI* genes was decreased in *NR* whereas the situation was more contrasted in *etr3-ko* with one gene having more transcripts and another one less. *TBL* genes also exhibited a complex situation with a reduced transcript levels for one gene in *NR* and an increased transcript levels for two genes in NR or of one gene in *etr3-ko*. This could be due to the fact that the encoded enzymes could have different types of substrates, either hemicelluloses or pectins. Finally, the transcript levels of two genes encoding PAC proteins showed opposite variations in *NR*, whereas one of them had less transcripts in *etr3-ko*.

Altogether, a significant proportion of the cell wall-related DEGs encoded proteins (i) exhibiting enzymatic activities (PG, PME, PL, PAE, and possibly TBL) directed against pectin polymers such as homogalacturonans (HGs) or rhamnogalacturonan I (RG-I) (Hocq et al., 2017, Stranne et al., 2018), (ii) regulating the enzymatic activity of PME (PMEI) (Giovane *et al.*, 2004) or (iii) able to interact with RG-I (Hijazi *et al.*, 2014).

Moreover, we observed that exogenous ethylene application stimulated the expression of three genes encoding PMEs (*Solyc01g057220, Solyc05g052120 and Solyc12g099410*) previously identified in the RNA-seq data set, and the application of 1-MCP slightly lowered their expression (Figure S4A). This further indicates that the expression of these genes is modulated by ethylene signaling.

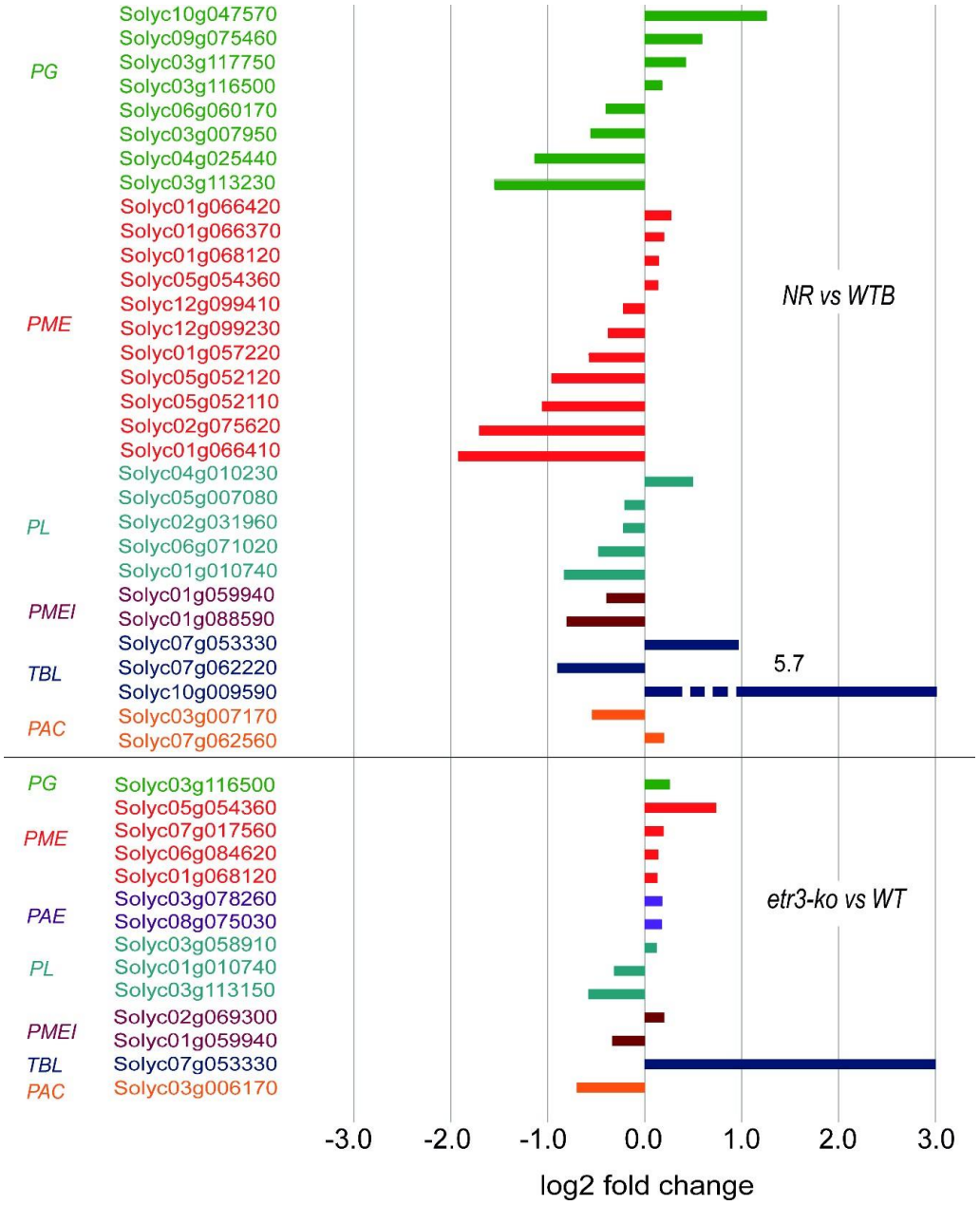

Figure 3. Changes in the level of transcript accumulation of genes possibly related to pectin modifications, in *NR* (upper part) and *etr3-ko* (lower part) compared to WTB and WT, respectively. These bar plots represent log2 (fold change) for the pectin-related DEGs *(P <0.05*). They are grouped in different families: PG (polygalacturonases), PME (pectin methylesterases), PAE (pectin acetylesterases), PL (pectate lyases), PMEI (PME inhibitors), TBL (trichome birefringence-like) and PAC (Proline-rich Arabinogalactan proteins conserved Cysteines). The pectin-related genes are listed in Table S4C.

3.6 Transcriptomic analyses of calcium signaling-related genes in NR and etr3-ko pollen tubes

The expression of 47 Ca^{2+} signaling-related genes was significantly altered in *NR* and *etr3-ko* (Figure 4). There were 34 DEGs (26 down- and 8 up-regulated) in *NR*, and 13 DEGs (6 down- and 7 up-regulated) in *etr3-ko* PTs. According to homologies with TAIR 11 annotation (Table S5), they belong to classes of Ca^{2+} pumps, Ca^{2+} channels, and Ca^{2+} sensors such as calmodulin-binding proteins (CaMBPs), calmodulin-like proteins (CMLs) or Ca^{2+} effectors including Ca^{2+}-dependent protein kinases (CPKs) and CBL-interacting protein kinases (CIPKs). The DEGs coding for some proteins of similar function, were up-regulated in *NR* and down-regulated in *etr3-ko*, or inversely. This could be related to inverse PT growth response in these mutants. Among these, *CPKs* were down-regulated in *NR* and up-regulated in *etr3-ko*. In contrast, *CIPKs* were down-regulated in *NR*, but not significantly affected in *etr3-ko*. Globally in *NR*, there were more down-regulated *CML* and *CaM* genes than in *etr3-ko*. Some of these down-regulated genes exhibited a high number of RNA copies, like *Solyc06g068960, Solyc05g050750* and *Solyc02g067220*, when looking at the 'base mean' (Table S5), thus even DEGs with a small log2 fold change may have an impact on cell functions.

Additional results showed that exogenous ethylene application stimulated the expression of three Ca^{2+} signaling-related genes previously identified in the RNA-seq data set (*Solyc01g010020*, and *Solyc02g063340*, encoding calmodulins, and *Solyc03g123890* encoding a Ca^{2+}-transporting ATPase 1), and that the application of 1-MCP inhibited their expression (Figure S4B). This further shows that expression of these calcium signaling-related genes is modulated by ethylene signaling.

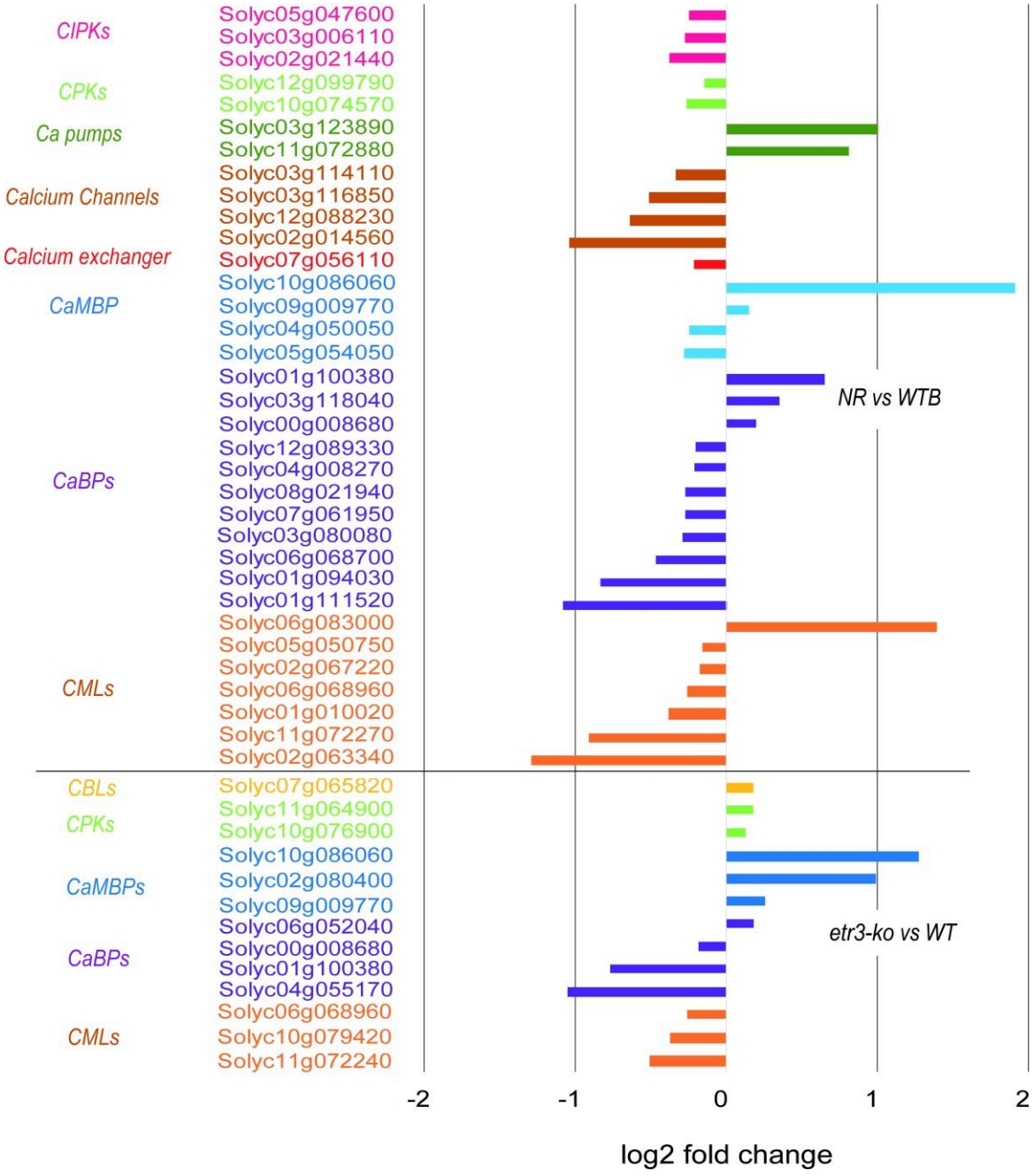

Figure 4. Changes in the level of transcripts related to calcium signaling, in *NR* (upper part) and *etr3-ko* (lower part) compared to WTB and WT, respectively These bar plots represent log2 (fold change) for the calcium-related DEGs *(P <0.05*). The genes are grouped in families: CIPKs (CBL-interacting protein kinases), CPKs (calcium-dependent protein kinases), CaMBPs (calmodulin binding proteins), CaBPs (calcium-binding proteins), CMLs (calmodulin-like proteins). The calcium signaling-related genes are listed in Table S5.

3.7 Immuno-localization of homogalacturonans in etr3-ko and NR pollen tubes

To check possible modifications of HGs in *etr3-ko* and *NR* PTs, we assessed the distribution of weakly and highly methylesterified HGs using LM19 and LM20, respectively. Labeling with LM20 revealed that the highly methylesterified HGs was, as expected, mainly located at the tip of the WT, WTB and *etr3-ko* PTs (Figure 5A). However, an unusual ring-like labeling pattern was observed along the *NR* PT cell wall (Figure 5A). Fluorescence intensity was measured in PT tips, using the same delimited area. The LM20 fluorescence intensity in *etr3-ko* PT apex slightly decreased compared to the WT, without being significant, while in *NR* PT tip, the intensity was significantly higher than in WTB and other lines (Figure 5B). Finally, the diameters of PTs grown in liquid and solid germination medium (GM) were measured in the tip region (Figure 5 C-D). No difference was observed in solid GM (Figure 5D), whereas in liquid GM, the diameters of *etr3-ko* PTs were smaller than in WT, while *NR* PT diameters were larger than in WTB (Figure 5 C-D).

The immuno-localization with LM19 of epitopes associated with weakly methylesterified HGs gave no significant difference (Figure S5A and B): 50% and 57% of the PT tips of WT and WTB were labeled, respectively. In *NR,* 39% of the PT tips were labeled, *vs* 67% in *etr3-ko*.

More LM19 labeling means an increase in cell wall stiffness (Parre and Geitmann, 2005), but no conclusion can be taken here. In addition to immuno-localization, the total PME activity was assayed on whole protein extracts of PTs, but no significant difference was observed, neither looking at activity per fresh mass (Figure S5C), nor looking at specific activity per µg proteins (Figure S5D).

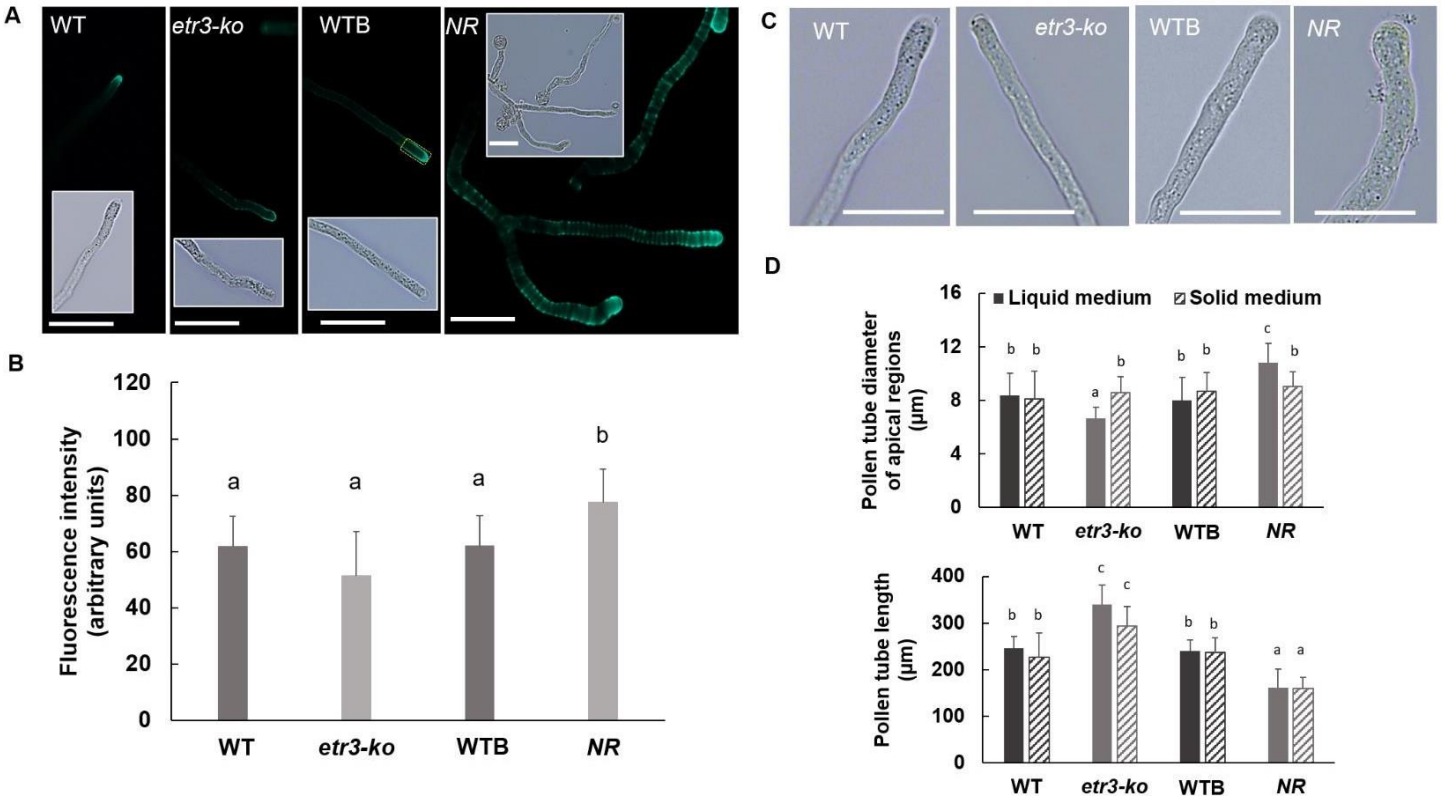

Figure 5. Immunolocalization of highly methylesterified homogalacturonan (HG) epitopes. **(A)** Immunolabeling of PTs of WT, etr3-ko, WTB and NR using LM20. **(B)** Fluorescence intensity was measured at PT apex. n = 80 PTs for each line, error bars show SE, different letters show significant differences at $P = 0.05$ (Dunn's test). The area delimited by a yellow dashed line (as shown on WTB) indicates the chosen zone for measuring the fluorescence mean intensity. **(C)** A representative picture of PTs cultured in the liquid germination medium for each line. **(D)** Measurement of PT length and diameter, in solid and liquid germination medium, 4 h after pollen grain imbibition, in the four tomato lines, n = 50 PTs for each line. Error bars show SE and different letters show significant differences at $P = 0.05$ (Tukey's HSD). Scale bars = 50 µm in panels A and C.

3.8 Calcium load in pollen tube tips is modulated by ETRs

To verify the ethylene signaling ability to change Ca^{2+} ion dynamics in PT apex, PTs were loaded with fluo-4/AM to highlight Ca^{2+} gradient from the tip to the base (Figure 6). Calcium

loading was observed in WT, WTB, *NR* and *etr3-ko* PT tips (Figure 6: panels A-D) and the zone over which fluorescence intensity was quantified is delimited by a yellow dashed line (see Methods for timing details). The fluorescence intensity in the apex region was higher in *etr3-ko* compared with WT, while it was lower in *NR* compared with WTB (Figure 6E), indicating that ethylene signaling modulates the Ca^{2+} accumulation in the PT apex. This corroborates RNA-seq results, as ethylene signaling modulates the expression of several genes encoding pumps and channels involved in Ca^{2+} homeostasis, or sensors (CaMs, CMLs) and effectors (CDPKs, CIPKs) involved in Ca^{2+} decoding. In addition to microscopic imaging, we observed the effects of lanthanum, an inhibitor of calcium transport (Qu et al., 2016) on the PT growth of the different lines. Figure S6 shows that the application of ethylene increased Ca^{2+} accumulation in the WT PTs and that application of 1-MCP decreased it. We also observed that the growth of all PTs was stopped after 2 h of lanthanum (La^{3+}) treatment, regardless of the tomato line and that the Ca^{2+} accumulation in PT decreased within 30 min following the La^{3+} treatment.

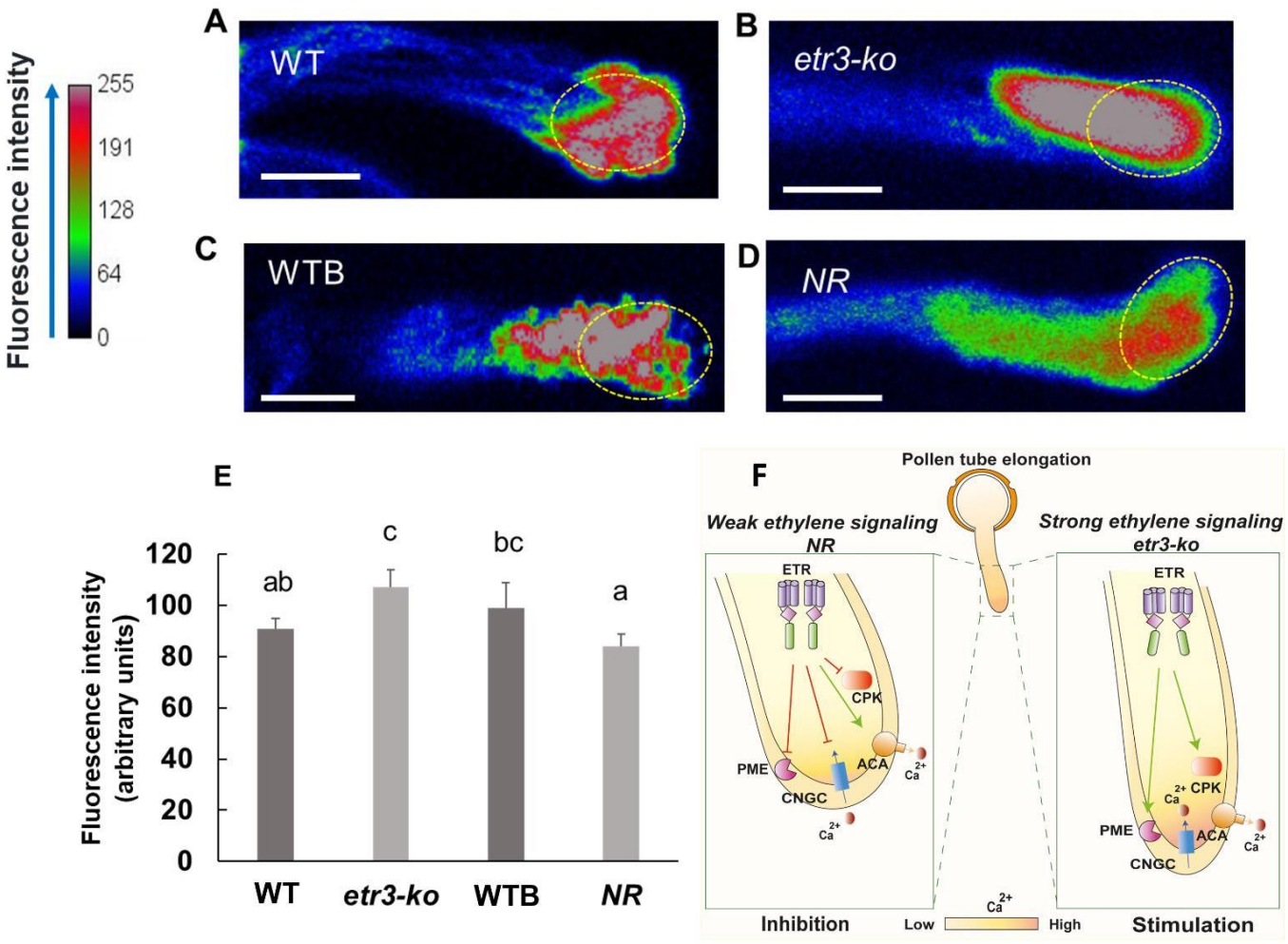

Figure 6. **Effects of *ETR* mutations on the Ca^{2+} gradient in the apical regions of pollen tubes. (A, B, C, D)** Representative images of Ca^{2+} gradient at maximal fluorescence over a 30 min growth period in WT, *etr3-ko*, WTB and *NR* respectively, scale bars = 10 µm. **(E)** Means of maximum fluorescence intensity measured in PT apex loaded with Fluo-4/AM over a 30 min growth period, n = 10 PTs, error bars are SE, different small letters show significant differences at $P = 0.05$ (Tukey's HSD). The zone delimited by a yellow dashed line indicates the region where the maximum fluorescence intensity has been measured. **(F)** Model showing that ethylene signaling regulates PT elongation through cell wall reshuffling by affecting activities of pectin methylesterases (PME) and through modifications in calcium gradient by affecting calcium channels (CNGC), calcium pumps (ACA) and Ca^{2+} effectors (CPK). Only enzyme families showing strong regulation in *ETR* LOF or GOF mutants are represented.

4. Discussion

4.1 Ethylene signaling modulates pollen tube growth

A few previous studies have suggested a role for ethylene in PT growth (Holden et al., 2003; Jia et al., 2018), but the expression of *ETRs* in PTs has been rarely analysed. We observed that three genes, *ETR3, ETR4 and ETR5,* are expressed in tomato growing PTs, confirming recent observations showing expression of the same three *ETRs* in tomato flower tissues (Jegadeesan et al., 2018).

Using various *etr* mutants, we observed that LOF *etr3-ko* and *etr4-ko* led to longer PTs, and GOF *NR,* led to shorter PTs. This latter result confirms recent observations of shorter PTs in the *Arabidopsis etr1-1* GOF mutant (Jia et al., 2018). The ethylene being produced without significant difference between all lines, this suggests that PT growth depends on signaling arising from ETRs. Then, PT growth enhancement observed in WT and WTB after adding ethylene suggests that ethylene releases the blocking effect imposed by ETRs, while the dominant *NR* mutation imposes a strong inhibition that ethylene cannot release at the chosen dose. Additionally, our results showing a significant increase in PT length upon ethylene treatment of the *etr3-ko* line, suggest that, as expected, knocking-out one *ETR* renders PTs more sensitive to ethylene signaling. PT growth stimulation in LOF mutants was modulated with a low dose of 1-MCP, and a significant decrease in PT length was observed in *etr3-ko,* whereas no significant decrease in PT length was observed in WT and WTB. Here, we confirm results regarding the effects of 1-MCP on PT growth in *P. inflata* (Holden et al., 2003), but unlike *Arabidopsis* (Jia et al., 2018), tomato PT growth does not appear to be governed by *ETR1* alone. Altogether, it seems that ethylene signaling partially governs PT elongation. Indeed, blocking ethylene action by 1-MCP led to minimal PT growth, whatever the *ETR* alteration.

Before these experiments with LOF and GOF mutants, we ran preliminary trials with WT at various doses of ethylene and 1-MCP to determine optimal concentrations (Figure S7). The best stimulation of PT growth by ethylene was observed at 100 ppm, but adding ethylene up to 1000 ppm led to a decreasing effect on PT growth, may be due to slight toxicity. For 1-MCP, the

dose chosen for all trials was 2 ppm, as the PT growth decrease seems to saturate beyond 4 ppm. It can be postulated that the remaining PT growth is independent of ethylene signaling.

4-2-Transcriptome profiling of NR and etr3-ko PTs revealed that the GOF mutation has a stronger impact than the LOF mutation

Then we detected gene expression changes in *ETR3* mutants using a RNA-seq survey. We showed that the number of DEGs between *NR* and WTB was higher than between *etr3-ko* and WT. These observations are logical considering that in *NR*, the ethylene-insensitive ETR3, dominates the signaling of the surrounding ETRs and blocks ethylene signaling (Chen *et al.*, 2019), while the *etr3-ko* mutation impairs only one out of the three mostly expressed *ETRs* in PTs.

In addition, the expression of *ETR3* was repressed in *etr3-ko*, without any consequence as a functional ETR3 protein is not produced. This negative feedback on other *ETRs* is not similar to recent observations in *etr7-ko* fruit tissues in which the expression of *ETR3*, *ETR4*, *ETR5* and *ETR6* was increased at the inception of ripening (Chen et al., 2020a). Thus, it is possible that the regulation of *ETR* expression is tissue-dependent. It is also possible that ETR3 and ETR7 do not exert similar feedback on *ETR* expression. In *NR*, the *ETR4* and *ETR5* transcriptsare up-regulated. The related proteins would increase the potential blockage of PT growth.

4-3-Cell wall remodeling is a main output of ethylene signaling in pollen tubes: A focus on pectins

The transcriptomics study revealed the importance of the changes observed in the expression levels of cell wall-related genes in both *NR* and *etr3-ko* PTs. The expression of genes encoding proteins involved in HG remodeling was the most impacted, as expected since HGs are abundant pectin components of PT cell walls (Dehors *et al.*, 2019). Consequently, two kinds of enzymes could be modulated: HG-modifying enzymes demethylating or deacetylating HGs, such as PMEs and PAEs; or enzymes degrading HGs, thus producing oligogalacturonides, such

as PGs or PLs (Hocq et al., 2017). In *NR* PTs, seven PME-, four PG-, and four PL-encoding genes were down-regulated. This observation is consistent with PT length reduction. Indeed, PT elongation requires cell wall flexibility brought in part by the active remodeling of HGs at the PT tip, such as demethylation and reduction of HG chain length. When these modifications do not happen, the cell wall remains stiff, thus inhibiting PT elongation. Conversely, only a few genes encoding pectin-related genes were DEGs in *etr3-ko* PTs. Four *PMEs* were only slightly up-regulated, suggesting a little effect on HG methylesterification, but sufficient to explain the fastest growth compared to the other lines. Only one of these four *PMEs* was clearly down-regulated in *NR*, *Solyc05g054360*. Its level of expression went down from a log2 of 0.74 in *etr3-ko* to 0.1 in *NR*. Thus, the massive decrease in *PME* expression levels in *NR* was related to other genes.

Besides, transcript levels of TBL-encoding genes were strongly modified in *NR* and in *etr3-ko*. The precise role of the *Arabidopsis* 46 TBLs is unknown. However, they were grouped in five clusters, and clusters IV and V are linked to *O*-acetylation of hemicelluloses, like xyloglucan, mannan and xylan, whereas the other clusters gather TBLs possibly involved in *O*-acetylation of pectins (Stranne et al., 2018). The two *TBL* genes up-regulated in *NR* are homologous to *Arabidopsis TBLs* of cluster IV and V (Solyc07g053330, 2-fold; Solyc10g009590, 52-fold), suggesting a re-organization of the cell wall to cope with changes occurring at the pectin level. The third *TBL* gene with modified level of transcripts is down-regulated (about 2-fold) and is homologous to *Arabidopsis TBL* genes of cluster II among which the *TBL44*/*PMR5* gene was shown to play a role in pectin esterification (Vogel *et al.*, 2004). The expression of the *Solyc07g053330* gene, coding for a putative cell wall polysaccharide *O*-acetyltransferase, was lower in *etr3-ko* than in *NR*, also suggesting modifications of hemicelluloses.

Since pectins are critical components for cell wall changes at the PT apex (Mollet et al, 2013), mainly by affecting cell wall rheological properties (Parre and Geitmann, 2005), and since

regulation of genes involved in HG remodeling was affected in *NR* and *etr3-ko*, our study focused on HG distribution in PT cell walls. In WT, the weakly methylesterified HGs are located in the PT shank where they can be cross-linked by Ca^{2+} ions, promoting cell wall stiffness and providing mechanical support for the tip-polarized elongation (Lehner *et al.*, 2010; Chebli *et al.*, 2012; Mollet *et al.*, 2013; Dehors *et al.*, 2019). In contrast, the highly methylesterified HGs are mainly located at the PT apical region providing sufficient flexibility required for the turgor-driven PT elongation (Parre & Geitmann, 2005; Vogler et al., 2013; Mollet et al., 2013)

The surprising LM20 labeling has revealed rings of highly methylesterified HGs all along *NR* PTs. These observations could be related to the down-regulation of eight *PMEs* and associated to the pulsating-growth of PTs. As such, in *Arabidopsis pme48* pollen grains, in which PME activity was reduced and the degree of methylesterification of HGs was higher than in WT, germination was delayed and PT length was reduced (Leroux., *et al.*, 2015). On the other hand, in *Solanum chacoense*, exogenous application of PME to germinating pollen grains induced a reduction of PT growth, an increase of cell wall stiffness and a reduction of its visco-elasticity (Parre and Geitmann, 2005), suggesting that tight regulations of PME activity are required for proper cell wall remodeling and PT growth. The fact that no change in global PME activity was observed among the various lines is not surprising, as temporal and spatial changes revealed by the immuno-localization of methylesterified HG are more refined than the measurement of global activity after crushing whole PTs.

The rate of PT elongation is determined by the equilibrium between turgor-pressure and cell wall ability to extend under this pressure (Kroeger *et al.*, 2011). We observed that PTs exhibited larger diameters in *NR* than in WTB in liquid medium only. In contrast, in *etr3-ko*, the diameter of PTs in liquid medium was smaller than in WT. The down-regulation of *PMEs* in *NR* presumably did not allow the proper demethylesterification of HGs in the sub-apical dome of

the tip and consequently the normal Ca^{2+} bridging of deesterified HGs, thus decreasing the stiffness of the cell wall in the shank of PTs. This led to an increase of PT diameter under the internal turgor-pressure. This increase was also observed in liquid medium in *pme48* (Leroux et al., 2015). These data demonstrate that solid medium can provide a mechanical support to PTs and that the stiffness of the medium can also differently modulate PT growth (Gossot and Geitmann, 2007; Reimann *et al.*, 2020).

Taken together, our results suggest that ethylene signaling can modify the cell wall structure of PTs by regulating the transcription of genes encoding enzymes involved in pectin and hemicellulose modifications. These changes, especially those observed in the degree of methylesterification of HGs, induce a reduction in the length of PTs and an increase in their diameters when ethylene perception is constitutive as in *NR*, and the reverse phenotype when one of the major ETRs present in PTs is inactive like in *etr3-ko*.

4-5-Calcium signaling is a main target of ethylene signaling in pollen tubes

Tip-focused Ca^{2+} gradients generated by interplay between Ca^{2+} pumps and channels are observed during PT elongation and correlated with pulses in growth rates (Pierson *et al.*, 1996 and for a recent review see Zheng et al., 2019). In our study, more than 30 genes coding for proteins involved in Ca^{2+} homeostasis and decoding were de-regulated in the two *ETR* mutants. Such a high DEG number indicates the tight link that exists between ethylene and Ca^{2+} signaling, and highlights the importance of the latter in modulating tomato PT elongation. More than 25 of these DEGs were repressed in *NR*.

Interestingly, a few DEGs were inversely de-regulated in *NR* and *etr3-ko,* in agreement with the observed opposite growth and tip-focused Ca^{2+} gradient phenotypes. This is the case for the calreticulin gene (*Solyc01g100380*), which expression is down-regulated in *etr3-ko* and up-regulated in *NR*. This protein was already shown to be important for Ca^{2+} homeostasis during PT growth in *P. hybrida* (Suwińska *et al.*, 2017). Conversely, *CPK17* (*Solyc12g099790*) is up-

regulated in *etr3-ko* and down-regulated in *NR*. *CPK17* was shown to be preferentially expressed in *Arabidopsis* PTs and to have a redundant function with *CPK34* during PT growthand tropism (Myers *et al.*, 2009). The PTs of the double mutant *cpk17/cpk34* display a slower growth and impaired tropism. The *CPK17* ortholog being up-regulated in *etr3-ko* and down- regulated in *NR* could fit with longer PTs observed in *etr3-ko* and shorter PTs observed in *NR*. Genes encoding two other Ca^{2+} effectors, *CPK20* (*Solyc10g076900*) and *calcineurin B-like protein3 (CBL3)* (*Solyc07g065820*) are also up-regulated in *etr3-ko* PTs. These two Ca^{2+} effectors have been reported to be associated with PT growth by activating the slow anion channel SLAH3 at the PT tip (Gutermuth *et al.*, 2013), whereas CBL3 activates CIPK12 to promote a fast PT growth (Steinhorst *et al.*, 2015). The gene (*Solyc10g086060*) that showed the strongest amplitude between inhibition (in *NR*) and stimulation (in *etr3-ko*) is homologous to the *Arabidopsis* gene *At5g03040*. This gene encodes the Ca^{2+}-calmodulin binding protein IQD2, of the large IQD family. These family members participate in microtubule organization during plant development and are modulated by auxin (Bürstenbinder *et al.*, 2017). Here, it appears that removing the ETR3, in the LOF, leads to the up-regulation of *IQD2* that could promote PT expansion by favoring the cytoskeleton organization required for a proper elongation of the cell.

Regarding *NR*, there were only a few up-regulated genes: two encoding Ca^{2+}-ATPases, *calcium-transporting ATPase 4 (ECA4)* (*Solyc11g072880*), *ACA9* (*Solyc03g123890*) and one encoding CML7 (*Solyc06g083000*). Considering that PTs were shorter in *NR* than in *etr3-ko*, we can speculate that these ATPases and CML7 could contribute to dissipate the Ca^{2+} gradient by extruding the Ca^{2+} ions from the cytosol. Indeed, in *NR*, the Fluo-4 fluorescence is systematically lower than in WTB, indicating a lower Ca^{2+} concentration in PT tips. However, we cannot exclude a membrane permeability disturbance due to the mutation, which would affect the loading of the probe in PTs.

In *NR*, there were down-regulated genes encoding the CMLs 3, 13, 16, 27, 28 and 46 (*Solyc05g050750*, *Solyc11g072270*, *Solyc01g010020*, *Solyc06g068960*, *Solyc02g063340* and *Solyc02g067220*, respectively) and two genes encoding cyclic nucleotide-gated ion channels, CNGC8 and 16 (*Solyc03g116850* and *Solyc03g114110*, respectively). CNGCs together with iGLUr channels are the main players in generating the Ca^{2+} influx in PTs (Michard., *et al.*, 2017; Gu *et al.*, 2017; Tunc-Ozdemir *et al.*, 2013)(Michard., *et al.*, 2017). CNGC8 was recently shown to be involved in PT growth by antagonizing CNGC18 (Pan *et al.*, 2019). With respect to shorter PTs observed in *NR*, a reduced activity of these CNGC channels in conjunction witha supposed increased activity of Ca^{2+}-ATPases could result in a disruption/mitigation of the tip-focused Ca^{2+} gradient as confirmed by the lower Fluo-4 fluorescence observed in PT tips. Concerning CMLs, little is known about their targets in plants but most of the genes cited abovehave been already shown to be up-regulated during pollen germination and/or PT growth (Wang *et al.*, 2008). Moreover, it is not excluded that one of these down-regulated genes encode CMLsthat could participate in either a positive or a negative regulation of one of the two identified Ca^{2+}-ATPases as already shown (Astegno *et al.*, 2017). In addition, several other genes belonging to the Ca^{2+} toolkit are also down-regulated including several genes encoding CIPKsor cation exchangers. These are known to be directly involved in the regulation of ions channels governing ion homeostasis during PT growth. The *Arabidopsis* gene homologous to the down-regulated *annexin 5* gene (*Solyc04g008270*) was shown to be involved in pollen development and PT growth by promoting Ca^{2+}-dependent membrane trafficking necessary for PT elongation (Zhu *et al.*, 2014). The additional experiment, using La^{3+} to block calcium fluxes, proved that calcium is downstream of the ethylene signal, as no PT elongation was observed inany of the tomato lines in the presence of lanthanum, whatever the signals delivered by ETRs.

Overall, the calcium signaling-related DEGs in the two *ETR* mutants similarly point out the crucial role of ethylene in controlling the tip-focused Ca^{2+} gradient required for PT growth. The fact that the application of lanthanum inhibits calcium transport in all lines, wild types and loss-

or gain-of-function *ETR* mutants, is a proof that calcium transport is downstream of the ethylene signaling.

In summary (Figure 6F), our work suggests that ETR signaling blocks PT growth, in absence of a sufficient amount of ethylene. This blockade is notably mediated by cell wall modifying enzymes acting on the methylesterification status of HGs, and by an alteration of Ca^{2+} loading in PTs. Changes in ethylene signaling is also altering expression of other gene families, particularly related to hormone metabolism, that were not detailed in this study. Contributions of the ethylene precursor, 1-aminocyclopropane carboxylic acid, also has been suggested to play crucial roles in ovular PT attraction (Mou *et al.*, 2020). Ethylene has long been known to be involved in many plant development processes, and its contribution to fruit set has been under scrutiny over the last decades (An et al., 2020). Here, we unravel part of its crucial role in PT growth.

By altering ethylene perception, we show that ethylene signal acts on both cell wall- and calcium-related genes. Specific effects on HG methylesterification and calcium signaling were demonstrated.

Chapter III: 1-aminocyclopropane-1-carboxylic acid (ACC) stimulates tomato pollen tube growth independently of ethylene perception

(Published in Physiologia Plantarum by Althiab-Almasaud et al., 2021) https://doi.org/10.1111/ppl.13579

The supplementary data of this chapter have been placed in Annex II

1-aminocyclopropane-1-carboxylic acid (ACC) stimulates tomato pollen tube growth independently of ethylene receptors

Abstract

The plant hormone ethylene plays vital roles in plant development, including pollen tube (PT) growth. Many studies have used the ethylene precursor, 1-aminocyclopropane-1-carboxylic acid (ACC), as a tool to trigger ethylene signaling. Several studies have suggested that ACC can act as a signal molecule independently of ethylene, inducing responses that are distinct from those induced by ethylene. In this study, we confirmed that ethylene receptor function is essential for promoting PT growth in tomato, but interestingly, we discovered that ACC itself can act as a signal that also promotes PT growth. Exogenous ACC stimulated PT growth even when ethylene perception was inhibited either chemically by treating with 1-methylcyclopropene (1-MCP) or genetically by using the ethylene-insensitive *Never Ripe* (*NR*) mutant. Treatment with aminoethoxyvinylglycine (AVG), which reduces endogenous ACC levels, led to reduction of PT growth, even in the *NR* mutant. Furthermore, GUS activity driven by an EIN3 Binding Site promoter (*EBS:GUS* transgene) was triggered by ACC in the presence of 1-MCP. Taken together these results suggest that ACC signaling can bypass the ethylene receptor step to stimulate PT growth and EBS driven gene expression.

1. Introduction

Enhancing crop yields to ensure global food security is becoming a pressing challenge, and in most crop species, flowers, fruit and seeds are key components for yield control (Dhankher and Foyer, 2018). As such, research efforts on plant reproduction are essential to increase fruit/seed yields.

Ethylene is a phytohormone regulating reproduction and the development of fruits and seeds, among numerous other processes (An et al., 2020; Binder, 2020). The biosynthesis of ethylene starts from methionine and the immediate precursor of ethylene is 1-aminocyclopropane-1-carboxylic acid (ACC), generated by ACC synthase (ACS) from S-adenosyl methionine. Oxidation of ACC to ethylene is then catalyzed by ACC oxidase (ACO) (Polko and Kieber, 2019). Plant ethylene responses are typically observed upon treatment with exogenous ACC, but several studies have indicated that ACC can act as an ethylene-independent signal (Xu *et al.*, 2008; Tsang *et al.*, 2011; Yin *et al.*, 2019; Vanderstraeten *et al.*, 2019; Mou *et al.*, 2020). Xu et al. (2008) suggested that ACC is involved in the regulation of a cell wall function in Arabidopsis roots even when ethylene perception is blocked by 1-MCP. Tsang et al. (2011) demonstrated that the isoxaben-induced inhibition of Arabidopsis primary root elongation depends on ACC biosynthesis, but does not depend on the perception of ethylene. An accumulation of recent studies has uncovered potential signalling roles of ACC in a number of other processes. Vanderstraeten *et al.* (2019) found that ACC can function as a negative regulator of Arabidopsis early vegetative development, *i.e.* reducing rosette development, hypocotyl elongation in darkness, and root growth, independently of ethylene signalling. In another study, it has also been shown that ACC itself positively regulates the symmetric division of guard mother cells into two guard cells (Yin et al, 2019). ACC signalling in Arabidopsis ovules was found to be involved in pollen tube (PT) attraction, by stimulating the secretion of the PT attractant LURE1.2 (Mou et al., 2020). Additionally, ethylene-independent ACC signalling has been demonstrated in the liverwort *Marchantia polymorpha* (Li et al., 2020).

Sexual plant reproduction necessitates pollen germination, the elongation of PTs through the style to reach the ovule and the release of sperm cells into the ovular embryo sac

for fertilization, among other steps (An *et al.*, 2020). There is evidence that ethylene plays a role in this complex process. For example, increased ethylene production was detected in the pistil after pollination in *Petunia* (Holden *et al.,* 2003). This ethylene burst is correlated with the expression of ACS and ACO genes in the pistil (Llop-Tous et al., 2000). Another study showed that PT growth is stimulated by an ethylene-driven metabolism leading to higher levels of actin filaments (Jia et al. 2018), which are important for the polarized growth of PTs (Mollet et al., 2013). The role of ethylene perception on PT elongation was first observed using 1-MCP (Holden et al., 2003), and later in Arabidopsis *etr1-1* ethylene-insensitive mutants (Jia et al., 2018).

In light of the emerging differences between ethylene- and ACC-induced responses, in this study we used various strategies to investigate the potential roles of ethylene versus ACC in tomato PT growth.

2. Material and methods

2.1 Plant material and growth conditions

This study was carried out with four lines of *Solanum lycopersicum,* cv. MicroTom: wild type (WT), *NR*, *EBS:GUS* in WT and *EBS:GUS* in the *NR* mutant. *NR* is a dominant ethylene receptor mutant that displays ethylene insensitivity (Wilkinson *et al.*, 1995). We obtained *NR* and its corresponding wild-type background from the L.E. Pereira Peres laboratory (Carvalho *et al.*, 2011). The *EBS:GUS* plasmid was obtained from A. Stepanova laboratory (Stepanova *et al.*, 2007) with EBS standing for EIN3 Binding Site. The *EBS:GUS* WT line was generated in our laboratory by transformation with *Agrobacterium tumefaciens* (Jones et al., 2002). The *EBS:GUS:NR* line was generated by crossing the homozygous *EBS:GUS:WT* line with *NR*. Two homozygous lines were chosen. Both *EBS:GUS:WT* and *EBS:GUS:NR* plant transformation were selected with the antibiotic hygromycine B (100 $mg.l^{-1}$). Seeds were sterilized with 5% NaClO for 8 min, then washed 3 times with sterilized water, and were sown directly on soil and maintained in a culture room, with a 16h day: 8h night cycle, associated with temperature 22°C:18°C cycle, respectively, under 80% relative humidity and a day light intensity of 250 $\mu mol \cdot m^{-2} \cdot s^{-1}$.

2.2 Pollen grain germination in *vitro* assays

Pollen grains were collected from ten anthers, from approximately five plants, at one and two days post-anthesis, in 1.5 ml centrifuge tubes, by using an electric toothbrush body (Oral-B, France). For imbibition, pollen grains were placed on the pollen germination medium (300 mM sucrose, 2 mM boric acid, 2 mM calcium nitrate, 2 mM magnesium sulfate and 1 mM potassium nitrate), as described previously (Firon et al., 2012). The pollen grains were incubated at 25°C, 80% relative humidity for various times, in the dark, in 2 ml vials with septum and screwed caps (Interchim, France). For the ACC and AVG treatments, solutions were added in the germination medium at 10 µM final concentration, unless otherwise stated. For the ethylene and 1-MCP treatments, these gases were injected at 100 ppm and 2 ppm final concentration, respectively, based on previously-described dose effects (Althiab-Almasaud et al., 2021). 1-MCP, which inhibits ethylene perception (Binder, 2020), was obtained from AgroFresh (Fran Nguyen-Kimce) and prepared according their recommendations. All other chemicals were from Sigma-Aldrich (France).

The germination medium was transferred onto a glass slide prior to microscopic observations. The images were acquired using an inverted microscope (Leitz DMIRB, Leica Microsystems, Germany) equipped with a camera CMOS 10Mpixels (LEÏCA MC 190HD). The objective in place was an NPlan 10x:0.22NA. The length of pollen tubes was measured using ImageJ software (Abràmoff et al., 2004).

2.3 ACC content

For pollen tube free ACC content, we optimized the protocol of Bulens *et al.*, (2011) with the following modifications. Two mg of crushed frozen pollen tube were placed in 1.5 ml centrifuge tubes, 1 mL of 5% sulfosalicylic acid solution was added to the frozen sample, and incubated and centrifuged as described. The supernatant was collected in a 5 ml glass vial. The ethylene was measured using a gas chromatograph and the following conditions: 2 m x 3 mm 80/100 alumina column, injector at 110°C, N_2 as carrier gas at 30 ml/min in an isocratic oven temperature at 70°C, and FID detector at 250°C.

2.4 GUS activity assay and GUS staining

GUS activity was assayed according to Melo *et al.*, (2016) with the following modifications. For each sample, two mg of crushed frozen pollen tubes were homogenized with 300µL mL extraction buffer composed of 50 mM Hepes-KOH (pH 7.0), 5 mM DTT and 0.5% PVP (w/v), then the samples were incubated at 4°C for 30 min with gentle shaking and spun at 16,000 *g* for 10 minutes at 4°C. Supernatants (100µl) were mixed with 100 µl of GUS extraction buffer containing 2 mM 4-methylumbelliferyl-b-D-glucuronide (MUG) and incubated at 37°C for 30 min. Then 30 µl of this reaction were mixed with 270 µl of stop reagent 0.2 M Na_2CO_3 (pH 9.5).

Pollen tubes of *EBS:GUS* transgenic plants were vacuum infiltrated for 5 min in GUS staining buffer (100 mM sodium phosphate buffer, pH 7.0, 10 mM EDTA, 0.1 % Triton X-100, and 1 mg/mL X-Gluc) and then incubated for 24 h at 37 °C. After staining, the pollen tubes were washed in distilled water. GUS-positive samples were examined with an inverted microscope (Leitz DMIRB, Leica Microsystems, Germany) equipped with a camera CMOS 10 Mpixels (LEÏCA MC 190HD). The objective was an NPlan 10x:0.22NA.

2.5 Statistical treatments

All data were processed with the R package (R Core Team, 2021), using ANOVAs and Tukey multiple comparison tests.

3. Results

3.1 Ethylene perception stimulates pollen tube growth

The impact of ethylene perception on pollen tube elongation in tomato was studied in the WT and ethylene-insensitive *NR* mutant, 4h after imbibition. We used exogenous ethylene and 1-MCP treatment as effector or inhibitor of ethylene receptors, respectively. We found that in WT, exogenous ethylene stimulates PT growth, and by contrast, 1-MCP inhibits it (Figure 1A), consistent with the results obtained by Holden et al. (2003) in *Petunia inflata*. Ethylene-stimulated growth was prevented by 1-MCP+ethylene treatment, in which ethylene was applied 30 min after adding 1-MCP, showing that the simulation of PT growth by ethylene goes through ethylene receptors as expected. This also demonstrated that even a small dose of 1-MCP is able to counteract the effect of large concentrations of ethylene. In contrast, *NR* pollen tube growth was not affected by the treatments **(Figure 1B)**, consistent with *NR* being disrupted in ethylene perception (Wilkinson et al. 1995).

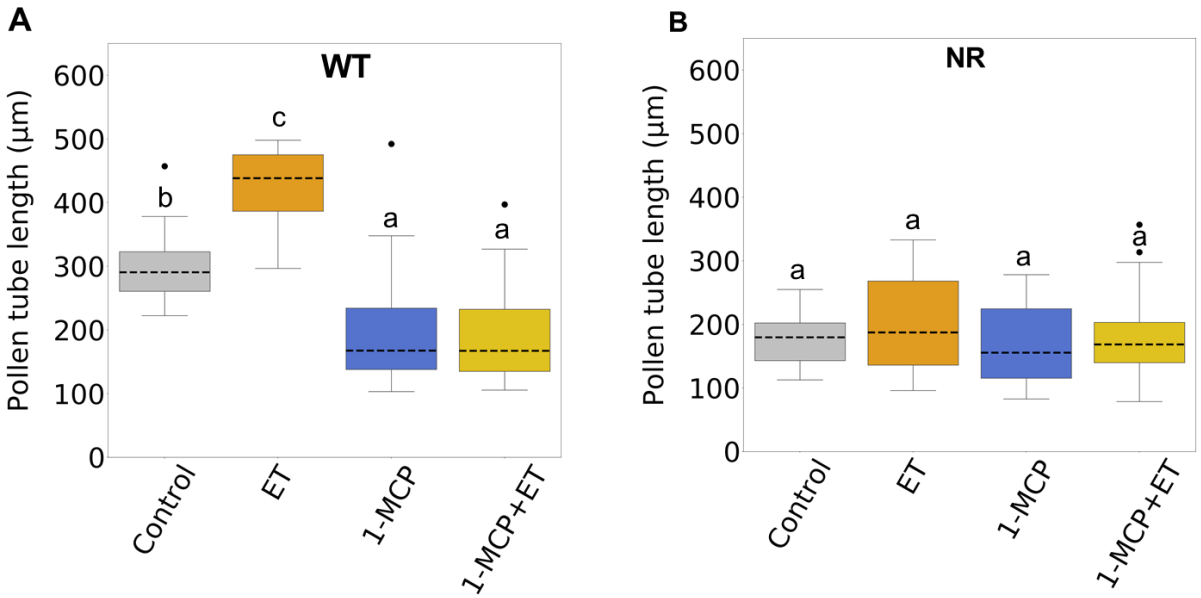

Figure 1. The effect of exogenous ethylene (ET) (100 ppm), 1-MCP (2 ppm), on PT growth in **A)** WT and **B)** NR, n=50 individual PTs, 4h after imbibition. In both panels, horizontal dashed lines show medians, and black dots show outliers, and different small letters show significant differences at the 0.05 level (Tukey's HSD).

3.2 ACC stimulates PT growth, even when ethylene perception is blocked

We next investigated the effect of ACC on PT growth by first performing dose-response experiments. We found that ACC stimulates WT PT growth with an optimal dose of 100 µM (Figure 2A). This biphasic response caused by ACC has already been observed in Marchantia with growth stimulation at 1 µM and growth inhibition at 100 µM (Li et al., 2020). Although this treatment likely causes PT growth due to the conversion of ACC toethylene, we discovered that ACC can also stimulate PT growth (albeit to a lesser extent) in the*NR* mutant (Figure 2B). This result was unexpected given that *NR* cannot perceive ethylene, and it suggested that exogenous ACC can stimulate PT growth independently of ethylene perception.

We then investigated whether endogenous ACC plays a similar role as treatment with exogenous ACC. We began by first measuring the free (non-conjugated) ACC content in PTs (Figure 2C). We did not assay conjugated ACC content, as this has not been shown to play a signaling role in plants. In WT PTs, the endogenous content of free ACC was found to decrease over the imbibition time to 50 nmoles.g^{-1} (Figure 2C). This corresponds roughly to 50 µM, which fits with a previous determination of ACC in plant tissues (Bulens et al., 2011). Next, we hypothesized that if endogenous ACC induces PT growth, then AVG, an inhibitor of ACC

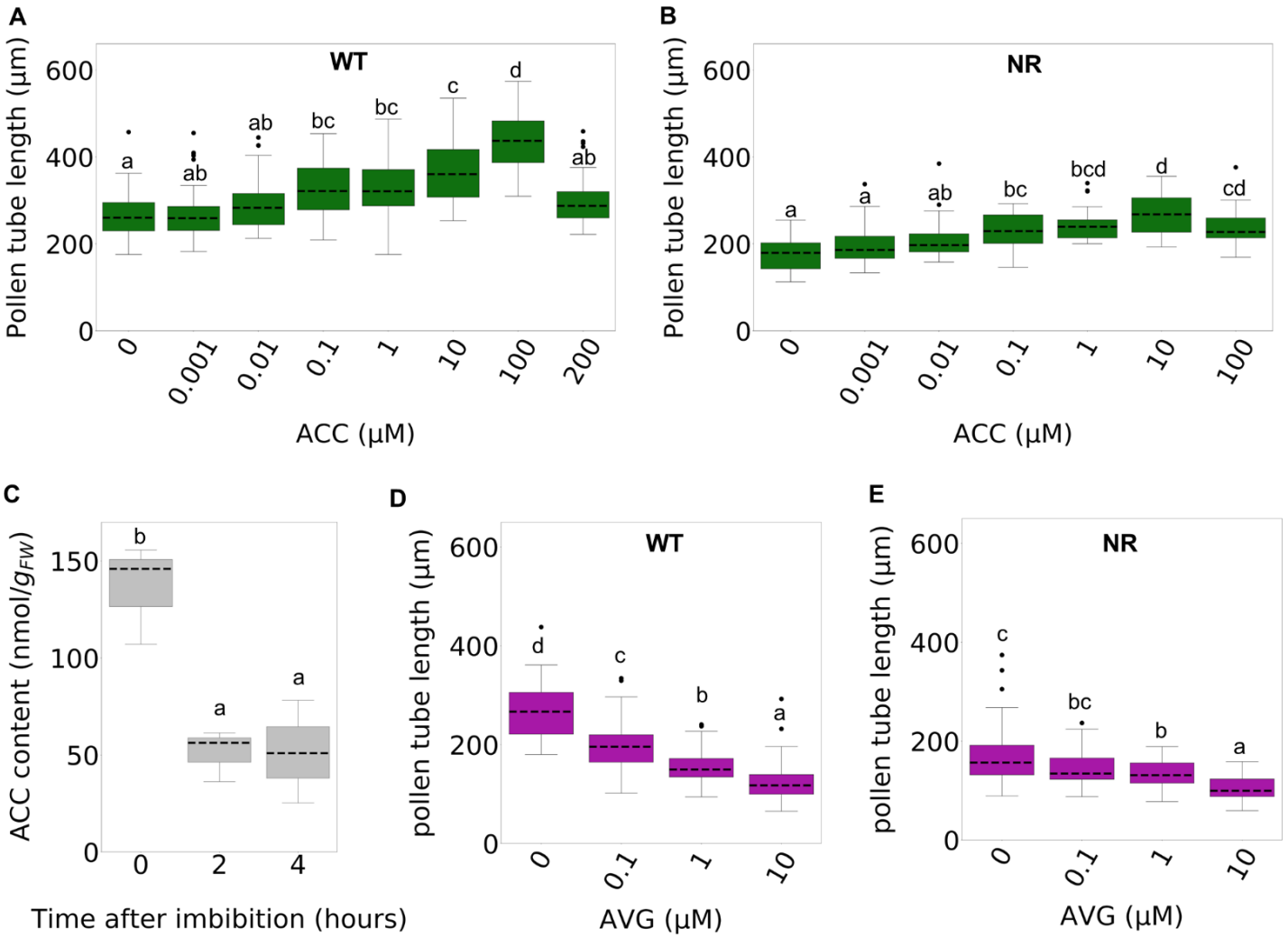

Figure 2. Effects of different concentrations of ACC **(A, B)** and AVG **(D, E)** on PT length in WT and NR, respectively, 4h after imbibition, n = 50 individual PTs. **C)** Free ACC content of pollen grains and PTs. In all panels, horizontal dashed lines show medians, and black dots show outliers, different small letters show significant differences at the 0.05 level (Tukey's HSD).

synthase, should exhibit reduced PT growth. By performing an AVG dose response in both WT and *NR*, we found that PT growth linearly decreased with increasing AVG doses up to 10µM (Figures 2D and 2E). We next confirmed that the effect of AVG (10 µM) was based on ACC content, rather than, say, a toxic effect; by adding ACC 30 min after the imbibition start in the presence of AVG, we found that ACC restored PT growth in the presence of AVG

in both the WT and *NR* (Figures 3A and 3B). Moreover, by measuring the free ACC content in PTs of both lines, we confirmed that free ACC is indeed reduced by AVG (Figure 3C). Taken together, these results indicated that the stimulation of PT growth by endogenous ACC is partially independent of ethylene perception.

Finally, to confirm that ACC action on PT growth is partially independent of ethylene perception, we treated PTs with exogenous ACC 30 min after imbibition in the presence of 1-MCP, which blocks ethylene perception. We found that we still observed the stimulating effect of ACC on PT growth in the WT and *NR* (Figure 3D). In this case, the relatively shorter PT lengths of all the samples were due to the inhibition of ethylene perception, because1-MCP did not affect the free ACC content (Figure 3E) and likely did not affect ethylene biosynthesis from ACC. These results confirmed that ACC stimulation of PT growth is partially independent of ethylene perception.

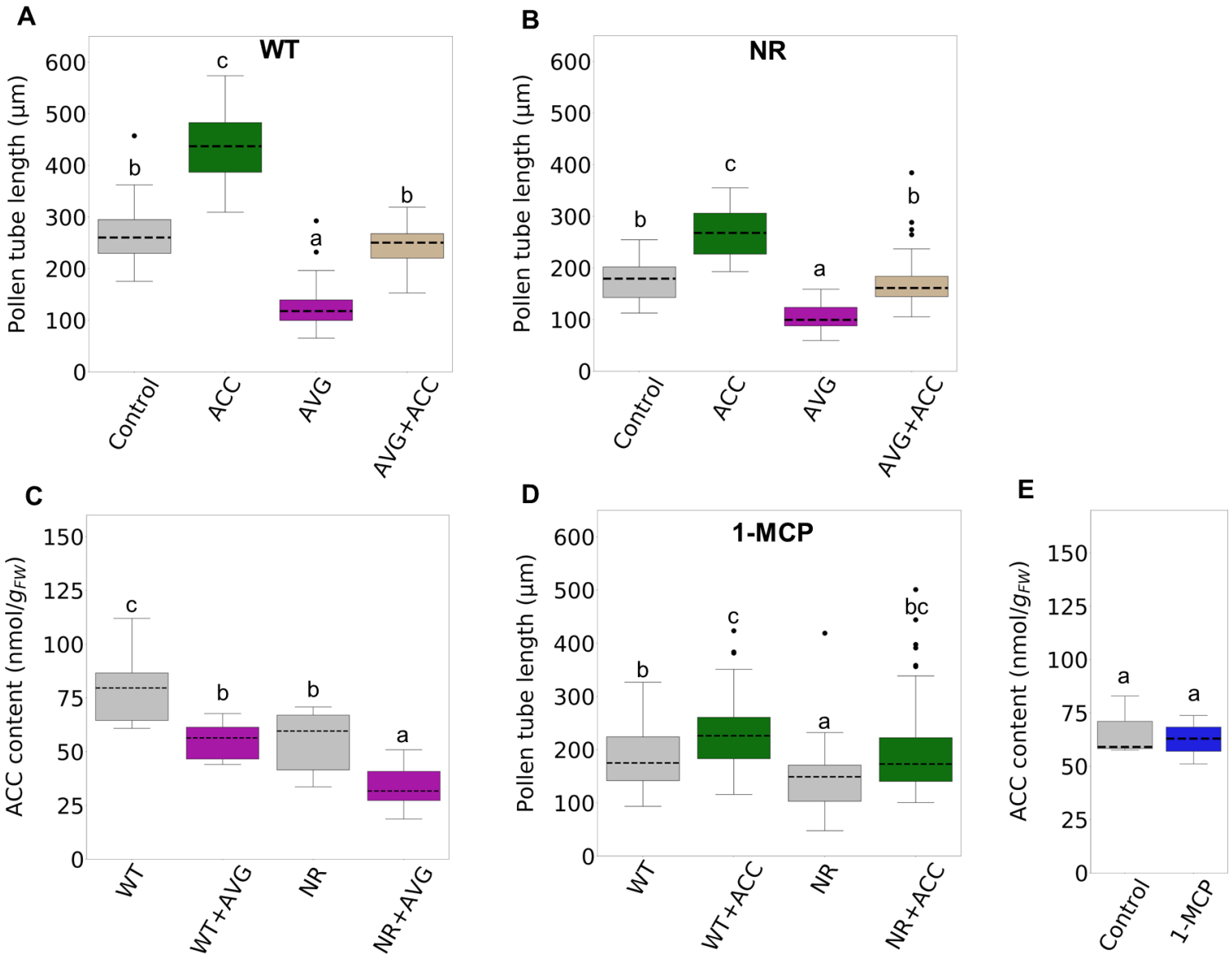

Figure 3. The effect of exogenous ACC (10µM) or AVG (10µM) on PT growth in **A)** WT and **B)** NR, n = 150 individual PTs. **C)** Free ACC content in WT and NR PTs with or without AVG, n = 12 biological replicates of 0.5 mg of pollen grains each. **D)** Effects of ACC on PT growth in presence of 1-MCP, n = 50 individual PTs. **E)** Effect of 1-MCP (2ppm) on ACC content in PTs, n = 3 biological replicates of 0.5 mg pollen grains each. All panel measurements were performed 4h after imbibition, horizontal dashed lines show medians, and black dots show outliers, different small letters show significant differences at the 0.05 level (Tukey's HSD).

3.3 ACC stimulates GUS driven by EBS, independently of ethylene perception.

Given that ethylene and ACC each stimulate PT growth, we asked if ACC is able to trigger a downstream step of the ethylene signaling pathway, *i.e.*, EIN3-LIKE (EIL)-dependent transcription. EILs are primary transcription factors of the ethylene signal cascade (Liu et al., 2015). We observed the effects of various treatments on *EBS:GUS* activity in pools of pollen grains, germinating grains and PTs. This GUS construct was shown to work in tomato fruit tissues (Bianchetti et al., 2017), but had not been tested in pollen cells. Firstly, we observed a degree of GUS activity and staining in the control WT (Figure 4), probably due to endogenous levels of ethylene (Althiab-Almasaud et al., 2021) or to free ACC (Figure 2C). Treatments with exogenous ACC and ethylene were able to stimulate the GUS activity, whereas 1-MCP repressed this activity (Figure 4A and 4B). Moreover, 30 min after applying 1-MCP, the ACC treatment was able to stimulate GUS activity and staining, despite ethylene perception being blocked (Figure 4A and 4B). Finally, 30 min after applying 1-MCP, the ethylene treatment was not able to stimulate GUS activity. These results suggest that ACC is able to activate EIL-dependent transcription, independently of the ethylene receptor step. To further confirm this, we conducted experiments in the *NR* mutant background, into which we crossed the EBS:35S:GUS transgene, and observed that ACC was able to stimulate GUS activity as in the WT, without or with 1-MCP application (Figure S1). The GUS activity profiles were similar between WT and NR lines (Figure 4B and Figure S1B). This should drive further research to better understand EBS activation in tomato pollen cells.

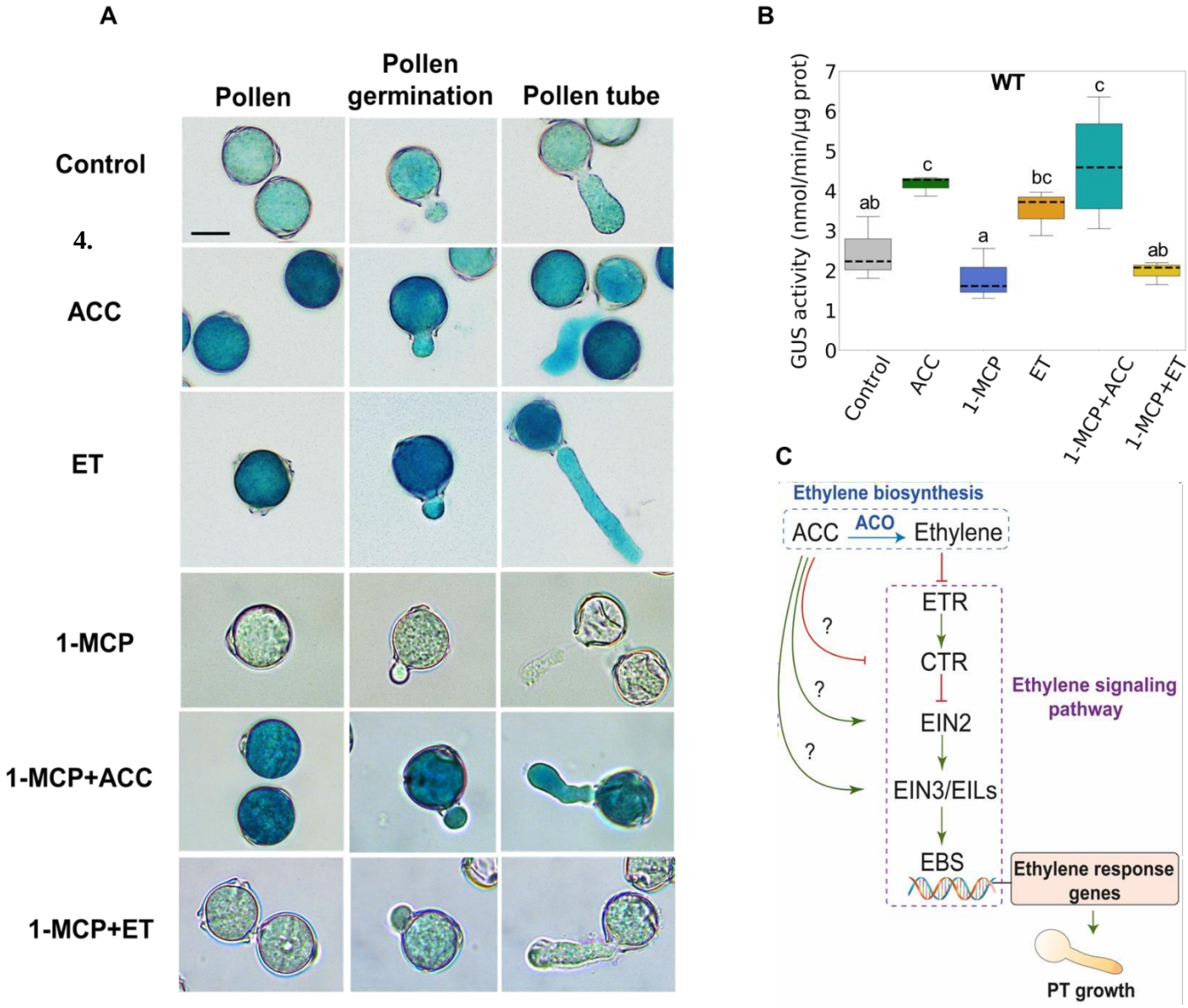

Figure 4. (A) Images of WT tomato pollen grains and tubes expressing the *EBS:GUS* reporter after various treatments. Scale bar = 30 µm**. (B)** GUS activity assayed 4h after imbibition in WT PTs. n = 3 biological replicates of 0.5 mg pollen grains each, horizontal dashed lines show medians, different small letters show significant differences at the 0.05 level (Fisher's LSD). **(C)** Proposed model showing ACC signaling bypassing ethylene perception to stimulate PT growth.

4. Discussion

Our results confirmed previous studies showing the essential role of ethylene in PT growth (Holden et al., 2003; Jia et al., 2018). However, we discovered that the ethylene precursor ACC can promote PT growth independently of ethylene perception, adding to the growing evidence that ACC itself can act as a signal. Indeed, when the ethylene receptors were either blocked by 1-MCP or genetically inhibited in the *NR* mutant, the addition of exogenous ACC was able to stimulate PT growth. It is possible that *NR* only partially blocks block ethylene perception as stated in Negi et al. (2010). Furthermore, the use of AVG to inhibit ACC synthesis in the *NR* mutant demonstrated that endogenous ACC plays a role in promoting PT growth independently of ethylene perception. In future experiments to further prove ACC roles independent of ethylene action, pyrazinamide, which blocks ACC oxidase (Sun et al., 2017), could be tested.

Ethylene-independent signaling by ACC has already been recently described invarious plant organs (Polko and Kieber, 2019; Vanderstraeten et al. 2019; Mou et al. 2020; Li et al., 2020). In contrast to previous findings, where ACC and ethylene induced distinct responses, we found that ACC and ethylene both promote tomato PT growth. Jia et al. (2018) also showed that exogenous ACC was able to promote Arabidopsis PT growth; they observed a reduced PT growth in the *etr1-1* mutant, a gain-of-function ethylene-insensitive mutant similar to *NR*, but they did not observe any stimulation effect by ACC in this mutant. Additionally, they neither tested the effect of ACC in the presence of 1-MCP or other ethyleneperception inhibitors, nor measured free ACC content.

In our experiments, we found that there was less free ACC in the *NR* mutant. Thus the slower PT growth in this mutant compared to WT could be due to a combined effect of impaired ethylene perception and lower free ACC levels.

By testing the downstream activation of the *EBS:GUS* reporter in various conditions impacting the ethylene perception step, we observed results suggesting that ACC can modulate reactions downstream of the ethylene receptor steps. The ACC targets could be signaling steps related to CTR1, EIN2 or EIN3/EILs, which all function upstream of EBS, as outlined in a

tentative model (Figure 4C). Previous results by Vanderstraeten et al. (2019) suggest that ACC signaling by-passes the ethylene receptor step and branches to EIN2. Indeed, Vanderstraeten et al. (2019) showed that exogenous ACC reduces Arabidopsis rosette area in Col-0, even when 1-MCP was applied, but the *ein2-1* ethylene-insensitive mutant was less responsive to the ACC effect. In contrast, Mou et al. (2020) showed that ACC action bypasses the *ein2-5* null mutant in ovules. Additionally, Mou et al. (2020) found that ACC can stimulate an intracellular Ca^{2+} increase in Arabidopsis ovules, and Ca^{2+} is known to enhance PT elongation (Michard et al., 2017). Whether or how Ca^{2+} connects with EBS remains an open question, and checking Ca^{2+} signaling after adding ACC and 1-MCP would be an interesting perspective for a further study.

In conclusion, we observed that both ethylene perception and ACC itself can stimulate tomato PT growth. These findings, particularly the newly uncovered role of ACC that is independent of ethylene perception, open new research perspectives, such as identifying the direct targets of ACC signalling upstream of the EIN3/EIL binding site and elucidating the underlying signalling mechanisms.

General Conclusion and Perspectives

With my doctorate work, I contributed to better characterize the involvement of ethylene and ACC signaling in the pollen tube germination and growth.

A large set of data supports the hypothesis that ethylene plays active roles in reproductive sexual organs formation and development which is critical to the successful initiation of the fruit set process (Vriezen et al., 2008; Pascual et al., 2009; Carbonell-Bejerano et al., 2011). I wrote a bibliographic review showing that ethylene is involved in the pollen germination once the pollen is released from anther and lands on the stigma, and the ethylene also regulates the pollen tube growth in the style by the transmission tissues degradation to facilitate pollen tube elongation, and finally the fertilization of the ovule (An et al., 2020).

In this study, I focused on the effect of ETR signaling on tomato PT growth. The data set of my main article (published in Plant Journal) showed that PT elongation was repressed in absence of a sufficient amount of ethylene. This repression related to the modification in the expression of cell wall and calcium related genes. Moreover, the ethylene perception mutants display specific effects on cell wall modifying enzymes acting on the methylesterification status of HGs, and effects on Ca^{2+} gradient alteration.

In the third chapter, I showed that ACC itself can stimulate tomato PT growth independently of ethylene signaling, as this ethylene precursor stimulated PT growth even when ethylene perception was blocked by NR mutant or 1-MCP. Furthermore, in the presence of 1-MCP, GUS activity driven by an EIN3 Binding Site promoter (EBS:GUS transgene) was stimulated by exogenous ACC treatment. These results suggest that ACC stimulates PT growth, independently of ethylene perception.

Further works could be performed to understand why the profile of HG methylesterification presents a ladder pattern in the NR ethylene insensitive mutant. Moreover, it would be interesting to check whether there is a correlation between the PMEs structure (presence of an PMEI domain (PME type I / group2) or absence (PME type 2 / group 1)) and the

regulation of these gene expression during pollen tube growth.

Analyses of ETRs expression patterns showed that ethylene receptor genes are differentially expressed in various tissues and organs (Chen et al., 2020a). Therefore, the ethylene receptor genes could show different responses to PTs growth. We generated series of ETR LOF mutants by using CRISPER CAS9 technology: *etr4-ko*, *etr5-ko* and *etr7-ko* as single mutants, and *etr1_2-ko*, *etr3_4-ko* and *etr5_7-ko* as double mutants. These mutants could be used to understand how the different ethylene receptor regulate the PTs growth.

Recently, it was found that ethylene plays a role in tomato pollen thermotolerance. They demonstrated that ethylene treatment, prior to heat-stress exposure, increased pollen quality (Jegadeesan et al., 2018). During my study, we aimed to investigate the role of ethylene receptors in pollen thermotolerance. Preliminary experiments showed that pollen tube growth was sill enhanced in *etr3-ko* at 34°C, when control PT growth wazs reduced compared to ambient temperature. We aimed also to check, pollen germination in vivo, the rate of burst, the callose plug formation in pollen tube, sperm cells division, and RNAseq analysis in *NR* and etr3-ko under heat stress. This study was blocked because of the Covid lockdown.

Our study was performed in vitro, studying the effect of ETRs on PTs growth in vivo would be helpful to extend our knowledge into the plant reproduction. I generated an ETR4-VENUS mutant, and preliminary fluorescence experiment showed strong fluorescence in the stigmatic papilla of pistil one day before anthesis (A-1) for ETR4-VENUS lines, suggesting that ETR4 play critical role for pollen germination in the stigma and may be PT elongation in the style.

Finally, further works could be performed to check what transcription factors activate the EBS:GUS expression, and to identify the direct targets of ACC signaling.

Moreover, studying whether ACC affect cell wall-modifying enzymes and calcium gradient in PTs, independently of ethylene perception in Arabidopsis by using 1-MCP or *etr1-1* for ethylene perception disruption, and *acs* octuple mutants in which ACC production is reduced.

Rasha Althiab-Almasaud contributions:

First chapter (review): I participated to the article design with all co-authors, I compiled the references and draw the illustrations in partnership with the other first joint author, and I participated to the writing of the text with all co-authors.

Second chapter (roles of ethylene perception in PT growth): I participated to the article design with all co-authors, I performed all experiments and data treatments, I wrote paragraphs about cell wall with E. Jamet and J.C. Mollet, and the paragraphs about calcium signaling with C Mazars, I wrote the first draft of all other parts with C. Chervin, and all co-authors edited the manuscript.

Last chapter (roles of ACC in PT growth): I participated to the design of the experiments with all co-authors, I performed all laboratory work and data analyses, and I wrote entirely the first draft, before edition with all co-authors

Annex I

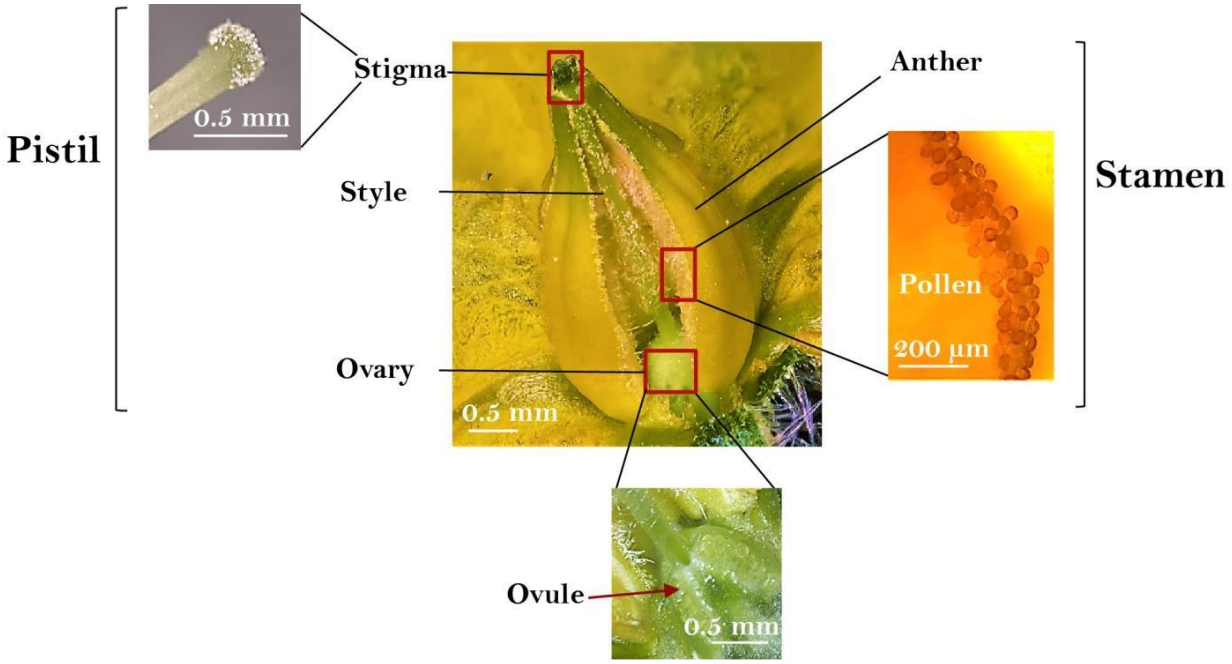

Figure S1. Flower morphology of *Solanum lycopersicum* (cv. MicroTom). The pictures show male and female reproductive parts of the tomato flower (stamen and pistil). Pictures were acquired with a ZEISS Axio ZoomV16 Microscope.

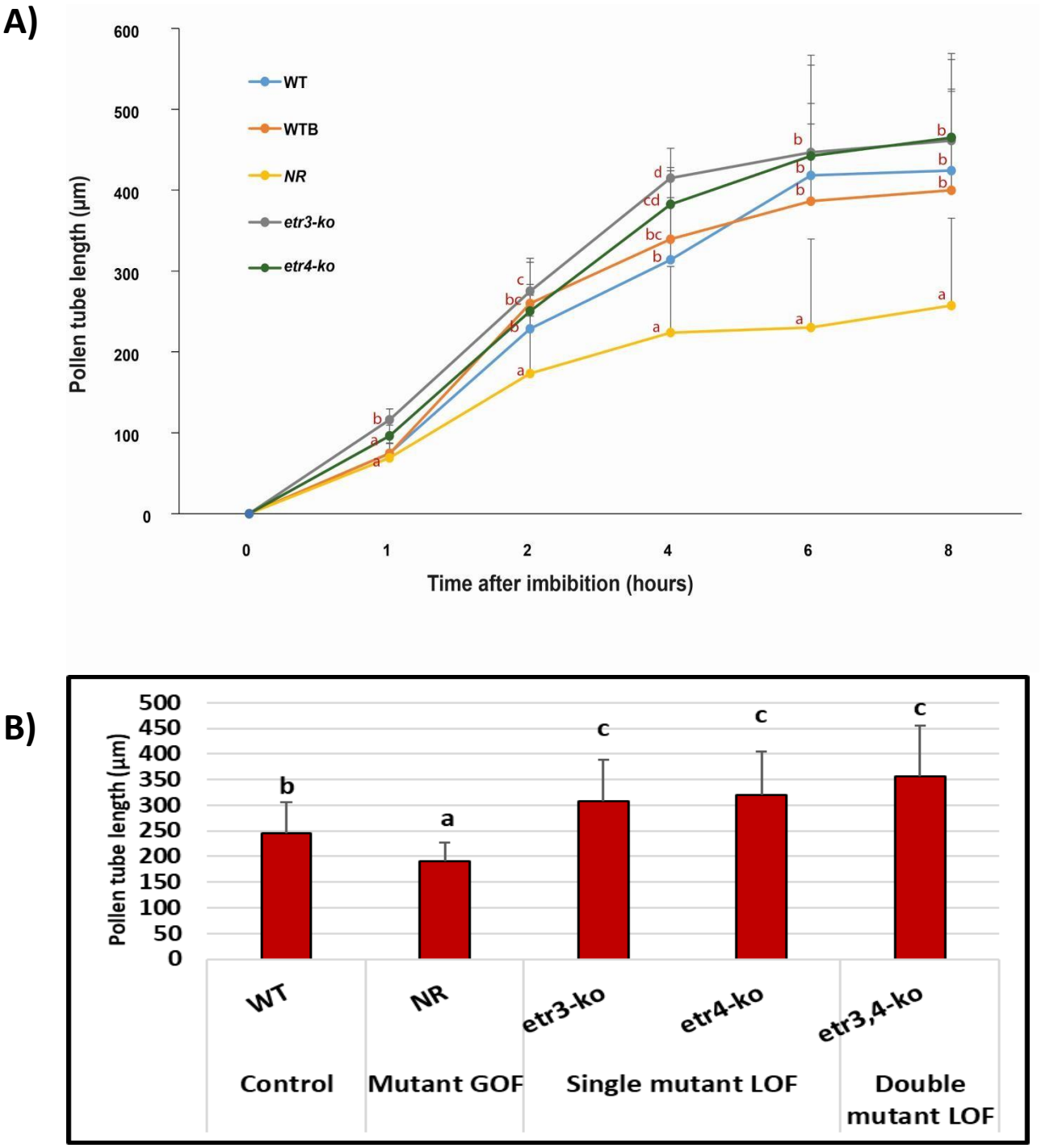

Figure S2. Tomato pollen tube (PT) growth as a function of time after imbibition. **A)** Five tomato line PTs were tested: WT, *etr3-ko*, *etr4-ko*, WTB, and *NR* grown on solid germination medium. n = 100 PTs. Error bars show SE and different letters indicate significant differences at $P < 0.05$ level (Tukey's HSD). **B)** Similar results of a different experiment, 4h after pollen grain imbibition, showing preliminary results with the *etr3,4-ko* double mutant. n = 50 PTs. Error bars show SE and different letters indicate significant differences at $P < 0.05$ level (Tukey's HSD).

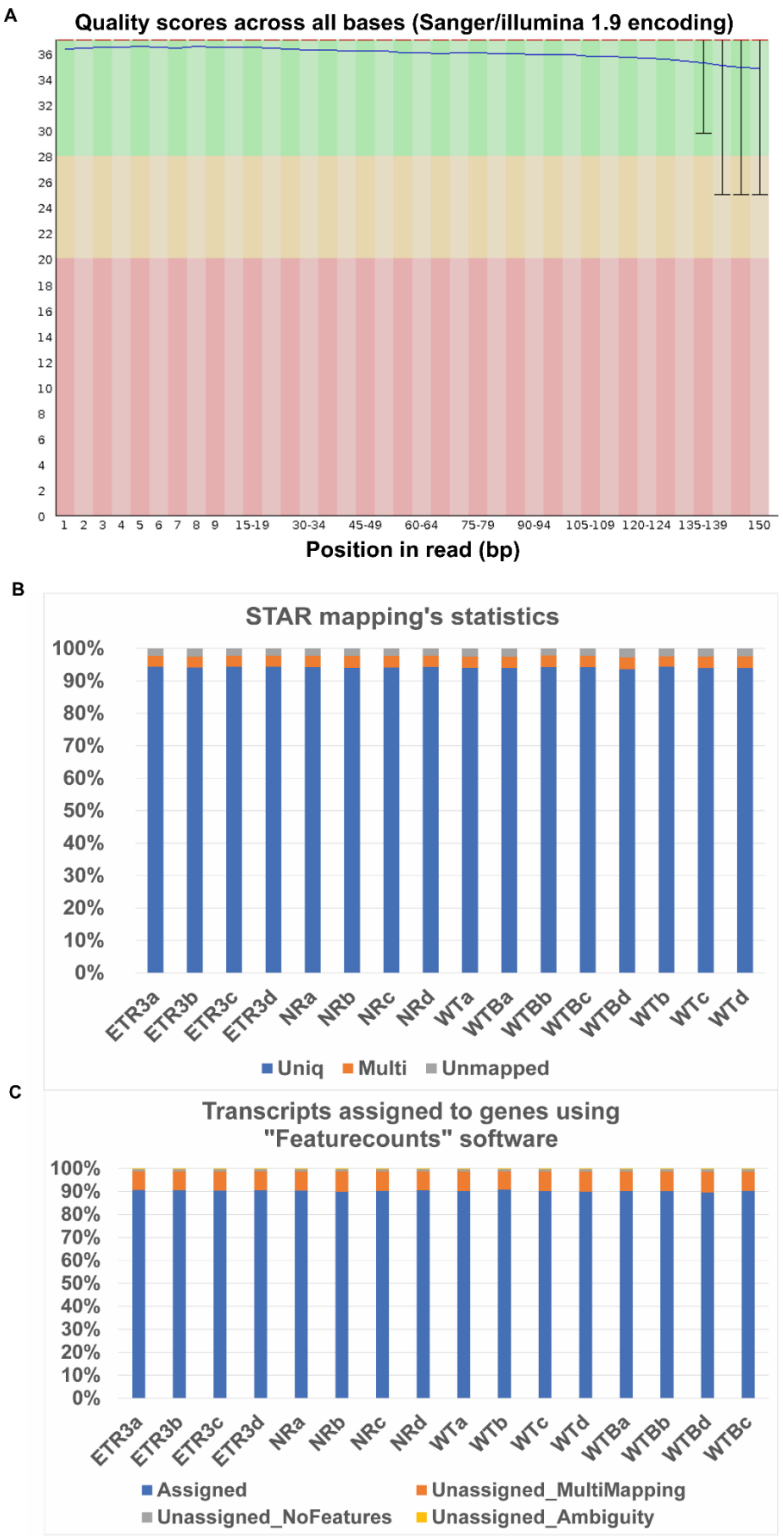

Figure S3. Quality indicators of RNAseq experiment. A. FastQC result describing quality scores across all bases along with the 150 bp long reads (Illumina 1.9 encoding). **B**. Percentage of reads mapped without any ambiguity. **C**. Percentage of the sequenced reads assigned to genes after the mapping process. In panels B and C, the four biological replicates are labeled a, b, c, and d. ETR3 stands for *etr3-ko*.

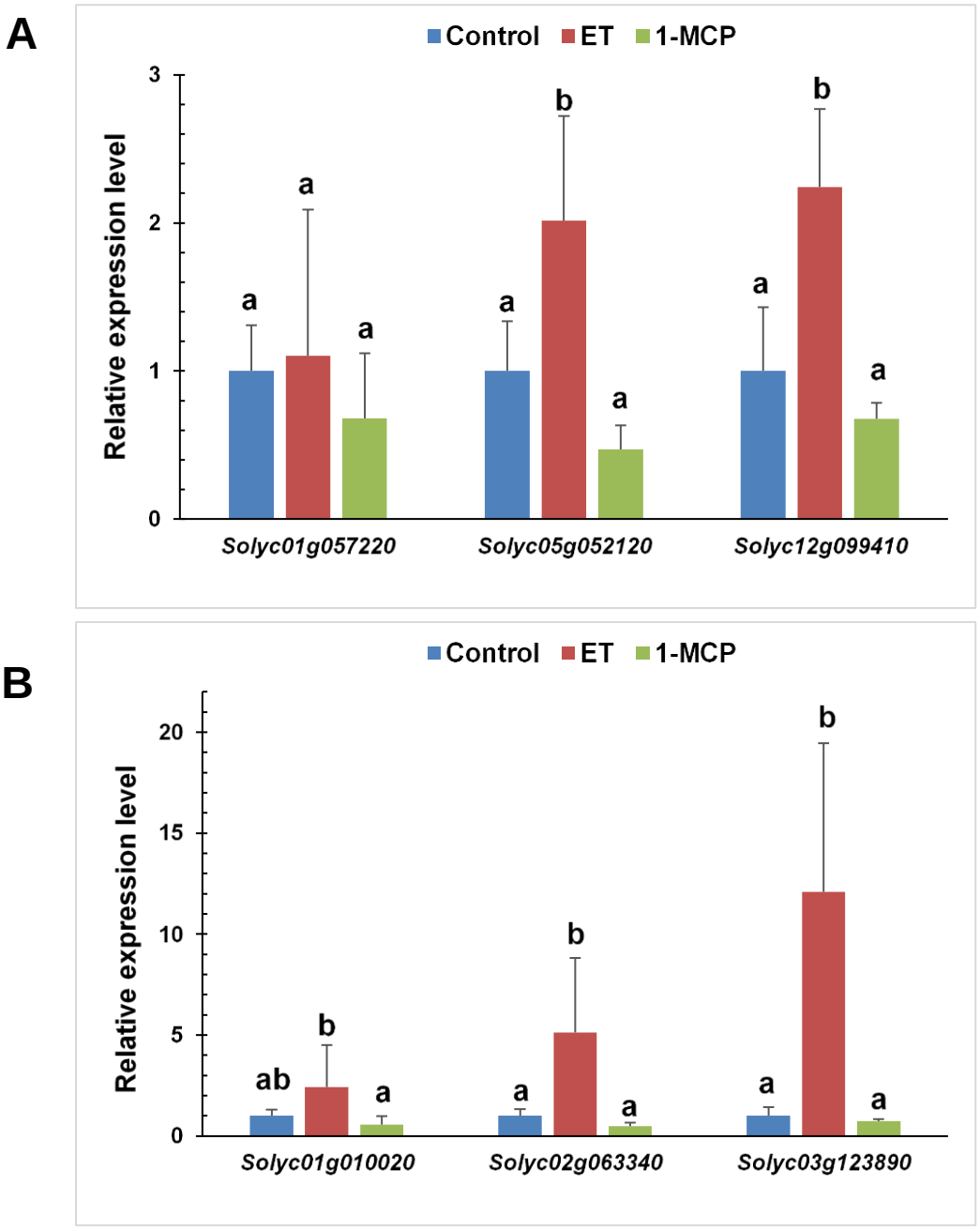

Figure S4. Expression levels of **A)** *PME* genes, and **B)** calcium related genes in germinating tomato pollen grains. ET stands for ethylene and 1-MCP for 1-methylcyclopropene, applied on WT pollen grains at 100 and 2 ppm, respectively, for 4 h over the imbibition and germination processes. n = 4 biological replicates, error bars show SE, different letters show significant differences at 0.05 level (Fisher's LSD). Relative expression was calculated with regard to each "Control", set as 1.

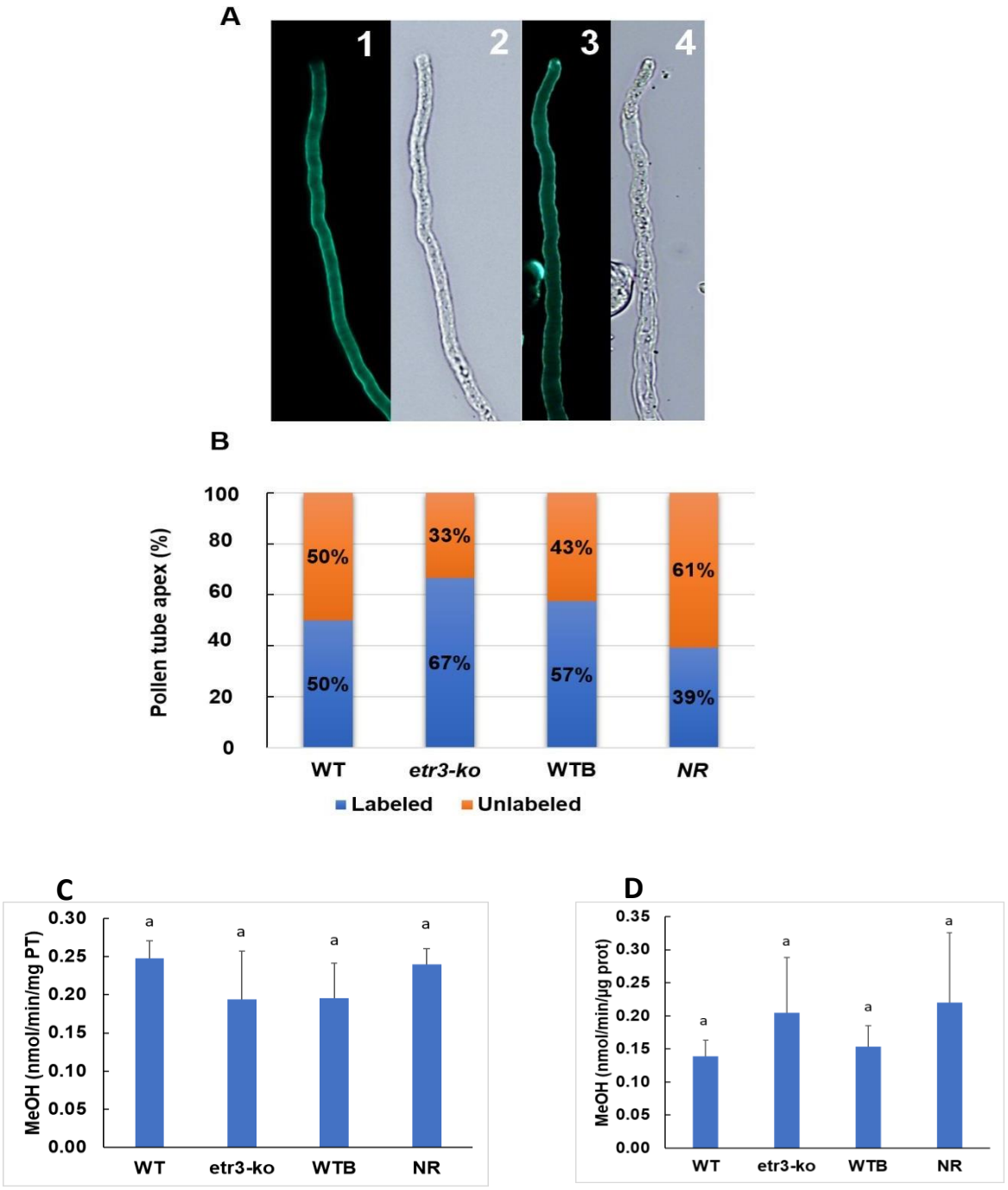

Figure S5. Immunolabeling of weakly methylesterified HG epitopes probed with LM19, and PME acitivity. **A**. Immunolabeling of wild-type PTs grown in liquid germination medium showing two cases: unlabeled PT tip (1-2) and labeled PT tip (3-4); 1 and 3: LM19 labeling; 2 and 4: bright field. **B**. Distribution of the two types of labeling: labeled and unlabeled PT tips, in the different tomato lines; n = 50 PTs were measured in each tomato line. Chi-square of independence between tomato lines and % labeled tips, $P = 0.072$. **C.** PME activity per PT fresh weight and **D.** Specific PME activity per µg protein; n = 3 biological replicates of 50 PTs, error bars show SE, absence of difference tested by Tukey's HSD at $P = 0.05$.

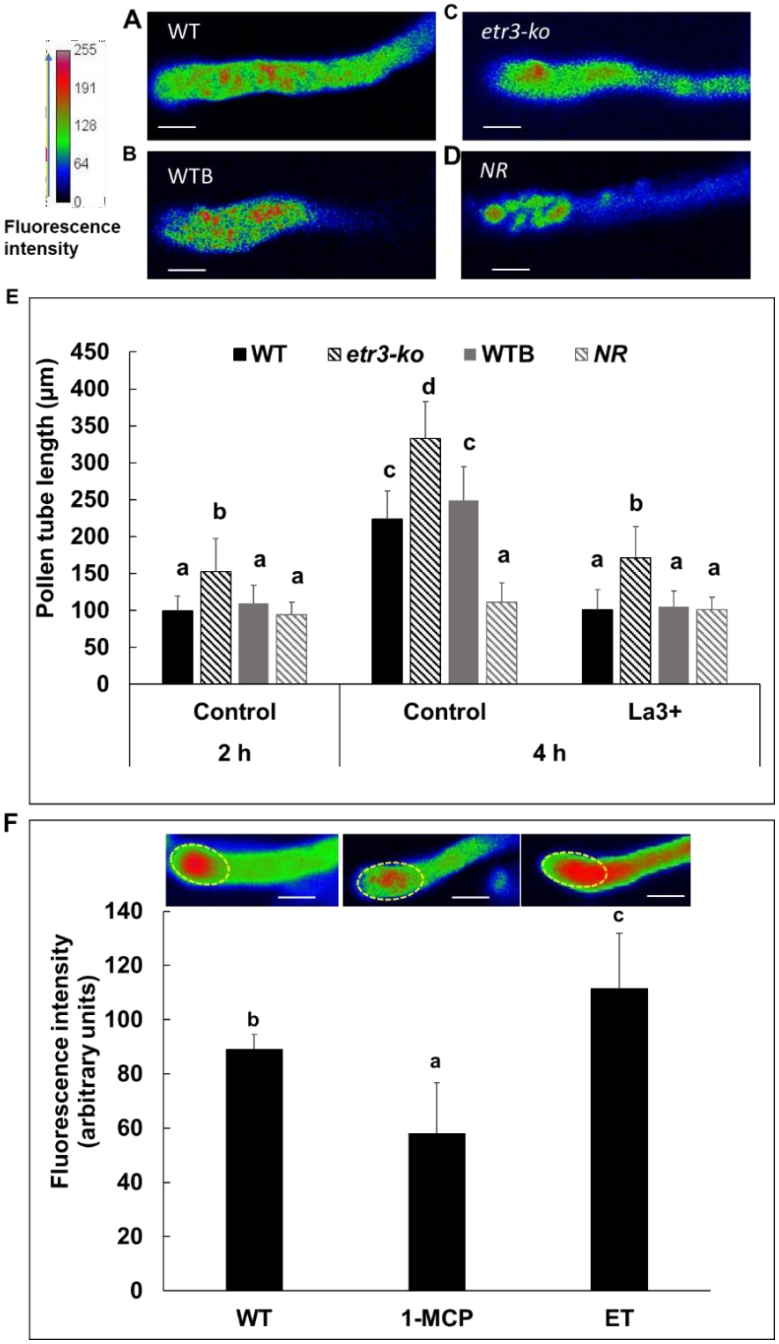

Figure S6. Ca2+ gradients in apical regions of pollen tubes. **A, B, C, D** are representative images of Ca^{2+} gradient 30 min after adding lanthanum (La^{3+}) in four tomato lines WT, *etr3-ko*, WTB and *NR* respectively, scale bars = 10 µm. Images of the controls without La^{3+} are shown in Figure 6. **E)** Tomato pollen tube (PT) growth on solid medium over time after imbibition and after La^{3+} application, same lines as above, n = 50 PTs. Error bars show SE and different letters indicate significant differences at $P < 0.05$ level (Tukey's HSD). La^{3+} was applied at 50 µM, two hours after imbibition of pollen grains, after the readings at "2h". **F)** Effect of 1-MCP (2 ppm) and exogenous ethylene ET (100 ppm), on Ca^{2+} gradient in WT pollen tubes, fluorescence intensity was assessed as in Fig. 6, n = 12 PTs for each line. Error bars show SE and different letters show significant differences at 0.05 level (Tukey's HSD).

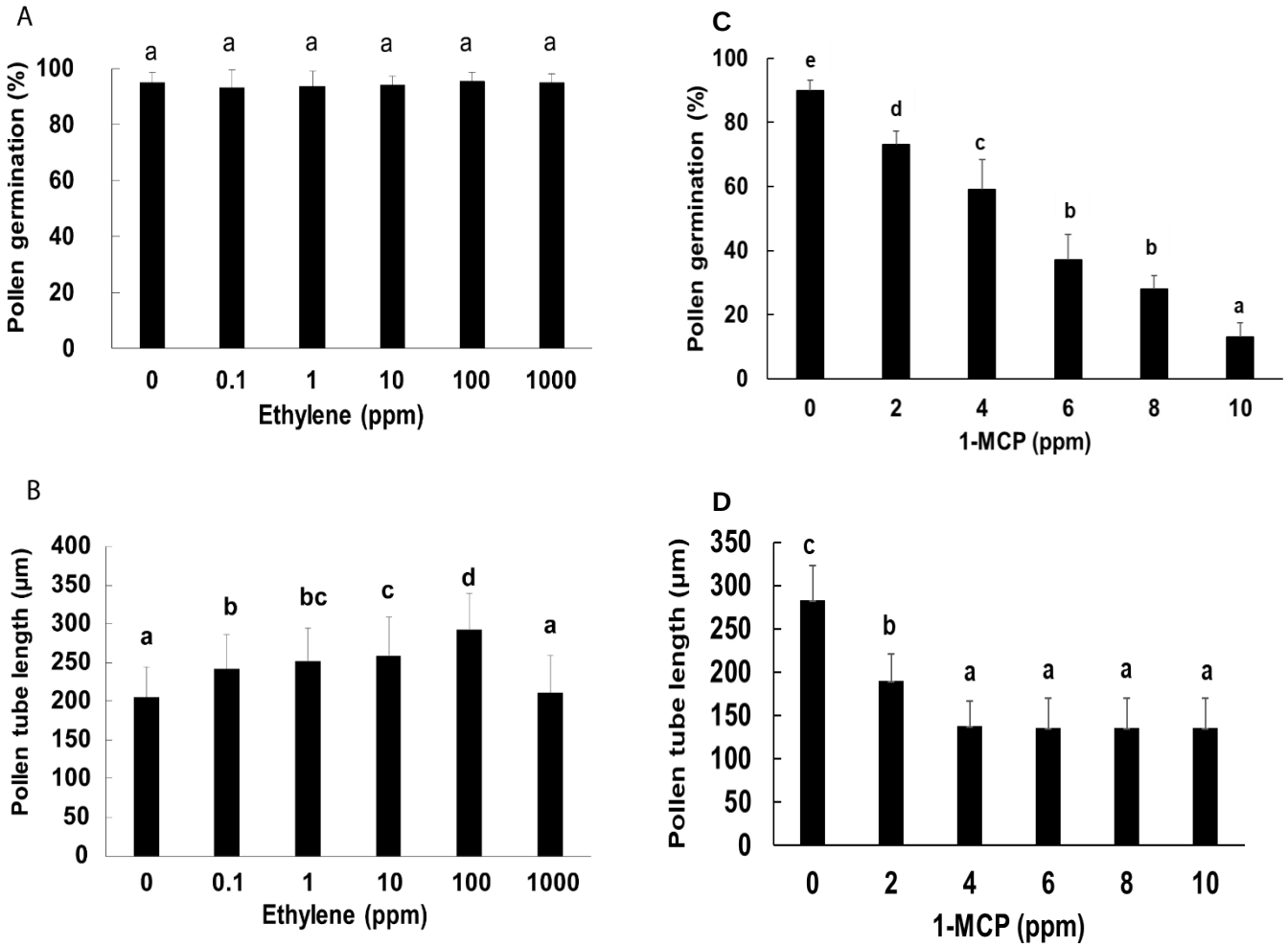

Figure S7. Effects of ethylene concentrations on (**A**) the rate of pollen germination and (**B**) the pollen tube growth of WT. Effects of 1-MCP concentration on (**C**) the rate of pollen germination and (**D**) the pollen tube growth of WT. These gases were added in the headspace over solid GM at the time of pollen grain imbibition and the measurements were performed 4 h after. n = 150 pollen grains. Error bars show SE. Different letters show significant differences at $P = 0.05$ (Tukey's HSD).

Figure S8. *etr3-ko* and *etr4-ko* tomato protein sequences with their relative wild-type sequences, the beginning of the ethylene binding pocket starts at AYFSIP, which is not translated in the mutants.

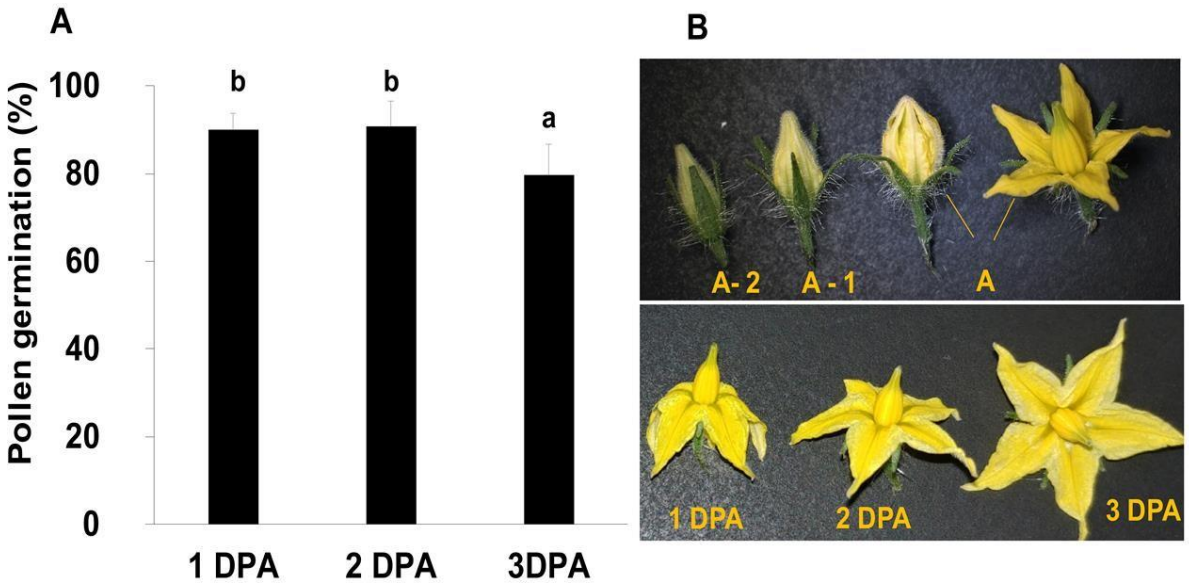

Figure S9. Pollen viability at different stages of flower development. **A.** Rate of pollen germination at 1, 2 and 3 days post-anthesis (DPA) (n = 100 pollen grains). **B.** Aspect of a tomato flower at 2 and 1 days before anthesis (A-2 and A-1, respectively), 0 day of anthesis (A) and 1, 2 and 3 DPA. The rate of pollen germination in solid germination medium at 1 and 2 DPA was about 90% and slightly decreased at 3 DPA. Error bars show SE. Different letters show significant differences at $P < 0.05$ level (Tukey's HSD).

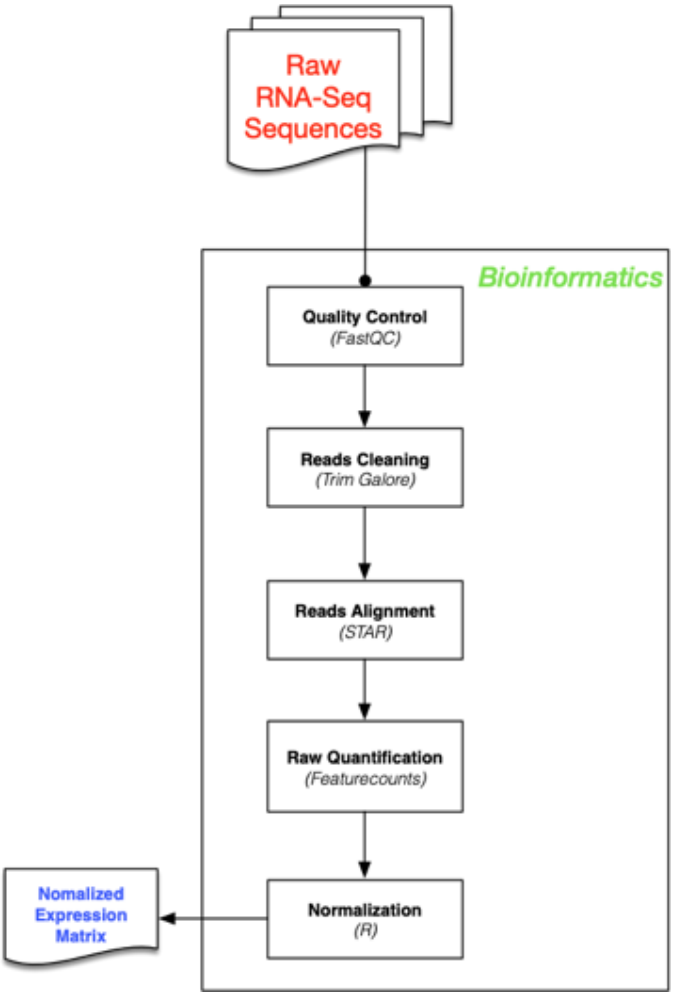

Figure S10. Overview of the RNA-Seq analysis pipeline. Different tools were used for the pre-processing steps of the raw sequencing data. FastQC is used to check the quality of raw reads, then the reads cleaning and filtering are performed by Trim Galore, Cleaned sequences are then mapped to the reference genome using STAR, gene expression are quantified by featureCounts, and differentially expressed genes are identified by DESeq2.

Table S1. Genes and primer sequences used for RT-qPCR analyses

Sly	Solyc	Description	Gene name	Forward primer	Reverse primer
Sly12g0054571	Solyc12g011330	Ethylene receptor 1	*ETR1*	5'-GCCTTTTATCTTCCATCGTGGA-'3	5'-GATACTTCATTAGCAAGTCGTCAGCA-'3
Sly07g0127601	Solyc07g056580	Ethylene receptor 2	*ETR2*	5'-TGGCATTCCTGGTCGCTTA-'3	5'-TCTGCATGTGATTTGCAGGC-'3
Sly09g0098021	Solyc09g075440	Never ripe-2	*ETR3/NR*	5'-GCTTTGGCTCTGGATTTACCTATTC-'3	5'-TTCCCGCCACGTTTAAGAGA-'3
Sly06g0363951	Solyc06g053710	Ethylene receptor homolog (ETR4)	*ETR4*	5'-GCCATACTGGTTTTGGTTCTACCTA-'3	5'-CCACAACCCTGACTATCTCAATTTC-'3
Sly11g0287841	Solyc11g006180	Ethylene receptor homolog (ETR5)	*ETR5*	5'-TGTTCAGATGATGCAGGGAAAT-'3	5'-ATGAGTGTCATCCCCTGCG-'3
Sly05g0160141	Solyc05g055070	Ethylene receptor homolog	*ETR7*	5'-CGCTTTTCCACGGATGTTCC-'3	5'-ATCATTCCCGCCCTCGATTC-'3
Sly01g0036821	Solyc01g101060	S-adenosyl-L-methionine synthetase	*SAM1*	5'-CCCATCTGGCCGATTCGTTA-'3	5'-GAGCACCCCAACCACCATAA-'3
Sly09g0079511	Solyc09g008280	S-adenosyl-L-methionine synthetase Z24743	*SAM2*	5'-AGGCATTGGGTTCGTCTCAG-'3	5'-AACTCCTTGGGCGATGTCAG-'3
Sly10g0167081	Solyc10g011660	Auxin-responsive GH3 family protein	*JAR1*	5'-TCTGAAGGATGGGTCGGAGT-'3	5'-TGCTCCACGCCAATGAGATT-'3
Sly03g0228041	Solyc03g123890	Calcium-transporting ATPase 1	*ACA1*	5'-AGGCTTGGCAAGATCTGACT-'3	5'-CCAGCCATCAAGAAAGGTGC-'3
Sly01g0005421	Solyc01g010020	Calmodulin 1	*CAM1*	5'-ACTAGAGTTAGCCGCGCTTC-'3	5'-TCGATGAACCCGTTGCCATT-'3
Sly02g0324371	Solyc02g063340	Calmodulin 4	*CAM4*	5'-CGCGAACGAATCTTCAAGCG-'3	5'-AGGCTTGCAATGTCTCTCCA-'3
Sly01g0015111	Solyc01g057220	Pectin Methylesterase	*PME*	5'-GCCAGCAATACAAAGAGCGG-'3	5'-GTTCTTAGGGTACGCAGCCA-'3
Sly05g0156841	Solyc05g052120	Pectin Methylesterase	*PME*	5'-CAGCACCAAGACCAGATGGA-'3	5'-CATGTGCTGTTACCATTGCCA-'3
Sly12g0075751	Solyc12g099410	Pectin Methylesterase	*PME*	5'-GCATTCGCTAACACGACTGG-'3	5'-GCCTTGCAACCCAACCATTT-'3

Table S2. A. Correlation between RNAseq and RT-qPCR data; B. Feedback of *ETR* mutations on *ETR* expressions

sorted from low to high expression levels in RNAseq

15 genes x 4 tomato lines = 60 samples

A.

gene	RNAseq counts	qPCR deltaCt	line
ETR2	0.000087	0.29	*etr3-ko*
ETR2	0.000262	1.36	WT
ETR2	0.000262	0.41	*NR*
ETR2	0.000698	1.65	WTB
ETR1	0.001342	0.27	*etr3-ko*
ETR1	0.002505	0.07	*NR*
ETR1	0.002774	1.08	WTB
ETR1	0.003132	1.73	WT
ETR7	0.001850	1.53	*etr3-ko*
ETR7	0.004183	1.41	*NR*
ETR7	0.004263	2.74	WTB
ETR7	0.004344	2.43	WT
ETR3	0.007987	47.80	*etr3-ko*
ETR3	0.014137	91.70	WTB
ETR3	0.016374	75.14	WT
ETR3	0.020687	138.42	*NR*
ETR5	0.030096	88.24	*etr3-ko*
ETR5	0.036425	116.72	WT
ETR5	0.036489	106.07	WTB
ETR5	0.090351	238.60	*NR*
ETR4	0.042133	56.77	*etr3-ko*
ETR4	0.046418	83.32	WTB
ETR4	0.057724	96.60	WT
ETR4	0.059926	108.35	*NR*
sam1	0.073538	9.76	*etr3-ko*
sam1	0.088719	12.99	WTB
sam1	0.137187	2.85	*NR*
sam1	0.202089	25.69	WT
CAM1	0.238729	209.96	*NR*
CAM1	0.259468	626.70	*etr3-ko*
CAM1	0.297791	340.74	WT
CAM1	0.300271	391.97	WTB
ACA1	0.195509	128.08	WTB
ACA1	0.226300	502.51	*etr3-ko*
ACA1	0.238905	109.84	WT
ACA1	0.406972	161.37	*NR*
sam2	0.352383	200.60	*NR*
sam2	0.368920	1189.29	*etr3-ko*
sam2	0.481639	276.46	WT
sam2	0.487476	311.09	WTB
CAM4	0.251938	236.89	*NR*
CAM4	0.406202	1069.21	*etr3-ko*
CAM4	0.510078	708.22	WT
CAM4	0.598450	832.25	WTB
PME Solyc01g057220	1.493015	937.34	*NR*
PME Solyc01g057220	1.707009	6245.20	*etr3-ko*
PME Solyc01g057220	2.158357	6202.50	WTB
PME Solyc01g057220	2.265294	2645.31	WT
PME Solyc05g052120	1.368004	805.35	*NR*
PME Solyc05g052120	1.958763	8455.75	*etr3-ko*
PME Solyc05g052120	2.404271	1986.78	WT
PME Solyc05g052120	2.576031	3153.37	WTB
JAR1	3.379268	1148.04	WTB
JAR1	3.511792	4281.60	*etr3-ko*
JAR1	3.659816	2293.50	WT
JAR1	4.486860	3959.67	*NR*
PME Solyc12g099410	41.865520	16355.93	NR
PME Solyc12g099410	44.722125	74966.51	*etr3-ko*
PME Solyc12g099410	47.019965	52546.94	WTB
PME Solyc12g099410	49.204294	25254.70	WT

B. Down- or up-regulation of *ETR* expression in *ETR* mutants, checked by RT-qPCR

	etr3-ko vs WT	*NR vs* WTB
ETR1	0.16	0.06
ETR2	0.21	0.25
ETR3	0.64	1.51
ETR4	0.59	1.30
ETR5	0.76	2.24
ETR6	too low	too low
ETR7	0.63	0.52

For full names of the genes see Table S1.

Genes in black: associated with ethylene perception

Genes in red: associated with ethylene synthesis and ACC conjugation

Genes in blue: associated with calcium signaling

Genes in green: associated with cell wall modification

coeff Pearson
with Excel 0.86

Pearson Product Moment Correlation
with SigmaPlot v11.0

Correlation Coefficient	0.864
P Value	6.681E-19
Number of Samples	60
Power	1

See https://doi.org/10.1111/tpj.15353 for

Supplemntal table 3

Supplemntal table 4

Supplemntal table 5

Annex II

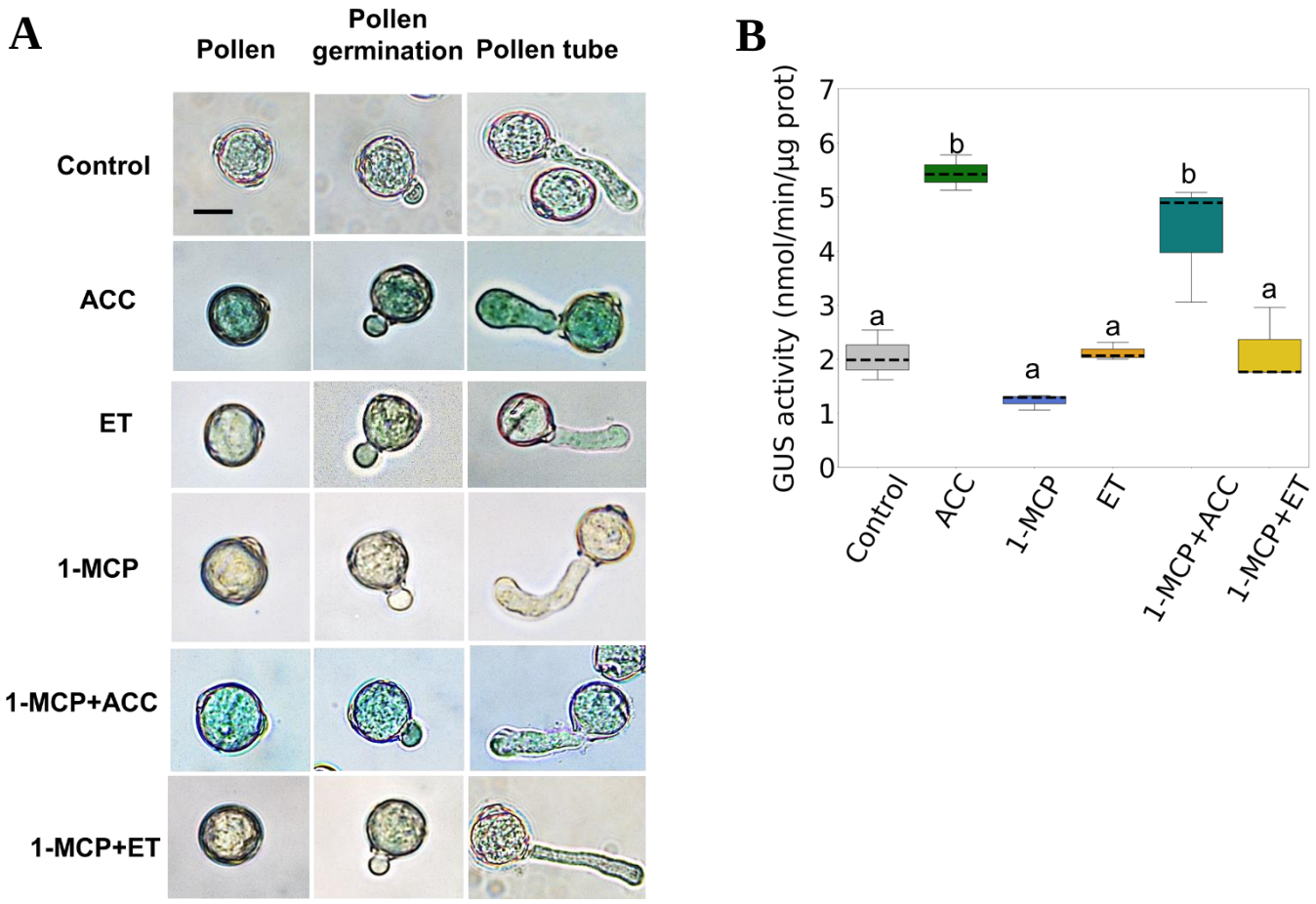

Figure S1. (A) Pictures showing expression of the EBS:GUS reporter in NR tomato pollen grains and tubes, after various treatments. Scale bar = 30 µm. **(B)** GUS activity assayed 4h after imbibition in NR PTs. n = 3 biological replicates of 0.5 mg pollen grains each, horizontal dashed lines show medians, different small letters show significant differences at the 0.05 level (Fisher's LSD).

Annex III (article in preparation)

Fruit set stages identification using deep learning

Abstract

The research in the plant reproduction was rapidly progressed considering the growth of population. For scientific research, the identification of different fruit set stages in tomato is important methods. Traditional detection methods of different stage of fruit set are identified manually by tagging and observation of the development stages, these methods consume time to precise the different growth stages. In recent years, AI (Artificial Intelligence) has been introduced in agriculture research, especially in the field of automated image analysis, which have shown their efficiency in image processing with high accuracy. In this study, we propose an improved YOLOV3-tiny model for detecting different fruit set stages in tomato. Our dataset contains more than 1145 images and 3315 annotations in total. The dataset contains class information for seven stages of a tomato fruit set. Images are initially collected, and subsequently augmented. The augmented images are used to create training sets with 3000 annotations. The training of the model was performed by 800 epochs, the trained model is tested on a test dataset. The test results show that the proposed improved YOLOV3-tiny model is superior to the original YOLOV3 and YOLOV3-tiny models, with average detection time of the model is 0.203 s per frame, which can provide real-time detection of tomato fruit set stages however under overlapping flowers. Moreover, this model is small and efficient that it would increase the applicability of real-time even when small hardware devices are used.

1- Introduction

In recent years, the research in the plant reproduction was rapidly progressed considering the growth of population **(Pereira & Coimbra, 2019)**. Tomato is one of the most popular vegetables that play a significant role in the agricultural economy. Previously, the studies focus on plant reproduction processes for increasing crop productivity. The transition from flower to young fruit, namely fruit set, is an initial step of fruit

development to ensure successful sexual plant reproduction, and fruit set efficiency is important features that determine the production and yield of various crops **(An *et al.*, 2020).**

Besides its importance as an economically important crop with large production, and its nutritional importance, tomato (Solanum lycopersicum L.) has been considered as a model for scientific research **(Sun *et al.*, 2006)**. Most of these researchers based on the application of molecular biology techniques to understandthe genetic and molecular mechanisms that regulate plant reproduction **(Hu *et al.*, 2020).**

The accurate identification of the different stage of tomato fruits set as well as the identification of their ripening stage is considered challenging and essential tasks for the researchers: Althiab-almasaud et al 2021 studied the impacts of Ethylene signaling on pollen tubes collected from 1DPA and 2DPA stages. In the usual case, the different stage of fruit set is identified manually by tagging and observation of the development stages which could take several days. Moreover, tagging preselected flowers constraint the independency in the experimental plan if several stages are required.

Recently, the interest in the development of deep learning as a powerful technique in the artificial intelligence field for various agricultural procedures was increased.

The beginning of its applications was in the diseases and fruit detection, which can solve the main problems with fruit-and vegetable-picking robots, like the complex scenes such as backlighting, direct sunlight, overlapping fruit and branches, blocking leaves, etc. **(Xu et al, 2020)**

Li et al (2019) purpose a deep learning-based system to identify and count a very small pest, wheat mites. Similarly, in tomato for the early detection of gray leaf spot disease **(Liu & Wang, 2020a, b).** Also, **Tsironis et al, (2020)** demonstrated that deep learning-based classification and detection could provide information for the ripening stage of tomato fruit**.** Moreover, deep learning methods can effectively provide apple fruit detection under overlapping apples and identify their growth stages for yield estimation **(Tian et al, 2019).**

In this study, we aim to develop a robust tool, based on deep learning, provide an accurate detection and identification of seven different fruit-set stages and able to be used by researchers in real time application.

2- Materials and methods

2-1. Dataset used in the research

This study was performed on *Solanum lycopersicum,* cv. MicroTom: wild type (WT), Seeds were sterilized with 5% NaClO for 8 min, then washed 3 times with sterilized water, the seedling were grown in a culture room, with a 16h day: 8h night cycle, associated with temperature 22°C:18°C cycle, respectively, under 80% relative humidity and a day light intensity of 250 $\mu mol \cdot m^{-2} \cdot s^{-1}$. Seven different stages of flower development were used, at two and one days before anthesis (A-2 and A-1), 0 day of anthesis (A), one, two, three and four days post-anthesis (DPA). We check the different stages by tagging and observing the flower over all their development stages. The images of flowers were captured using a digital camera Panasonic, DMC-FZ62. To ensure the diversity of tomato flower image dataset, the images are obtained from different patches and different greenhouse. The aforementioned dataset is annotated using the "makesense.ai tool" which it is given output files that correspond relationship between labels and data, the dataset is randomly divided into training and test datasets according to the proportion of 80 and 20% respectively. The training and detection of the tomato fruit set object detection network model was programmed in Python. We use the precision, f1-score parameters and time (s) evaluation indexes to evaluate our method. The calculation formulas of precision (P) and f1-score (F1) are shown in formula (1)

(1) $$Precision = \frac{TP}{Total\ positive\ results} \quad Recall = \frac{TP}{Total\ predicted\ cases} \quad F1 = 2 * \frac{Precision * Recall}{Precision + Recall}$$

where TP is the number of true positive samples

2.3 Models:

The YOLO ("You Only Look Once") algorithm was proposed by **Redmon et al. in 2016** and based on Darknet object detection neural network architecture. In a single pass through its network, YOLO combines detection, classification, and localization of objects inside an image. This makes it more computationally efficient and robust than other networks that only perform one or two of these tasks simultaneously.

Principle of YOLOv3 model

YOLOv3 is the third generation of YOLO with faster object detection network and improved detection precision compared with that of YOLO1 and YOLOv2. YOLOv3 uses darknet-53 for feature extraction, with

74 CNN and 32 more deep learning layers (Figure1), which is more powerful than the YOLOv2 with darknet-19. The model size of YOLOv3 is approximately 247 MB, with detection speed is only 1-2 frames/s on an embedded platform, which makes it undesirable for embedded devices. YOLOv3-tiny is the lightweight version containing a reduced number of layers that led to accelerate the detection much more comparing to YOLOv3 model. The model size is only 34.7MB. It can run on embedded or mobile devices. However, its backbone network has only 7 layers, and then features are extracted by using a small number of 1x1 and 3x3 convolutional layers so it cannot extract higher level semantic features, and its precision is low.

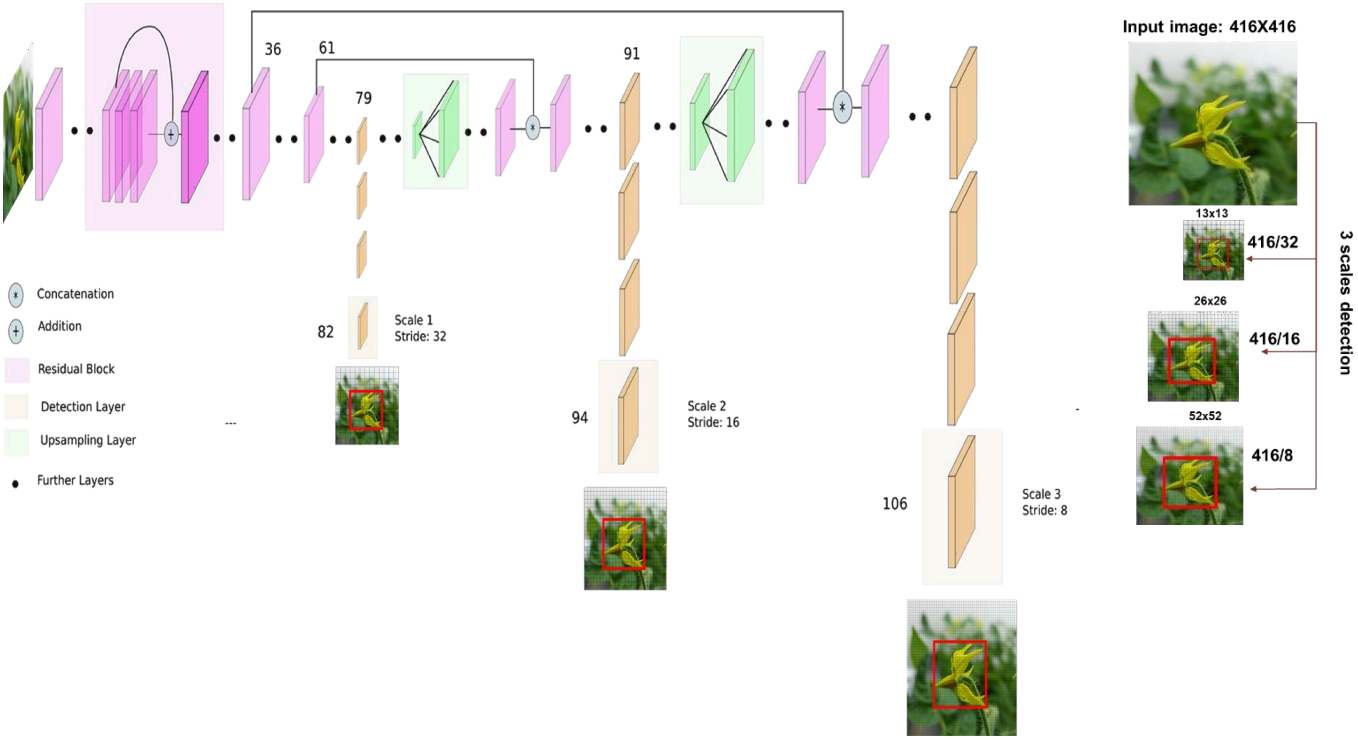

Figure1. YOLOv3 network model

How it works:

YOLO v3 makes prediction at three scales given by downsampling the dimensions of the input image following three ratios: 32, 16 and 8 which are the strides of the network. For example, if we have an input image with 416X416, the resultant feature map would be of size 13 x 13 at first scale then of dimensions of 26 x 26 and 52 x 52 at both second and third scale. To perform the prediction, YOLO uses 9 anchor boxes to trace of bounding box corresponding to three at each grid cell. Those bounding box have similar shape and size is to those of objects in the training dataset. The network applies the anchor to the following formulae to obtain bounding box predictions:

$$b_x = \sigma(t_x) + c_x$$
$$b_y = \sigma(t_y) + c_y$$
$$b_w = p_w e^{t_w}$$
$$b_h = p_h e^{t_h}$$

Where: b_x, b_y, bw, b_h are the x,y center co-ordinates, width and height of the prediction. t_x, t_y, t_w, t_h are the parameters predicted by the network to fit the detected object. cx and cy are the adding offset of the cell origin from the image origin. pw and p_h are width and height of the anchor box.

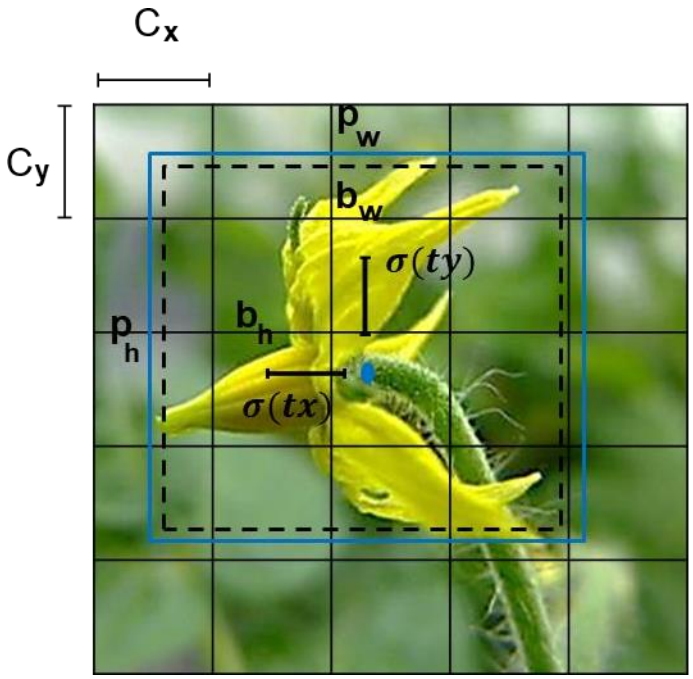

$$b_x = \sigma(t_x) + c_x$$
$$b_y = \sigma(t_y) + c_y$$
$$b_w = p_w e^{t_w}$$
$$b_h = p_h e^{t_h}$$

For an input image of size 416 x 416, YOLO predicts ((52 x 52) + (26 x 26) + 13 x 13)) x 3 = **10647** bounding boxes. However, the algorithm predicts the "objectness" score for each bounding box, which presents the likelihood that the predicted bounding box contains an object, as well as its class score. Thus, Yolo filter out detections with low probability below a predefined probability threshold (e.g., 0.15). However, the network still ends up with a lot of duplicate detections since it makes 3 predictions at each cell. Those could be filtered out via non-maximum suppression (NMS) which calculates the Intersection over Union IOU to identify the level of overlapping between predicted bounding boxes and keep only those with highest confidence score.

3- Results

After the training of the model, the test results are shown in (Figure2). In our model, F1 score is increased by 2 %, and the mean average precision (mAP) was increased from 80.7 to 86.5% comparing with the YOLOv3-tiny. Moreover, the average detection time of our model is 0.205 s per frame comparing with 1s per frame in original YOLOv3.

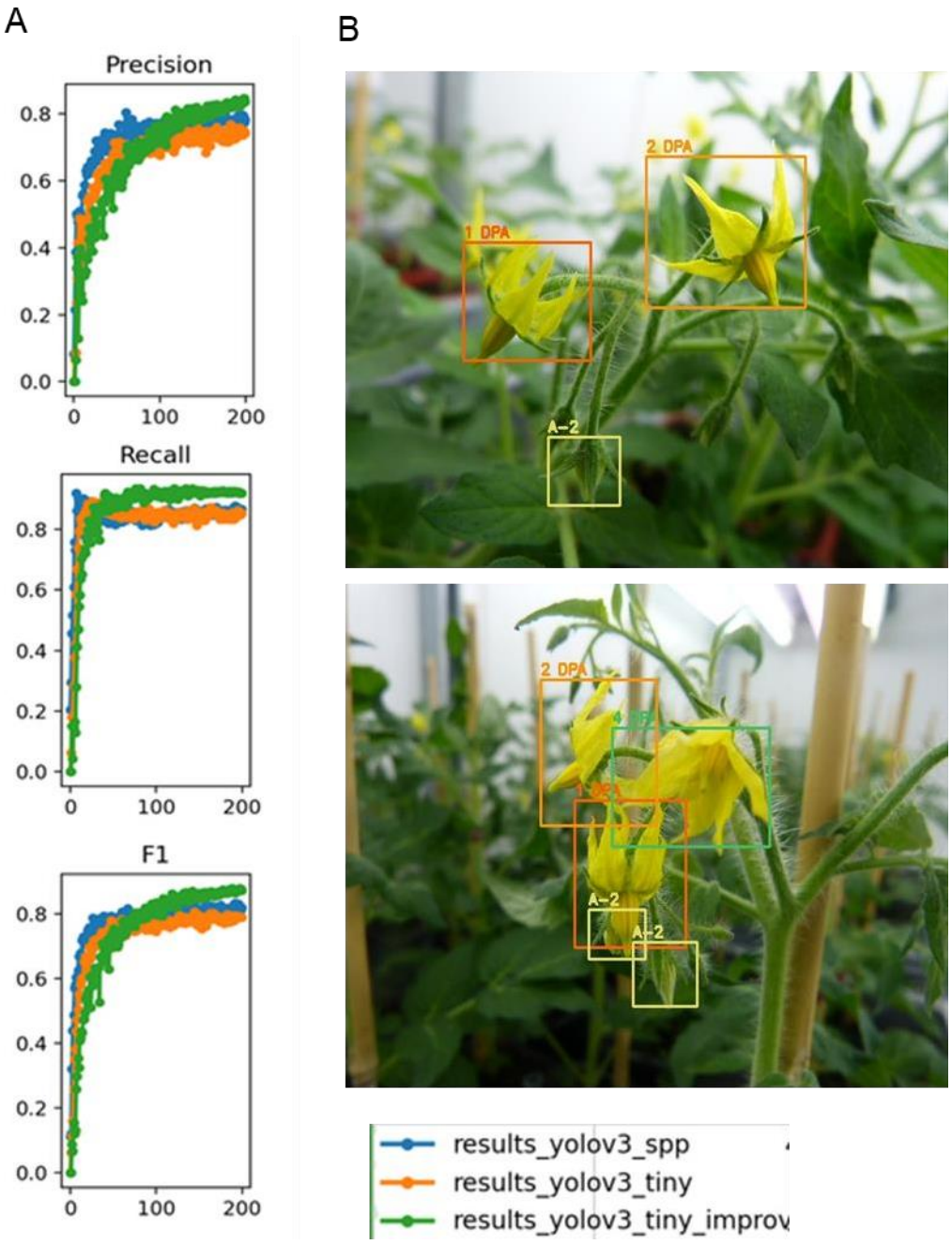

Figure2. **A)** Precision, Recall and FI curves of the original YOLOv3, tiny and tiny improved models which were evaluated on tomato fruit set images. **B)** Images show the detection results of YOLOv3-tiny improved in tomato fruit-set stages.

4- Conclusion

Considering that the deep network model increases the detection time, which is not feasible to real-time performance. Thus, deepening the network layer of YOLOv3-tiny can make it more abundant convolution features. In this study, we combine the high precision of original YOLOv3 and the fast detection of YOLOv3-tiny to provide at the end a real-time detection that is based on improved convolutional neural networks. Our data show that YOLOv3-tiny improved model detects the different stages of tomato fruit set with high accuracy in real time that could be used it to embedded devices, mobile devices and other smaller systems.

5- References (of the Annex III)

Althiab Almasaud R., Chen Y., Maza E., Djari A., Frasse P., Mollet J.C., Mazars C., Jamet E., Chervin C. (2021). Ethylene signaling modulates tomato pollen tube growth, through modifications of cell wall remodeling and calcium gradient. *Plant J.*, https://doi.org/10.1111/tpj.15353

An, J., Althiab Almasaud, R., Bouzayen, M., Zouine, M. and Chervin, C. (2020) Auxin and ethylene regulation of fruit set. *Plant Sci.*, **292**. 110381

Chen, P., Li, W.L., Yao, S.J., Ma, C., Zhang, J., Wang, B., Zheng, C.H., Xie, C.J. and Liang, D. (2021) Recognition and counting of wheat mites in wheat fields by a three-step deep learning method. *Neurocomputing*, **437**, 21–30.

Hu, G., Huang, B., Wang, K., et al. (2020) Histone posttranslational modifications rather than DNA methylation underlie gene reprogramming in pollination-dependent and pollination-independent fruit set in tomato. *New Phytol.*, nph.16902.

Liu, J. and Wang, X. (2020a) Early recognition of tomato gray leaf spot disease based on MobileNetv2-YOLOv3 model. *Plant Methods*, **16**, 1–16.

Liu, J. and Wang, X. (2020b) Tomato Diseases and Pests Detection Based on Improved Yolo V3 Convolutional Neural Network. *Front. Plant Sci.*, **11**, 1–12.

Pereira, A.M. and Coimbra, S. (2019) Advances in plant reproduction: From gametes to seeds. *J. Exp. Bot.*, **70**, 2933–2936.

Sun, H.-J., Uchii, S., Watanabe, S. and Ezura, H. (2006) A Highly Efficient Transformation Protocol for Micro-Tom, a Model Cultivar for Tomato Functional Genomics. *Plant Cell Physiol.*, **47**, 426–431..

Tian, Y., Yang, G., Wang, Z., Wang, H., Li, E. and Liang, Z. (2019) Apple detection during different growth stages in orchards using the improved YOLO-V3 model. *Comput. Electron. Agric.*, **157**, 417–426.

Tsironis, V., Bourou, S. and Stentoumis, C. (2020) Tomatod: Evaluation of object detection algorithms on a new real-world tomato dataset. *Int. Arch. Photogramm. Remote Sens. Spat. Inf. Sci. - ISPRS Arch.*, **43**, 1077–1084.

Xu, Z.F., Jia, R.S., Liu, Y.B., Zhao, C.Y. and Sun, H.M. (2020) Fast method of detecting tomatoes in a complex scene for picking robots. *IEEE Access*, **8**, 55289–55299.

References of the PhD thesis

Althiab Almasaud R., Chen Y., Maza E., Djari A., Frasse P., Mollet J.C., Mazars C., Jamet E., Chervin C. (2021). Ethylene signaling modulates tomato pollen tube growth, through modifications of cell wall remodeling and calcium gradient. *Plant J.*, 107, 893–908. https://doi.org/10.1111/tpj.15353

Abràmoff, M.D., Magalhães, P.J. and Ram, S.J. (2004) Image Processing with ImageJ. *Biophotonics Int.*, **11**, 36–42.

Aloni, R., Aloni, E., Langhans, M. and Ullrich, C.I. (2006) Role of auxin in regulating Arabidopsis flower development. *Planta*, **223**, 315–328.

An, J., Althiab Almasaud, R., Bouzayen, M., Zouine, M. and Chervin, C. (2020) Auxin and ethylene regulation of fruit set. *Plant Sci.*, **292**, 110381

Andrews, S. (2010). FastQC: A quality control tool for high throughput sequence data [Online]. http://www.bioinformatics.babraham.ac.uk/projects/fastqc/

Astegno, A., Bonza, M.C., Vallone, R., Verde, V. La, D'Onofrio, M., Luoni, L., Molesini, B. and Dominici, P. (2017) Arabidopsis calmodulin-like protein CML36 is a calcium (Ca2+) sensor that interacts with the plasma membrane Ca2+-ATPase isoform ACA8 and stimulates its activity. *J. Biol. Chem.*, **292**, 15049–15061.

Baldwin, L., Domon J.M., Klimek J.F., Fournet F., Sellier H., Gillet F., Pelloux J., Lejeune-Hénaut I., Carpita N.C., Rayon C. (2014). Structural alteration of cell wall pectins accompanies pea development in response to cold. *Phytochem*. **104**, 37-47.

Benjamini, Y. and Hochberg, Y. (1995) Controlling the False Discovery Rate: A Practical and Powerful Approach to Multiple Testing. *J. R. Stat. Soc. Ser. B*, **57**, 289–300.

Berger, F., Hamamura, Y., Ingouff, M. and Higashiyama, T. (2008) Double fertilization - caught in the act. *Trends Plant Sci.*, **13**, 437–443.

Bernardi, J., Lanubile, A., Li, Q.-B., Kumar, D., Kladnik, A., Cook, S.D., Ross, J.J., Marocco, A. and Chourey, P.S. (2012) Impaired auxin biosynthesis in the defective endosperm18 mutant is due to mutational loss of expression in the ZmYuc1 gene encoding endosperm-specific YUCCA1 protein in maize. *Plant Physiol.*, **160**, 1318–28.

Bianchetti, R.E., Cruz, A.B., Oliveira, B.S., Demarco, D., Purgatto, E., Peres, L.E.P., Rossi, M. and Freschi, L. (2017) Phytochromobilin deficiency impairs sugar metabolism through the regulation of cytokinin and auxin signaling in tomato fruits. *Sci. Rep.*, **7,** 7822.

Binder, B.M. (2020) Ethylene signaling in plants. *J. Biol. Chem.*, **295**, 7710–7725.

Binder, B.M., Walker, J.M., Gagne, J.M., Emborg, T.J., Hemmann, G., Bleecker, A.B. and Vierstra, R.D. (2007) The Arabidopsis EIN3 binding F-Box proteins EBF1 and EBF2 have distinct but overlapping roles in ethylene signaling. *Plant Cell*, **19**, 509–523.

Bisson, M.M.A. and Groth, G. (2015) Targeting Plant Ethylene Responses by Controlling Essential Protein-Protein Interactions in the Ethylene Pathway. *Mol. Plant*, **8**, 1165–1174.

Bosch, M. (2005) Pectin Methylesterase, a Regulator of Pollen Tube Growth. *Plant Physiol.*, **138**, 1334–1346.

Brummell, D.A. (2006) Cell wall disassembly in ripening fruit. *Funct. Plant Biol.*, **33**, 103-119.

Bulens, I., Poel, B. Van de, Hertog, M.L.A.T.M., Proft, M.P. De, Geeraerd, A.H. and Nicolaï, B.M. (2011) Protocol: An updated integrated methodology for analysis of metabolites and enzyme activities of ethylene biosynthesis. *Plant Methods*, **7**, 17.

Bürstenbinder, K., Mitra, D. and Quegwer, J. (2017) Functions of IQD proteins as hubs in cellular calcium and auxin signaling: A toolbox for shape formation and tissue-specification in plants? *Plant Signal. Behav.*, **12**, e1331198.

Cai, X., Xu, P., Zhao, P., Liu, R., Yu, L. and Xiang, C. (2014) Arabidopsis ERF109 mediates cross-talk between jasmonic acid and auxin biosynthesis during lateral root formation. *Nat. Commun.*, **5**, 1–13.

Carbonell-Bejerano, P., Urbez, C., Granell, A., Carbonell, J. and Perez-Amador, M.A. (2011) Ethylene is involved in pistil fate by modulating the onset of ovule senescence and the GA-mediated fruit set in Arabidopsis. *BMC Plant Biol.*, **11**. 84.

Carvalho, R.F., Campos, M.L., Pino, L.E., Crestana, S.L., Zsögön, A., Lima, J.E., Benedito, V.A. and Peres, L.E.P. (2011) Convergence of developmental mutants into a single tomato model system: "Micro-Tom" as an effective toolkit for plant development research. *Plant Methods*, **7**, 18.

Cecchetti, V., Altamura, M.M., Falasca, G., Costantino, P. and Cardarelli, M. (2008) Auxin Regulates Arabidopsis Anther Dehiscence, Pollen Maturation, and Filament Elongation. *Plant Cell Online*, **20**, 1760–1774.

Chang, C. (2016) Q and A: How do plants respond to ethylene and what is its importance? *BMC Biol.*, **14**, 7.

Chapman, E.J. and Estelle, M. (2009) Mechanism of Auxin-Regulated Gene Expression in Plants. *Annu. Rev. Genet.*, **43**, 265–285.

Chebli, Y., Kaneda, M., Zerzour, R. and Geitmann, A. (2012) The Cell Wall of the Arabidopsis Pollen Tube Spatial Distribution, Recycling, and Network Formation of Polysaccharides. *Plant Physiol.*, **160**, 1940–1955.

Chen, D. and Zhao, J. (2008) Free IAA in stigmas and styles during pollen germination and pollen tube growth of Nicotiana tabacum. *Physiol. Plant.*, **134**, 202–215.

Chen, Y., Hu, G., Rodriguez, C., Liu, M., Binder, B.M. and Chervin, C. (2020a) Roles of SlETR7, a newly discovered ethylene receptor, in tomato plant and fruit development. *Hortic. Res.*, **7**, 17.

Chen, Y., Althiab Almasaud, R., Carrie, E., Desbrosses, G., Binder, B.M. and Chervin, C. (2020b) Ethanol, at physiological concentrations, affects ethylene sensing in tomato germinating seeds and seedlings. *Plant Sci.*, **291**, 110368.

Chen, Y., Rofidal, V., Hem, S., et al. (2019) Targeted proteomics allows quantification of ethylene receptors and reveals SlETR3 accumulation in never-ripe tomatoes. *Front. Plant Sci.*, **10**, 1-10.

Cheng, Y., Dai, X. and Zhao, Y. (2006) Auxin biosynthesis by the YUCCA flavin monooxygenases controls the formation of floral organs and vascular tissues in Arabidopsis. *Genes Dev.*, **20**, 1790–1809.

Dearnaley, J.D.W. and Daggard, G.A. (2001) Expression of a polygalacturonase enzyme in germinating

pollen of Brassica napus. *Sex. Plant Reprod.*, **13**, 265–271.

Dehors, J., Mareck, A., Kiefer-Meyer, M.-C., Menu-Bouaouiche, L., Lehner, A. and Mollet, J.-C. (2019) Evolution of Cell Wall Polymers in Tip-Growing Land Plant Gametophytes: Composition, Distribution, Functional Aspects and Their Remodeling. *Front. Plant Sci.*, **10**, 1–28.

Dhankher, O.P. and Foyer, C.H. (2018) Climate resilient crops for improving global food security and safety. *Plant Cell Environ.*, **41**, 877–884.

Dharmasiri, N., Dharmasiri, S., Estelle, M., Kepinski, S. and Leyser, O. (2005) The F-box protein TIR1 is an auxin receptor. *Nature*, **435**, 441–445.

Dobin, A., Davis, C.A., Schlesinger, F., Drenkow, J., Zaleski, C., Jha, S., Batut, P., Chaisson, M. and Gingeras, T.R. (2013) STAR: Ultrafast universal RNA-seq aligner. *Bioinformatics*, **29**, 15–21.

Du, L., Bao, C., Hu, T., Zhu, Q., Hu, H., He, Q. and Mao, W. (2016) SmARF8, a transcription factor involved in parthenocarpy in eggplant. *Mol. Genet. Genomics*, **291**, 93–105.

Duan, Q.-H., Wang, D.-H., Xu, Z.-H. and Bai, S.-N. (2008) Stamen development in Arabidopsis is arrested by organ-specific overexpression of a cucumber ethylene synthesis gene CsACO2. *Planta*, **228**, 537–543.

Dumont, M., Lehner, A., Bouton, S., Kiefer-Meyer, M.C., Voxeur, A., Pelloux, J., Lerouge, P. and Mollet, J.C. (2014) The cell wall pectic polymer rhamnogalacturonan-II is required for proper pollen tube elongation: Implications of a putative sialyltransferase-like protein. *Ann. Bot.*, **114**, 1177–1188.

Edlund, A.F., Swanson, R. and Preuss, D. (2004) Pollen and stigma structure and function: the role of diversity in pollination. *Plant Cell*, **16 Suppl**, S84-97.

Feng, X.L., Ni, W.M., Elge, S., Mueller-Roeber, B., Xu, Z.H. and Xue, H.W. (2006) Auxin flow in anther filaments is critical for pollen grain development through regulating pollen mitosis. *Plant Mol. Biol.*, **61**, 215–226.

Ferrándiz, C., Fourquin, C., Prunet, N., Scutt, C.P., Sundberg, E., Trehin, C. and Vialette-Guiraud, A.C.M. (2010) Carpel Development. *Adv. Bot. Res.* **55,** 1-73.

Figueiredo, D.D., Batista, R.A., Roszak, P.J. and Köhler, C. (2015) Auxin production couples endosperm development to fertilization. *Nat. Plants*, **1**, 15184.

Firon, N., Pressman, E., Meir, S., Khoury, R. and Altahan, L. (2012) Ethylene is involved in maintaining tomato (Solanum lycopersicum) pollen quality under heat-stress conditions. *AoB Plants*, **2012**, pls024–pls024.

Gan, Z., Feng, Y., Wu, T., Wang, Y., Xu, X., Zhang, X. and Han, Z. (2019) Downregulation of the auxin transporter gene SlPIN8 results in pollen abortion in tomato. *Plant Mol. Biol.*, **99**, 561–573.

Giovane, A., Servillo, L., Balestrieri, C., Raiola, A., D'Avino, R., Tamburrini, M., Ciardiello, M.A. and Camardella, L. (2004) Pectin methylesterase inhibitor. *Biochim. Biophys. Acta - Proteins Proteomics*, **1696**, 245–252.

Goetz, M., Hooper, L.C., Johnson, S.D., Carlyle, J., Rodrigues, M., Vivian-smith, A. and Koltunow, A.M. (2007) Expression of Aberrant Forms of AUXIN RESPONSE FACTOR8 Stimulates Parthenocarpy in Arabidopsis. *Plant physiol*, **145**, 351–366.

Goetz, M., Vivian-Smith, A., Johnson, S.D. and Koltunow, A.M. (2006) AUXIN RESPONSE FACTOR8 is a negative regulator of fruit initiation in Arabidopsis. *Plant Cell*, **18**, 1873–1886.

Goldberg, R.B., Beals, T.P. and Sanders, P.M. (1993) Anther development: basic principles and practical applications. *Plant Cell*, **5**, 1217–1229.

Gossot, O. and Geitmann, A. (2007) Pollen tube growth: coping with mechanical obstacles involves the cytoskeleton. *Planta*, **226**, 405–416.

Gu, L.L., Gao, Q.F. and Wang, Y.F. (2017) Cyclic nucleotide-gated channel 18 functions as an essential Ca2+ channel for pollen germination and pollen tube growth in Arabidopsis. *Plant Signal. Behav.*, **12**, 17–19.

Gustavsson, Jenny , Cederberg Christel, S.U. (2011) Global Food losses and Food waste. FAO report, Rome, http://www.fao.org/3/a-i2697e.pdf.

Gutermuth, T., Lassig, R., Portes, M., Maierhofer, T., Romeis, T., Borst, J., Hedrich, R. and Konrad, K.R. (2013) Pollen Tube Growth Regulation by Free Anions Depends on the Interaction between the Anion Channel SLAH3 and Calcium-Dependent Protein Kinases CPK2 and CPK20. *Plant Cell*, **25**, 4525–4543.

Hijazi, M., Velasquez, S.M., Jamet, E., Estevez, J.M. and Albenne, C. (2014) An update on post-translational modifications of hydroxyproline-rich glycoproteins: Toward a model highlighting their contribution to plant cell wall architecture. *Front. Plant Sci.*, **5**, 1–10.

Hocq, L., Guinand, S., Habrylo, O., et al. (2020) The exogenous application of AtPGLR, an endo-polygalacturonase, triggers pollen tube burst and repair. *Plant J.*, **103**, 617–633.

Hocq, L., Pelloux, J. and Lefebvre, V. (2017) Connecting Homogalacturonan-Type Pectin Remodeling to Acid Growth. *Trends Plant Sci.*, **22**, 20–29.

Holden, M.J., Marty, J.A. and Singh-Cundy, A. (2003) Pollination-induced ethylene promotes the early phase of pollen tube growth in Petunia inflata. *J. Plant Physiol.*, **160**, 261–269.

Hua, J., Sakai, H., Nourizadeh, S., Chen, Q.G., Bleecker, A.B., Ecker, J.R. and Meyerowitz, E.M. (1998) EIN4 and ERS2 are members of the putative ethylene receptor gene family in Arabidopsis. *Plant Cell*, **10**, 1321–1332.

Jegadeesan, S., Beery, A., Altahan, L., Meir, S., Pressman, E. and Firon, N. (2018) Ethylene production and signaling in tomato (Solanum lycopersicum) pollen grains is responsive to heat stress. *Plant Reprod.* **31**, 367–383

Jia, H., Yang, J., Liesche, J., Liu, X., Hu, Y., Si, W., Guo, J. and Li, J. (2018) Ethylene promotes pollen tube growth by affecting actin filament organization via the cGMP-dependent pathway in Arabidopsis thaliana. *Protoplasma*, **255**, 273–284.

Jones B, Frasse P, Olmos E, Zegzouti H, Li ZG, Latche A, Pech JC, Bouzayen M (2002). Down-regulation of DR12, an auxin-response-factor homolog, in the tomato results in a pleiotropic phenotype including dark green and blotchy ripening fruit. *Plant J.*, **32**, 603–613

Jong, M. de, Wolters-Arts, M., García-Martínez, J.L., Mariani, C. and Vriezen, W.H. (2011) The Solanum lycopersicum AUXIN RESPONSE FACTOR 7 (SlARF7) mediates cross-talk between auxin

and gibberellin signalling during tomato fruit set and development. *J. Exp. Bot.*, **62**, 617–626.

Jung, T., Lee, J.H., Cho, M.H. and Kim, W.T. (2000) Induction of 1-aminocyclopropane-1-carboxylate oxidase mRNA by ethylene in mung bean roots: Possible involvement of Ca^{2+} and phosphoinositides in ethylene signalling. *Plant, Cell Environ.*, **23**, 205–213.

Koning, R.E. (1983) The role of auxin, ethylene, and acid growth in filament elongation in Gaillardia Grandiflora(Asteraceae). *Am. J. Bot.*, **70**, 602–610.

Kovaleva, L. V., Dobrovolskaya, A., Voronkov, A. and Rakitin, V. (2011) Ethylene is Involved in the Control of Male Gametophyte Development and Germination in Petunia. *J. Plant Growth Regul.*, **30**, 64–73.

Kovaleva, L. and Zakharova, E. (2003) Hormonal status of the pollen-pistil system at the progamic phase of fertilization after compatible and incompatible pollination in Petunia hybrida L. *Sex. Plant Reprod.*, **16**, 191–196.

Kroeger, J.H., Zerzour, R. and Geitmann, A. (2011) Regulator or driving force? The role of turgor pressure in oscillatory plant cell growth. *PLoS One*, **6**, e18549.

Kumar, R., Khurana, A. and Sharma, A.K. (2013) Role of plant hormones and their interplay in development and ripening of fleshy fruits. *J. Exp. Bot.*, **65**, 4561–4575.

Lamarre, S., Frasse, P., Zouine, M., Labourdette, D., Sainderichin, E., Hu, G., Berre-Anton, V. Le, Bouzayen, M. and Maza, E. (2018) Optimization of an RNA-Seq Differential Gene Expression Analysis Depending on Biological Replicate Number and Library Size. *Front. Plant Sci.*, **9**, 108.

Lehner, A., Dardelle, F., Soret-Morvan, O., Lerouge, P., Driouichl, A. and Mollet, J.C. (2010) Pectins in the cell wall of Arabidopsis thaliana pollen tube and pistil. *Plant Signal. Behav.*, **5**, 1282–1285.

Leroux, C., Bouton, S., Kiefer-Meyer, M.-C., et al. (2015) PECTIN METHYLESTERASE48 Is Involved in Arabidopsis Pollen Grain Germination. *Plant Physiol.*, **167**, 367–380.

Li D, Flores-Sandoval E, Ahtesham U, Coleman A, Clay JM, Bowman JL, Chang C (2020) Ethylene-independent functions of the ethylene precursor ACC in Marchantia polymorpha. *Nat. Plants* **6**, 1335-1344.

Li, J., Li, Y., Deng, Y., Chen, P., Feng, F., Chen, W., Zhou, X. and Wang, Y. (2018) A calcium-dependent protein kinase , ZmCPK32 , specifically expressed in maize pollen to regulate pollen tube growth. *PLoS One*, **13**, e0195787.

Liao, Y., Smyth, G.K. and Shi, W. (2014) FeatureCounts: An efficient general purpose program for assigning sequence reads to genomic features. *Bioinformatics*, **30**, 923–930.

Lindstrom, J.T., Lei, C., Jones, M.L. and Woodson, W.R. (1999) Accumulation of 1-Aminocyclopropane-1-carboxylic acid (ACC) in Petunia Pollen is Associated with Expression of a Pollen-specific ACC Synthase Late in Development. *J. Am. Soc. Hortic. Sci.*, **124**, 145–151.

Liu, M., Chen, Yao, Chen, Ya, Shin, J., Mila, I., Audran, C., Zouine, M., Pirrello, J. and Bouzayen, M. (2018) The tomato Ethylene Response Factor Sl-ERF.B3 integrates ethylene and auxin signaling via direct regulation of Sl-Aux/IAA27. *New Phytol.*, **219**, 631–640.

Liu, M., Pirrello, J., Chervin, C., Roustan, J.-P. and Bouzayen, M. (2015) Ethylene control of fruit ripening:

revisiting the complex network of transcriptional regulation. *Plant Physiol.*, **169**, 2380–2390.

Llop-Tous, I., Barry, C.S. and Grierson, D. (2000) Regulation of Ethylene Biosynthesis in Response to Pollination in Tomato Flowers. *Plant Physiol.*, **123**, 971–978.

Love, M.I., Huber, W. and Anders, S. (2014) Moderated estimation of fold change and dispersion for RNA-seq data with DESeq2. *Genome Biol.*, **15**, 1–21.

Luschnig, C., Gaxiola, R.A., Grisafi, P. and Fink, G.R. (1998) EIR1, a root-specific protein involved in auxin transport, is required for gravitropism in Arabidopsis thaliana. *Genes Dev.*, **12**, 2175–2187.

Mao, J., Miao, Z., Wang, Z., Yu, L. and Cai, X. (2016) Arabidopsis ERF1 Mediates Cross-Talk between Ethylene and Auxin Biosynthesis during Primary Root Elongation by Regulating ASA1 Expression. *PLoS Genet*. **12**, e1005760.

Martin, M. 2011. Cutadapt removes adapter sequences from high-throughput sequencing reads. *EMBnet* **17**, 10-12

Martínez-Fernández, I., Sanchís, S., Marini, N., Balanzá, V., Ballester, P., Navarrete-Gómez, M., Oliveira, A.C., Colombo, L. and Ferrándiz, C. (2014) The effect of NGATHA altered activity on auxin signaling pathways within the Arabidopsis gynoecium. *Front. Plant Sci.*, **5**, 210.

Martínez, C., Manzano, S., Megías, Z., Garrido, D., Picó, B. and Jamilena, M. (2013) Involvement of ethylene biosynthesis and signalling in fruit set and early fruit development in zucchini squash (Cucurbita pepo L.). *BMC Plant Biol.*, **13**. 139.

Martinis, D. De and Mariani, C. (1999) Silencing gene expression of the ethylene-forming enzyme results in a reversible inhibition of ovule development in transgenic tobacco plants. *Plant Cell*, **11**, 1061–1072.

Maruyama, D., Völz, R., Takeuchi, H., et al. (2015) Rapid Elimination of the Persistent Synergid through a Cell Fusion Mechanism. *Cell*, **161**, 907–918.

Maza, E. (2016) In papyro comparison of TMM (edgeR), RLE (DESeq2), and MRN normalization methods for a simple two-conditions-without-replicates RNA-seq experimental design. *Front. Genet.*, **7**, 1–8.

Maza, E., Frasse, P., Senin, P., Bouzayen, M. and Zouine, M. (2013) Comparison of normalization methods for differential gene expression analysis in RNA-Seq experiments. *Commun. Integr. Biol.*, **6**, e25849.

Melo, N.K.G., Bianchetti, R.E., Lira, B.S., et al. (2016) Nitric Oxide, Ethylene, and Auxin Cross Talk Mediates Greening and Plastid Development in Deetiolating Tomato Seedlings. *Plant Physiol.*, **170**, 2278–2294.

Michard, E., Simon, Alexander A, Tavares, B., Wudick, M.M. and Feijó, J.A. (2017) Signaling with Ions: The Keystone for Apical Cell Growth and Morphogenesis in Pollen Tubes. *Plant Physiol.*, **173**, 91–111.

Mól, R., Filek, M., Machackova, I. and Matthys-Rochon, E. (2004) Ethylene synthesis and auxin augmentation in pistil tissues are important for egg cell differentiation after pollination in maize. *Plant Cell Physiol.*, **45**, 1396–1405.

Mollet, J.-C., Leroux, C., Dardelle, F. and Lehner, A. (2013) Cell Wall Composition, Biosynthesis and Remodeling during Pollen Tube Growth. *Plants*, **2**, 107–147.

Mou, W., Kao, Y.-T., Michard, E., Simon, A.A., Li, D., Wudick, M.M., Lizzio, M.A., Feijó, J.A. and Chang, C. (2020) Ethylene-independent signaling by the ethylene precursor ACC in Arabidopsis ovular pollen tube attraction. *Nat. Commun.*, **11**, 4082.

Muday, G.K., Rahman, A. and Binder, B.M. (2012) Auxin and ethylene: Collaborators or competitors? *Trends Plant Sci.*, **17**, 181–195.

Myers, C., Romanowsky, S.M., Barron, Y.D., et al. (2009) Calcium-dependent protein kinases regulate polarized tip growth in pollen tubes. *Plant J.*, **59**, 528–539.

Negi S, Sukumar P, Liu X, Cohen JD, Muday GK (2010) Genetic dissection of the role of ethylene in regulating auxin-dependent lateral and adventitious root formation in tomato. *Plant J.* **61**:3-15

Normanly, J., Cohen, J.D. and Fink, G.R. (1993) Arabidopsis thaliana auxotrophs reveal a tryptophan-independent biosynthetic pathway for indole-3-acetic acid. *Proc. Natl. Acad. Sci. U. S. A.*, **90**, 10355–10359.

Nguyen-Kim, H., San Clemente, H., Laimer, J., Lackner, P., Gadermaier, G., Dunand, C., Jamet, E. (2020). The Cell Wall PAC (Proline-Rich, Arabinogalactan Proteins, Conserved Cysteines) Domain-Proteins Are Conserved in the Green Lineage. *Int. J. Mol. Sci*., **21**, 2488.

O'Neill, S.D., Nadeau, J.A., Zhang, X.S., Bui, A.Q. and Halevy, A.H. (1993) Interorgan regulation of ethylene biosynthetic genes by pollination. *Plant Cell*, **5**, 419–432.

Okada, K., Ueda, J., Komaki, M.K., Bell, C.J. and Shimura, Y. (1991) Requirement of the Auxin Polar Transport System in Early Stages of Arabidopsis Floral Bud Formation. *Plant Cell*, **3**, 677–684.

Palanivelu, R., Brass, L., Edlund, A.F. and Preuss, D. (2003) Pollen Tube Growth and Guidance Is Regulated by POP2 , an Arabidopsis Gene that Controls GABA Levels. , **114**, 47–59.

Pan, Y., Chai, X., Gao, Q., Zhou, L., Zhang, S., Li, L. and Luan, S. (2019) Dynamic Interactions of Plant CNGC Subunits and Calmodulins Drive Oscillatory Ca 2+ Channel Activities. *Dev. Cell*, **48**, 710-725.

Pandolfini, T. (2009) Seedless Fruit Production by Hormonal Regulation of Fruit Set. *Nutrients*, **1**, 168–177.

Parre, E. and Geitmann, A. (2005) Pectin and the role of the physical properties of the cell wall in pollen tube growth of Solanum chacoense. *Planta*, **220**, 582–592.

Pascual, L., Blanca, J.M., Cañizares, J. and Nuez, F. (2009) Transcriptomic analysis of tomato carpel development reveals alterations in ethylene and gibberellin synthesis during pat3/pat4 parthenocarpic fruit set. *BMC Plant Biol.*, **9**, 67.

Pereira, A.M. and Coimbra, S. (2019) Advances in plant reproduction: From gametes to seeds. *J. Exp. Bot.*, **70**, 2933–2936.

Pertl, H., Himly, M., Gehwolf, R., Kriechbaumer, R., Strasser, D., Michalke, W., Richter, K., Ferreira, F. and Obermeyer, G. (2001) Molecular and physiological characterisation of a 14-3-3 protein from lily pollen grains regulating the activity of the plasma membrane H+ ATPase during pollen grain germination and tube growth. *Planta*, **213**, 132–141.

Petruzzelli, L., Sturaro, M., Mainieri, D. and Leubner-Metzger, G. (2003) Calcium requirement for ethylene-dependent responses involving 1-aminocyclopropane-1-carboxylic acid oxidase in radicle tissues of germinated pea seeds. *Plant, Cell Environ.*, **26**, 661–671.

Pierson, E.S., Miller, D.D., Callaham, D.A., Aken, J. Van, Hackett, G. and Hepler, P.K. (1996) Tip-localized calcium entry fluctuates during pollen tube growth. *Dev. Biol.*, **174**, 160–173.

Plcader, W., Sommer, H., Malepszy, S., Malinowski, R., Yin, Z. and Ziółkowska, A. (2006) The DefH9-iaaM-containing construct efficiently induces parthenocarpy in cucumber. *Cell. Mol. Biol. Lett.*, **11**, 279–290.

Poel, B. Van de, Smet, D. and Straeten, D. Van Der (2015) Ethylene and Hormonal Cross Talk in Vegetative Growth and Development. *Plant Physiol.*, **169**, 61–72.

Poel, B. Van de and Straeten, D. Van Der (2014) 1-aminocyclopropane-1-carboxylic acid (ACC) in plants: more than just the precursor of ethylene! *Front. Plant Sci.*, **5**, 1–11.

Qu, H., Xing, W., Wu, F. and Wang, Y. (2016) Rapid and Inexpensive Method of Loading Fluorescent Dye into Pollen Tubes and Root Hairs. *PLoS One*, **11**, e0152320.

Reimann, R., Kah, D., Mark, C., et al. (2020) Durotropic Growth of Pollen Tubes. *Plant Physiol.*, **183**, 558–569.

Rieu, I., Wolters-Arts, M., Derksen, J., Mariani, C. and Weterings, K. (2003) Ethylene regulates the timing of anther dehiscence in tobacco. *Planta*, **217**, 131–7.

Robles, L., Stepanova, A. and Alonso, J. (2013) Molecular mechanisms of ethylene-auxin interaction. *Mol. Plant*, **6**, 1734–1737.

Rotino, G.L., Perri, E., Zottini, M., Sommer, H. and Spena, A. (1997) Genetic engineering of parthenocarpic plants. *Nat. Biotechnol.*, **15**, 871–875.

Růzicka, K., Ljung, K., Vanneste, S., Podhorská, R., Beeckman, T., Friml, J. and Benková, E. (2007) Ethylene regulates root growth through effects on auxin biosynthesis and transport-dependent auxin

San Clemente, H. and Jamet, E. (2015) WallProtDB, a database resource for plant cell wall proteomics. *Plant Methods*, **11**, 1–7.

Sedbrook, J. C., Carroll, K. L., Hung, K. F., Masson, P. H.Somerville, C. R. (2002) The Arabidopsis SKU5 gene encodes an extracellular glycosyl phosphatidylinositol-anchored glycoprotein involved in directional root growth. *Plant Cell*, **14**, 1635-1648.

Serrani, J.C., Ruiz-Rivero, O., Fos, M. and García-Martínez, J.L. (2008) Auxin-induced fruit-set in tomato is mediated in part by gibberellins. *Plant J.*, **56**, 922–34.

Shin, J.H., Mila, I., Liu, M., Rodrigues, M.A., Vernoux, T., Pirrello, J. and Bouzayen, M. (2019) The RIN-regulated Small Auxin-Up RNA SAUR69 is involved in the unripe-to-ripe phase transition of tomato fruit via enhancement of the sensitivity to ethylene. *New Phytol.*, **222**, 820-836.

Shinozaki, Y., Hao, S., Kojima, M., et al. (2015) Ethylene suppresses tomato (Solanum lycopersicum) fruit set through modification of gibberellin metabolism. *Plant J.*, **83**, 237–251.

Silverstein, K.A., Moskal, W.A. Jr, Wu, H.C., Underwood, B.A., Graham, M.A., Town, C.D., VandenBosch, K.A. (2007). Small cysteine-rich peptides resembling antimicrobial peptides have been under-predicted in plants. *Plant J.* **51**, 262-280.

Sjut, V. and Bangerth, F. (1982) Induced parthenocarpy-a way of changing the levels of endogenous hormones in tomato fruits (Lycopersicon esculentum Mill.) 1. Extractable hormones. *Plant Growth Regul.*, **1**, 243–251.

Steinhorst, L., Mähs, A., Ischebeck, T., Zhang, C., Zhang, X., Arendt, S., Schültke, S., Heilmann, I. and Kudla, J. (2015) Vacuolar CBL-CIPK12 Ca2+-Sensor-Kinase complexes are required for polarized pollen tube growth. *Curr. Biol.*, **25**, 1475–1482.

Stepanova, A.N. and Alonso, J.M. (2009) Ethylene signaling and response: where different regulatory modules meet. *Curr. Opin. Plant Biol.*, **12**, 548–555.

Stepanova, A.N., Yun, J., Likhacheva, A. V. and Alonso, J.M. (2007) Multilevel Interactions between Ethylene and Auxin in Arabidopsis Roots. *Plant Cell Online*, **19**, 2169–2185.

Stranne, M., Ren, Y., Fimognari, L., et al. (2018) TBL10 is required for O-acetylation of pectic rhamnogalacturonan-I in Arabidopsis thaliana. *Plant J.*, **96**, 772–785.

Suwińska, A., Wasąg, P., Zakrzewski, P., Lenartowska, M. and Lenartowski, R. (2017) Calreticulin is required for calcium homeostasis and proper pollen tube tip growth in Petunia. *Planta*, **245**, 909–926.

Takada, K., Ishimaru, K., Kamada, H. and Ezura, H. (2006) Anther-specific expression of mutated melon ethylene receptor gene Cm-ERS1/H70A affected tapetum degeneration and pollen grain production in transgenic tobacco plants. *Plant Cell Rep.*, **25**, 936–941.

Takada, K., Ishimaru, K., Minamisawa, K., Kamada, H. and Ezura, H. (2005) Expression of a mutated melon ethylene receptor gene Cm-ETR1/H69A affects stamen development in Nicotiana tabacum. *Plant Sci.*, **169**, 935–942.

Tang, X. and Woodson, W.R. (1996) Temporal and Spatial Expression of 1-Aminocyclopropane-1-Carboxylate Oxidase mRNA following Pollination of Immature and Mature Petunia Flowers. *Plant Physiol.*, **112**, 503–511.

Tieman, D.M., Taylor, M.G., Ciardi J.A., Klee H.J. (2000). The tomato ethylene receptors NR and LeETR4 are negative regulators of ethylene response and exhibit functional compensation within a multigene family. *Proc. Natl. Acad. Sci. U. S. A.*, **97**, 5663-5668.

Tommaso, P. DI, Chatzou, M., Floden, E.W., Barja, P.P., Palumbo, E. and Notredame, C. (2017) Nextflow enables reproducible computational workflows. *Nat. Biotechnol.*, **35**, 316–319.

Trigueros, M., Navarrete-Gómez, M., Sato, S., Christensen, S.K., Pelaz, S., Weigel, D., Yanofsky, M.F. and Ferrándiz, C. (2009) The NGATHA genes direct style development in the Arabidopsis gynoecium. *Plant Cell*, **21**, 1394–409.

Tsang, D.L., Edmond, C., Harrington, J.L. and Nühse, T.S. (2011) Cell Wall Integrity Controls Root Elongation via a General 1-Aminocyclopropane-1-Carboxylic Acid-Dependent, Ethylene-Independent Pathway. *Plant Physiol.*, **156**, 596–604.

Tunc-Ozdemir, M., Rato, C., Brown, E., Rogers, S., Mooneyham, A., Frietsch, S., Myers, C.T., Poulsen, L. R., Malhó, R., and Harper, J.F. (2013) A cyclic nucleotide-gated channel Cyclic nucleotide gated channels 7 and 8 are essential for male reproductive fertility. *PLoS One* **8**, e55277.

Sun X, Li Y, He W, Ji C, Xia P, Wang Y, Du S, Li H, Raikhel N, Xiao J, Guo H (2017) Pyrazinamide and derivatives block ethylene biosynthesis by inhibiting ACC oxidase. *Nat Commun*. **8**:15758.

Vanderstraeten, L., Depaepe, T., Bertrand, S. and Straeten, D. Van Der. (2019) The Ethylene Precursor ACC Affects Early Vegetative Development Independently of Ethylene Signaling. *Front Plant Sci*. **10**, 1591.

Varoquaux, F., Blanvillain, R., Delseny, M. and Gallois, P. (2000) Less is better: new approaches for seedless fruit production. *Trends Biotechnol.*, **18**, 233–242.

Verhertbruggen, Y., Marcus, S.E., Haeger, A., Ordaz-Ortiz, J.J. and Knox, J.P. (2009) An extended set of monoclonal antibodies to pectic homogalacturonan. *Carbohydr. Res.*, **344**, 1858–1862.

Vogel, J.P., Raab, T.K., Somerville, C.R. and Somerville, S.C. (2004) Mutations in PMR5 result in powdery mildew resistance and altered cell wall composition. *Plant J.*, **40**, 968–978.

Völz, R., Heydlauff, J., Ripper, D., vonLyncker, L. and Groß-Hardt, R. (2013) Ethylene Signaling Is Required for Synergid Degeneration and the Establishment of a Pollen Tube Block. *Dev. Cell*, **25**, 310–316.

Vriezen, W.H., Feron, R., Maretto, F., Keijman, J. and Mariani, C. (2008) Changes in tomato ovary transcriptome demonstrate complex hormonal regulation of fruit set. *New Phytol.*, **177**, 60–76.

Wang, B., Chu, J., Yu, T., et al. (2015) Tryptophan-independent auxin biosynthesis contributes to early embryogenesis in *Arabidopsis*. *Proc. Natl. Acad. Sci.*, **112**, 4821–4826.

Wang, D.-H., Li, F., Duan, Q.-H., Han, T., Xu, Z.-H. and Bai, S.-N. (2010) Ethylene perception is involved in female cucumber flower development. *Plant J.*, **61**, 862–872.

Wang, H., Jones, B., Li, Z., et al. (2005) The tomato Aux/IAA transcription factor IAA9 is involved in fruit development and leaf morphogenesis. *Plant Cell*, **17**, 2676–2692.

Wang, H., Wu, H.M. and Cheung, A.Y. (1996) Pollination induces mRNA poly(A) tail-shortening and cell deterioration in flower transmitting tissue. *Plant J.*, **9**, 715–727.

Wang, Y. and Kumar, P.P. (2007) Characterization of two ethylene receptors PhERS1 and PhETR2 from petunia: PhETR2 regulates timing of anther dehiscence. *J. Exp. Bot.*, **58**, 533–544.

Wang, Y., Zhang, W.Z., Song, L.F., Zou, J.J., Su, Z. and Wu, W.H. (2008) Transcriptome analyses show changes in gene expression to accompany pollen germination and tube growth in arabidopsis. *Plant Physiol.*, **148**, 1201–1211.

Whitehead, C.S., Fujino, D.W. and Reid, M.S. (1983) Identification of the ethylene precursor, 1-aminocyclopropane-1-carboxylic acid (ACC), in pollen. *Sci. Hortic.*, **21**, 291-297.

Wilkinson, J.Q., Lanahan, M.B., Yen, H.C., Giovannoni, J.J. and Klee, H.J. (1995) An ethylene-inducible component of signal transduction encoded by Never-ripe. *Science,* **270**, 1807-1809

Wu, J., Qin, Y. and Zhao, J. (2008a) Pollen tube growth is affected by exogenous hormones and correlated with hormone changes in styles in Torenia fournieri L. *Plant Growth Regul.*, **55**, 137–148.

Wu, J.-Z., Lin, Y., Zhang, X.-L., Pang, D.-W. and Zhao, J. (2008b) IAA stimulates pollen tube growth and mediates the modification of its wall composition and structure in Torenia fournieri. *J. Exp. Bot.*, **59**, 2529–2543.

Xu, S., Rahman, A., Baskin, T.I. and Kieber, J.J. (2008) Two Leucine-Rich Repeat Receptor Kinases Mediate Signaling , Linking Cell Wall Biosynthesis and ACC Synthase in Arabidopsis. *Plant Cell*, **20**, 3065–3079.

Yau, Chi Ping (2004) Differential expression of three genes encoding an ethylene receptor in rice during development, and in response to indole-3-acetic acid and silver ions. *J. Exp. Bot.*, **55**, 547–556.

Yin, J., Zhang, X., Zhang, G., Wen, Y., Liang, G. and Chen, X. (2019) Aminocyclopropane-1-carboxylic acid is a key regulator of guard mother cell terminal division in Arabidopsis thaliana. *J. Exp. Bot.*, **70**, 897–907.

Yu, Jian, Niu, L., Yu, Jihua, Liao, W., Xie, J., Lv, J., Feng, Z., Hu, L. and Dawuda, M. (2019) The Involvement of Ethylene in Calcium-Induced Adventitious Root Formation in Cucumber under Salt Stress. *Int. J. Mol. Sci.*, **20**, 1047.

Zazímalová, E., Murphy, A.S., Yang, H., Hoyerová, K. and Hosek, P. (2010) Auxin transporters--why so many? *Cold Spring Harb. Perspect. Biol.*, **2**, a001552.

Zhang, X. S., & O'Neill, S.D. (1993) Ovary and Gametophyte Development Are Coordinately Regulated by Auxin and Ethylene following Pollination. *Plant Cell*, **5**, 403–418.

Zhang, C., Teng, X.-D., Zheng, Q.-Q., Zhao, Y.-Y., Lu, J.-Y., Wang, Y., Guo, H. and Yang, Z.-N. (2018) Ethylene signaling is critical for synergid cell functional specification and pollen tube attraction. *Plant J.*, **96**, 176–187.

Zhao, M.G., Tian, Q.Y. and Zhang, W.H. (2007) Ethylene activates a plasma membrane Ca^{2+}-permeable channel in tobacco suspension cells: Rapid report. *New Phytol.*, **174**, 507–515.

Zhao, Y. (2014) Auxin Biosynthesis. *Arabidopsis B.*, **12**, e0173.

Zheng, R., Su, S., Xiao, H. and Tian, H. (2019) Calcium: A Critical Factor in Pollen Germination and Tube Elongation. *Int. J. Mol. Sci.*, **20**, 420.

Zhu, J., Wu, X., Yuan, S., Qian, D., Nan, Q., An, L. and Xiang, Y. (2014) Annexin5 plays a vital role in Arabidopsis pollen development via Ca 2+-dependent membrane trafficking G. K. Pandey, ed. *PLoS One*, **9**, e102407.

Zouine, M., Maza, E., Djari, A., Lauvernier, M., Frasse, P., Smouni, A., Pirrello, J. and Bouzayen, M. (2017) TomExpress, a unified tomato RNA-Seq platform for visualization of expression data, clustering and correlation networks. *Plant J.*, **92**, 727–735.